MEASUREMENT AND STOCHASTIC MODELLING OF TORQUE AND THRUST IN TWIST DRILLING OPERATION

GURCHARAN SINGH CHAHIL

A Thesis

in

The Faculty

of

Engineering

Presented in Partial Fulfillment of the Requirement
for the degree of Master of Engineering at
Concordia University
Montréal, Québec, Canada

September, 1976

ABSTRACT

GURCHARAN SINGH CHAHIL

MEASUREMENT AND STOCHASTIC MODELLING OF TORQUE AND THRUST IN TWIST DRILLING

The present research work deals with the measurements and analysis of torque and thrust in twist drilling. Force and torque measurements were carried out using a specially designed two-component piezoelectric dynamometer. The dynamometer was both statically and dynamically calibrated and techniques for increasing the measuring accuracy and reducing cross-interference were employed.

The static calibration was performed under external torque and thrust force, using a specially designed fixture and force transducers. The dynamometer was dynamically calibrated by determining the frequency response of dynamometer under sinusoidal excitation ranging between 20 Hz to 4kHz. The frequency response shows that the natural frequency of a system consisting of only the workpiece and dynamometer is higher than that consisting of the dynamometer; workpiece and the machine-tool.

Experiments have been carried out to measure the drilling torque and thrust force in mild steel under different cutting conditions. Recorded data from the dynamometer was processed by a sequence of programs running on an EAI-690 hybrid computer

and a CDC-6400 digital computer and a statistical analysis was performed to determine the major statistical properties of the metal cutting torque and thrust.

For each recorded cutting force signal, analyses were carried out to determine the mean value, standard deviation, probability density, power spectral density and the auto-correlation function of the fluctuations in torque and thrust force.

Results of the analysis show that the dynamic fluctuations of torque and thrust in twist drilling are stationary and random with a Gaussian density function. An attempt is made to mathematically model the cutting torque and thrust in twist drilling. It is expected that this formulation will be of great value in an analytical study of the dynamic behaviour and stability of twist drilling machines under actual cutting operations.

ACKNOWLEDGEMENT

The author wishes to express his gratitude to his thesis supervisors, Dr. M.O.M. Osman and Professor G.D. Xistris for providing guidance during the course of the investigations.

The financial support of the National Research Council of Canada, Grant No. A5181, and Formation de chercheurs et d'action Concertée of the Government of Quebec, Grant No. 042110, is gratefully acknowledged.

The author is thankful also, to the engineering Machine Shop Staff and Mr. Korioth for their cooperation and help. Thanks are also due to Mr. Gordon Boast, for his help with the data reduction and transmission system. (E.A. 690 HYBRID COMPUTER)

TABLE OF CONTENTS

TABLE OF CONTENTS

LIST OF TABLES

LIST OF TABLES

LIST OF FIGURES

LIST OF FIGURES

NOMENCLATURE

NOMENCLATURE

D,d	Diameter of the drill
F	Friction force
F_c	Critical frequency
F_z	Thrust force in drilling
M_z	Torque in drilling
H	Interval between sample points
G	Spectral density
R	Auto-correlation function
R'	Reaction force
s,f	Feed in drilling
r	Radius of the drill at any point
w	Web thickness
Q	Electric charge
c	Gain
v	Volts
N	Number of data points
P	Probability density function
$\bar{Y}_i$	Mean value of sample points in i^{th} interval
$\bar{Y}_i^2$	Mean square value of sample points in i^{th} interval
Y(R)	Digitized sample record
α	Rake angle
η	Friction angle
ϕ	Shear angle
ρ	Point angle of drill
ν	Inclination angle

γ	Relief angle
σ	Standard deviation
σ^2	Variance
τ	Shear stress
μ	Mean value

CHAPTER I

INTRODUCTION

CHAPTER I

INTRODUCTION

1.1 INTRODUCTION

The kinematics of the drilling process basically consists of rotary motion of a twist drill combined with axial movement by either the drill or the workpiece. The twist drill possesses two symetrically located cutting edges known as lips which perform an oblique cutting action. The cutting action of a twist drill along its lips is characterised by a more complex process compared to that of the turning operation. The geometry of the chip formation changes along the cutting edges due to the variation of the tangential velocities and rake angles along the radius of the drill. This results in a non-uniform stress distribution along the tool-cutting edge which in turn affects the cutting forces on the drill.

The initial history of drilling is obscure. From the available data it appears that research work on drilling dates back to 1900 A.D. At that time, many researchers tried to determine the power absorbed in drilling experimentally. Among these, the names of Boston and Gilbert [1]* are prominent. They offered many empirical relations for calculating torque and thrust in drilling different materials.

---

*Numbers in brackets [] designate references at the end of the thesis.

Merchant [2], using the principle of minimum energy, carried out investigations in cutting forces in machining and assumed the process to be a steady state one. In 1952, Shaw, Cook and Smith [3] demonstrated the similarity between drill point and conventional turning tool, Figures 1.1 and 1.2. Oxford, Jr. [4] employed the principle of quick stop to study the mechanism of chip formation and concluded that this mechanism is not the same along the cutting lip. The action of the cutting edge is similar to the other cutting processes but under the chisel edge, the process is known as the extrusion process. Shaw and Oxford, Jr. [5] applied dimensional analysis and arrived at certain equations for thrust and torque, and found them to be in good agreement with the experimental results.

All these researchers have assumed that the cutting process is a steady state process and the theories put forward only give a steady state mean value of the force and neglect the fluctuating components. Knowledge of the nature of fluctuations of these cutting forces is essential, to have an insight into the dynamic behaviour and stability of machine tools. Other parameters such as the machinability of a workpiece, the surface texture of machined parts, power requirements, the tool life, etc., depend upon the magnitude and frequency of these forces.

The study and analysis of the dynamic behaviour of cutting forces is very important in understanding the vibratory response of a machine tool. De Vries [6] has given a brief description of dynamometers of different types used in orthogonal and oblique machining. He shows that semi-conductor strain gauge dynamometers have high natural frequencies and high sensitivity. Normally, a dynamometer with high natural frequency is required for accurate measurements of cutting forces. Under these conditions, frequencies of cutting forces encountered will be far less than the natural frequency of the dynamometer and the chances of resonance occurring will be remote. Crisp and Seidel [7] used a dynamometer with a natural frequency of 60 kHz to measure the exact fluctuations of cutting forces between single grain on grinding wheels and work piece. Piezoelectric quartz elements are commonly used in such high natural frequency devices.

Bickel [8], was the first to recognise the stochastic nature of cutting forces in metal cutting. He used piezoelectric elements for the cutting force measurement and showed that the degree of randomness could be a high percentage of a steady state cutting force. Based upon this reasoning, Kwiatkowski and Al Samarai [9] and Optiz and Weck [10] developed a relationship between the cutting forces and displacement of machine systems. Osman and Sankar [11], treated random force variations as stationary and Gaussian, and developed a short time acceptance test by determining the response of machine tool spindle systems.

Maragos [13] has proved experimentally that the cutting forces in the turning operation are stochastic in nature and Gaussian distributed only in the finishing operations. Subsequent work by Rakhit [14], verified that cutting forces in turning, are random and Gaussian distributed and furthermore, they play an important part in characterising the surface texture of the machined parts.

In the present investigation, the torque and thrust force in drilling is measured dynamically and a stochastic representation of these quantities is made by evaluating such statistical properties as probability density, auto-correlation function and spectral density.

In the second chapter, the steady state equation for thrust and torque in drilling is given. The similarity of the mechanics of cutting between drilling and turning operations is also developed.

The third chapter outlines the experimental measurements undertaken and discusses the characteristics of the various dynamometers used to measure static and dynamic components, followed by a description of the two component dynamometers used in this investigation.

The fourth chapter covers the complete experimental set-up for measurements. The static and dynamic calibrations

of the dynamometer are explained. A method for measuring small variations in thrust and torque with greater accuracy is given and the experimental results are recorded.

The data processing and reduction techniques employed are presented in the fifth chapter, and the statistical properties of the fluctuating components are evaluated and a standard mathematical model of their distribution is presented.

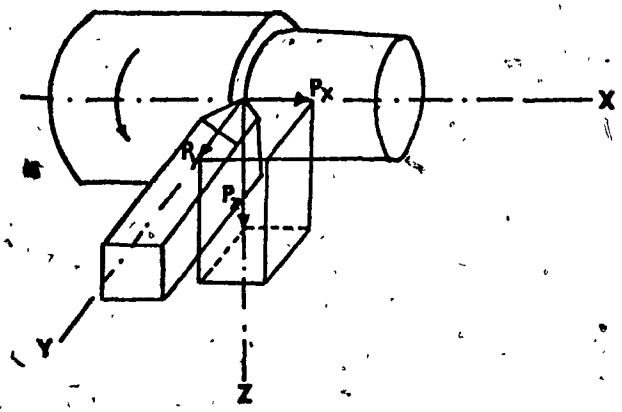

FIG. 1.1 Component Forces on a Conventional Turning Tool

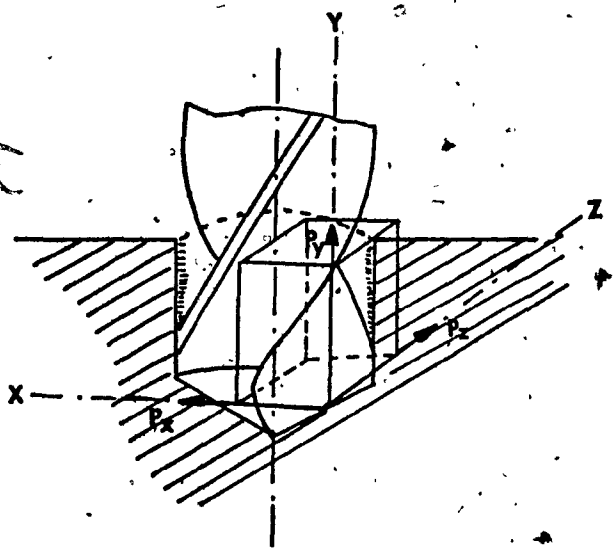

FIG. 1.2 Component Forces at the Cutting Edge of a Drill

CHAPTER II

THRUST FORCE AND TORQUE IN DRILLING

CHAPTER II

THRUST FORCE AND TORQUE IN DRILLING

The drilling operation is basically an oblique cutting operation having two cutting edges. In oblique machining, the cutting edge is inclined to the cutting velocity vector whereas, in othrogonal cutting, the cutting is at a 90 degree angle to the cutting velocity vector, Figure 2.1.

The resulting force in drilling required to develop plastic deformation of the layer under cutting lip can be resolved into two components, a tangential component P_z and a thrust force P_{xy} perpendicular to the cutting edge. The force P_{xy} can be further resolved into a radial force P_x and an axial force P_y acting axially along the drill. P_y is known as the thrust force and P_z is known as the power component of the force and is used to caloulate the torque.

From Figure 2.2

$$P_y = P_{xy} \sin \rho$$

where ρ = the half-point angle of drill.

Taking into account the thrust on both the lips

$$\text{total thrust } F_z = 2P_y = 2P_{xy} \sin \rho$$

Figure 2.3 shows the cutting action of the lips in plan view when the total torque is given by the couple.

Further, there is a friction force occurring at the flank surface, since this surface is in contact with the work surface. These forces are distributed along the cutting edge. Since an ideal sharpness of the cutting edge cannot be maintained, these forces are bound to occur.

K_f = specific friction force per unit active length of lip

Then, friction force

$$F = K_f \times \frac{d-d_o}{2 \sin \rho}$$

d = outer diameter of the drill

d_o = chisel edge diameter

On the basis of the force diagram shown in Figure 2.4, P_z [15] & [18] is calculated as follows:

$P_z = R \cos(\eta-\alpha)$

α = rake angle

η = friction angle

τ_s = shear stress along the shear plane

$$\tau_s = \frac{P_z \cos\phi - P_{xy} \sin\phi}{A_0} \sin\phi \qquad (2.1)$$

A_0 = undeformed chip cross-sectional area

w = width of cut in mm

t_1 = undeformed thickness in mm

$$P_z = \frac{A_0\ \tau_s \cos(\eta-\alpha)}{\sin\phi\ \cos(\phi+\eta-\alpha)} \qquad (2.2)$$

ϕ = shear angle in degree

$A_0 = wt_1$

In drilling

$$A_0 = \frac{d-d_0}{2} \times \frac{s}{2} \qquad (2.3)$$

s = feed/revolution

For thrust force analysis

$$P_y = P_{xy} \cos(90-\rho)$$

$$= P_{xy} \sin\rho$$

$$\tau_s = \frac{P_z \cos\phi - P_{xy} \sin\phi}{A_0} \times \sin\phi$$

$$P_{xy} = P_z \frac{\cos\phi}{\sin\phi} - \frac{\tau_s A_0}{\sin^2\phi}$$

$$P_y = \left[P_z \frac{\cos\phi}{\sin\phi} - \frac{\tau_s A_0}{\sin^2\phi}\right] \sin\rho$$

After putting the value of P_z from eq. (2.2)

$$P_y = \left[\frac{A_0\ \tau_s \cos(\eta-\alpha)}{\sin\phi\ \cos(\phi+\eta-\alpha)} \times \frac{\cos\phi}{\sin\phi} - \frac{\tau_s A_0}{\sin^2\phi}\right] \sin\rho$$

$$= \frac{A_0\ \tau_s \sin\phi}{\sin^2\phi} \left[\frac{\cos(\eta-\alpha)}{\cos(\phi\ \eta-\alpha)} \times \cos\phi - 1\right]$$

After simplification

$$P_y = \frac{A_0 \tau_s \sin\rho \cos[\phi - (\eta-\alpha)]}{\sin^2\phi \cos[\phi + (\eta-\alpha)]}$$

Total thrust force

$$F_z = 2P_y$$

From the geometry of the drill, Fig. 2.5,

$$W = \frac{d}{2 \sin \rho}$$

$$t_u = \frac{s}{2} \sin \rho$$

2.1 THE EFFECTIVE RAKE ANGLE AT VARIOUS RADII ALONG THE CUTTING EDGE

A simple three-dimensional tool is a conventional turning tool with an inclined cutting edge, Fig. 2.1. There are three angles of interest for such a tool.

α_n = normal rake angle (measured in a plane perpendicular to cutting edge)

α_e = effective rake angle (measured in a plane containing relative velocity factor and chip flow direction)

ν = inclination angle between cutting edge and a line perpendicular to cutting velocity vector.

These three angles can be derived in terms of ordinary lathe tool angles.

$$\tan i = \tan\alpha_b \cos C_s - \tan\alpha_s \sin C_s$$

$$\tan \alpha_n = [\tan\alpha_s \cos C_s + \tan\alpha_b \sin C_s] \cos i$$

$$\sin \alpha_e = \sin^2 i + \cos^2 i \sin\alpha_n$$

α_b = back rake angle

α_s = side rake angle

C_s = side cutting edge angle

The drill is a complex tool and visualization of these angles is difficult. By identifying the drill angles that correspond to α_b, α_s, C_s for the lathe tool, the i, α_n, and α_e for the drill can be calculated.

$$\alpha_b(\text{Lathe}) = \theta \text{ Helix Angle}$$

$$C_s(\text{Lathe}) = \cos^{-1}\left(\frac{\cos \rho}{\cos \nu}\right)$$

where

$$\rho = \sin^{-1}\left(\frac{W}{2\ r/\sin \rho}\right)$$

$$\alpha_s(\text{Lathe}) = \tan^{-1}\left[\frac{\tan\theta}{\tan C_s} - \frac{\tan i}{\sin C_s}\right]$$

W = web thickness

r = radius of drill

The above equation indicates that ν changes with the radius of the drill. As a result of the change of ν, α_n the normal rake angle, changes.

The above mathematical analysis assumes drilling to be a steady state process and does not take into account any fluctuations of thrust and torque in drilling. Pal, Bhattacharya and Sen [18], treated drilling as composed of two parts: (i) chisel edge cutting is by extrusion process; (ii) the other portion of lip is normal cutting. They developed an equation for torque in drilling and verified it experimentally. They also treated it as a steady state process. The subsequent analysis takes into account fluctuations and experimentally shows that drilling is not a steady state process.

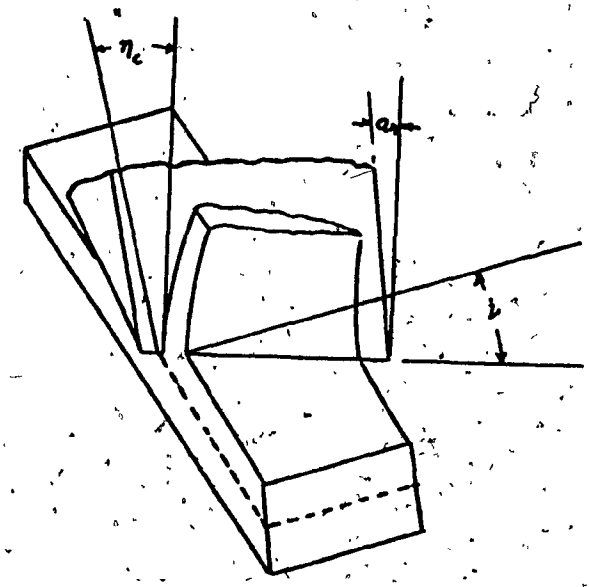

(View a)

FIG. 2.1 View of Cutting Tool With Inclined Cutting Edge

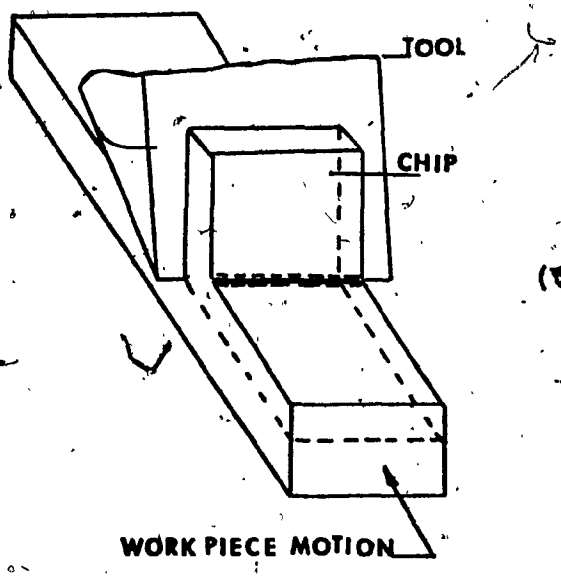

(View b)

FIG. 2.1 View of Orthogonal Cutting Edge

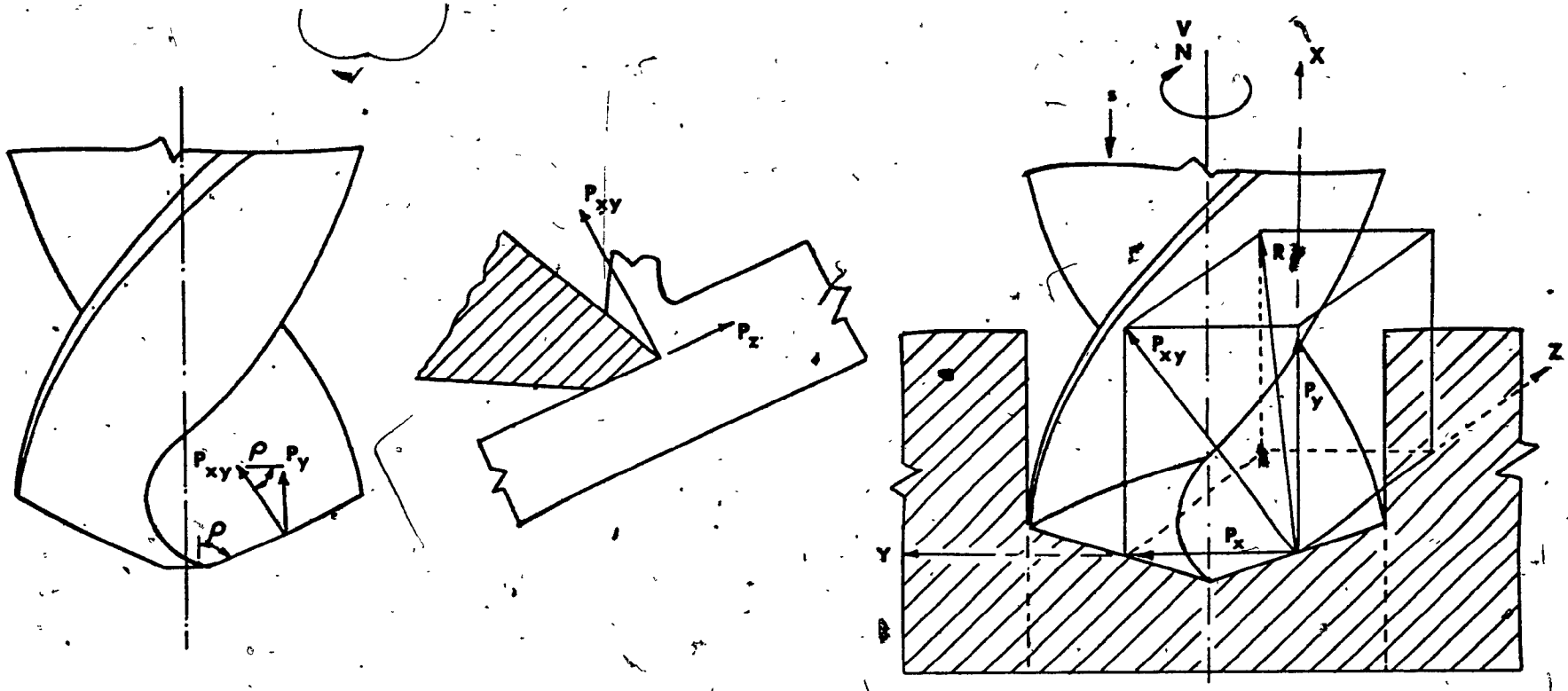

FIG. 2.2 Cutting Forces in Drilling at Cutting Edge of a Lip

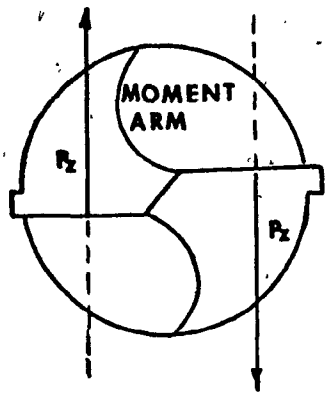

FIG. 2.3 The Cutting Action of Drill in Plan View

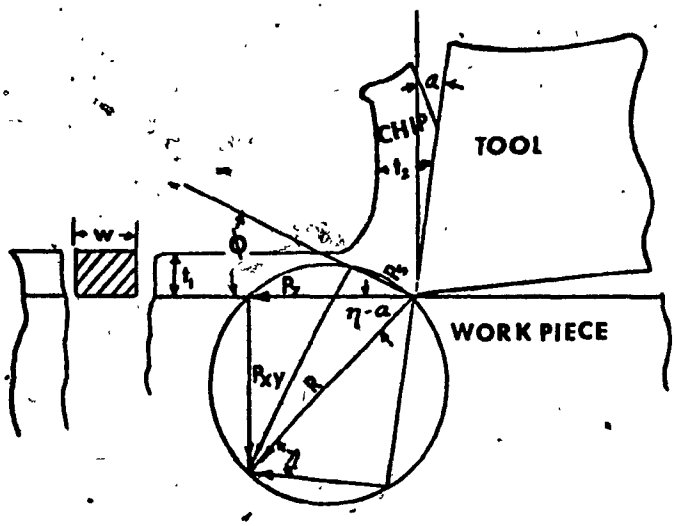

FIG. 2.4 Combined Force Diagram

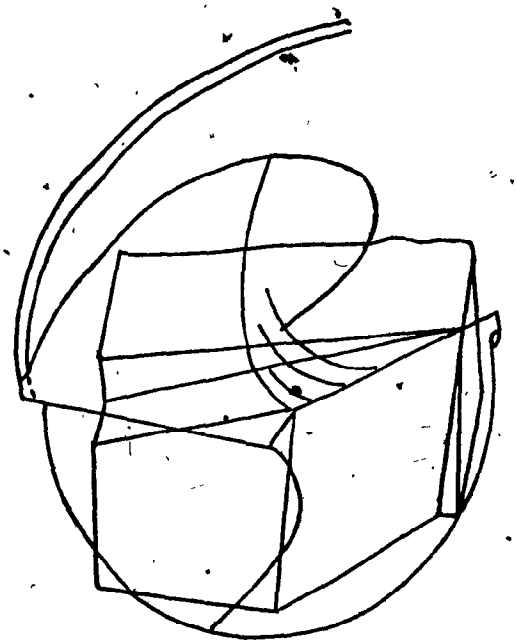

FIG. 2.6 Drill Superimposed on the Basic Turning Tool

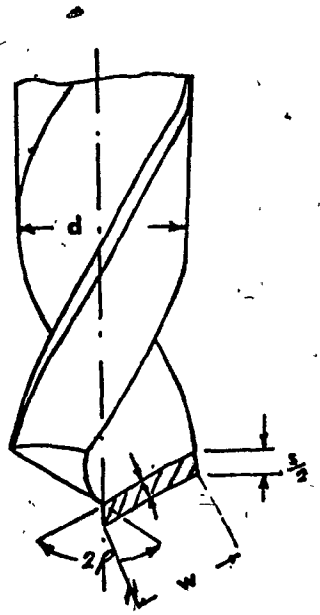

FIG. 2.5 Geometry of Chip Formation in Drilling Process

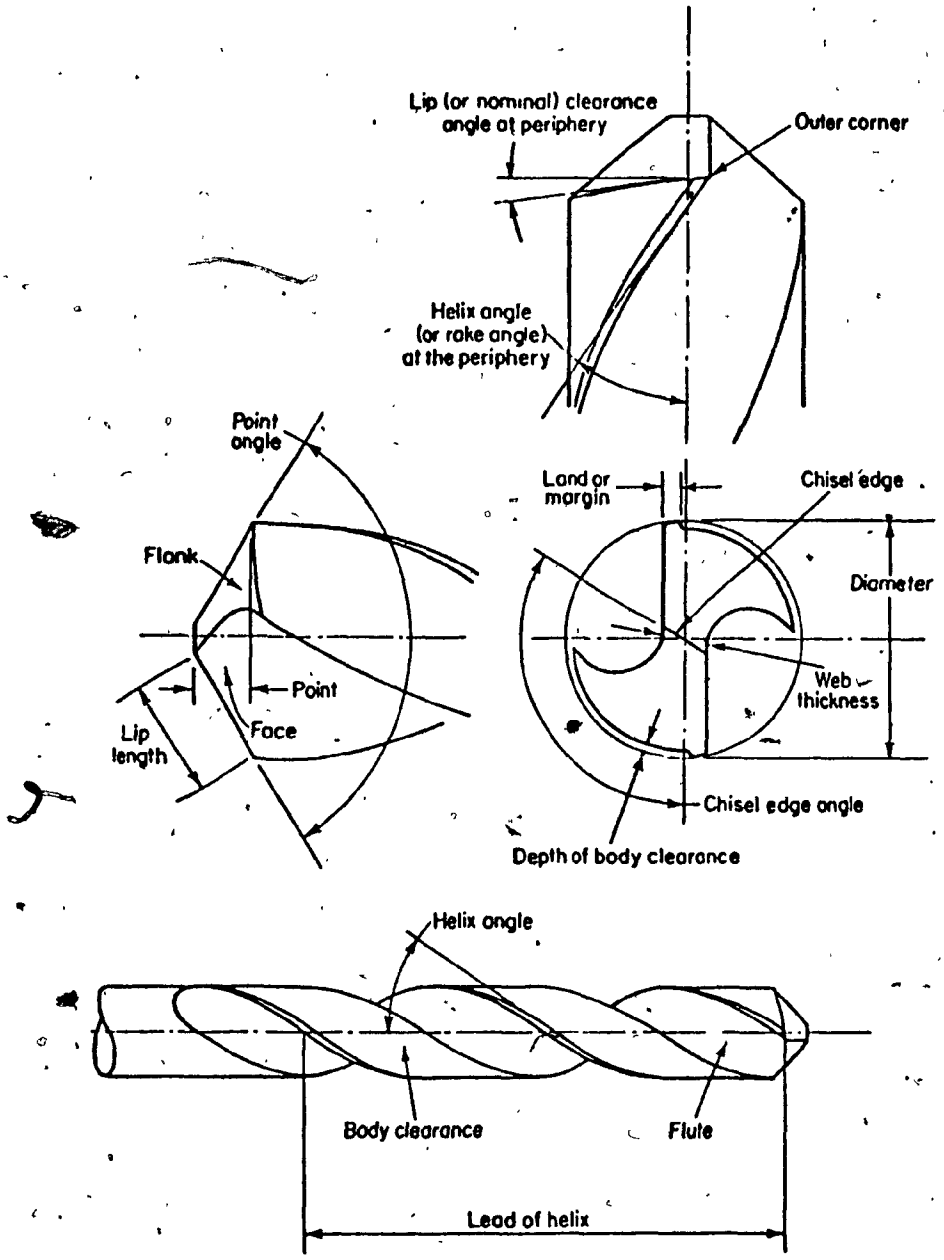

FIG. 2.7 Twist Drill Specification

CHAPTER III

MEASUREMENT OF TORQUE AND THRUST FORCE

CHAPTER III

MEASUREMENT OF TORQUE AND THRUST FORCE

Dynamometers are normally used for measurement of cutting forces in machining. In earlier stages, dynamometers were available which would measure only the static component of forces. With the advancement of technology, better measuring systems were developed which were capable of accurate measurements of the dynamic forces to make dynamic force measurement possible. A good deal of description about these systems is given in the literature. In general, there are two types of dynomometers; (i) strain gauge dynamometers more suitable for static force measurement; (ii) Piezoelectric dynamometers suitable for dynamic force measurement.

The strain gauge dynamometers have been widely used to measure cutting forces. The natural frequencies of these dynamometers are of the order of 200-1000 Hz and their response time is large. Hence, they are suitable for the measurement of steady components of forces.

For measurement of rapidly fluctuating forces, the natural frequency of the dynamometer should be far removed from the frequencies of cutting forces being measured. Under these conditions, chances of occurrence of resonance will be remote.

The piezoelectric crystal dynamometers have such characteristics and can be used for the measurement of dynamic

forces. Kistler and Micheletti [24] have developed dynamometers using piezoelectric crystals. The piezoelectric crystal systems have the following properties which are not found in other systems.

(i) The sensitivity of quartz transducers is, barring damage by mechanical overload or extreme temperature, constant for an indefinite time.

(ii) It is linear and free of hysteresis.

(iii) Only dynamic measurements are possible with a piezoelectric transducer.

It is possible to reliably measure quasi-static forces for periods of minutes to hours, the limiting factor being the drift of the amplifier and quality of insulation of the transducer cable and the input of the charge amplifier.

3.1 FORCE MEASUREMENT IN ORTHOGONAL CUTTING

In orthogonal metal cutting, analysis of the mechanics of cutting shows that there is a resultant force between the tool and chip. This force can be resolved into two components, a horizontal and a vertical static component. A strain gauge dynamometer will measure these two components.

This assumption is true only in the case where for a single force R between the tool and the chip. But, in addition to R, there is a friction force and the tool may also exert a

force directly on the surface of the workpiece. This extra force may result in a plastic deformation of the finished surface of the workpiece. Figure 3.2a shows a strain gauge dynamometer used to measure forces in orthogonal cutting.

3.2 STATIC THRUST AND TORQUE MEASUREMENT

In drilling, there are two cutting lips. The tangential component is the power component and gives rise to torque. Because of the symmetry of the two lips, the radial components cancel each other. The third component becomes the feed component or thrust component. So, in drilling, the thrust force and the torque are two obvious forces to be measured. It is convenient to mount the workpiece on the measuring platform, rather than to attempt to measure the reactions on the rotating drill. Figure 3.4 shows a two-component measuring platform.

3.3 DYNAMIC MEASUREMENTS OF THE TORQUE AND THRUST IN DRILLING

The dynamic measurement is similar to the static measurement in oblique machining. The dynamometer must be capable of measuring the rapid fluctuations of torque and thrust force. The frequency response of they dynamometer should be flat for the range of frequencies encountered in metal cutting. The sensitivity of the dynamometer should be high, so as to measure the small variations in magnitude, phase and frequency and should also be free from hysteresis. Normally, the piezoelectric crystal dynamometer exhibits these desirable character-

istics. Figures 3.2b and 3.3 show some of these types of dynamometers developed by Kistler for measurement of dynamic force fluctuations.

3.4 THE DYNAMOMETER

The piezoelectric crystal converts physical deformations into an electric field. The crystals are arranged in such a way that the point of application of the cutting force on the platform does not affect the measurements. A two component measuring platform of the Kistler type, Fig. 3.4 was used in this investigation. It has a natural frequency of 3 kHz in both directions. Figure 3.6 depicts the layout of the dynamometer used. It has the following features:

(i) A measuring cell pre-loaded between the base-plate (2) and top plate (3) with an elastic shank bolt (4).

(ii) A protective jacket (4).

(iii) A central hole protected with a steel tube (7).

The platform may be clamped at the edge of the base plate in which 6 holes are provided for that purpose. The maximum axial thrust that can be measured is of the order of 4,500 lb and the torque is of the order of 900 lb/inch.

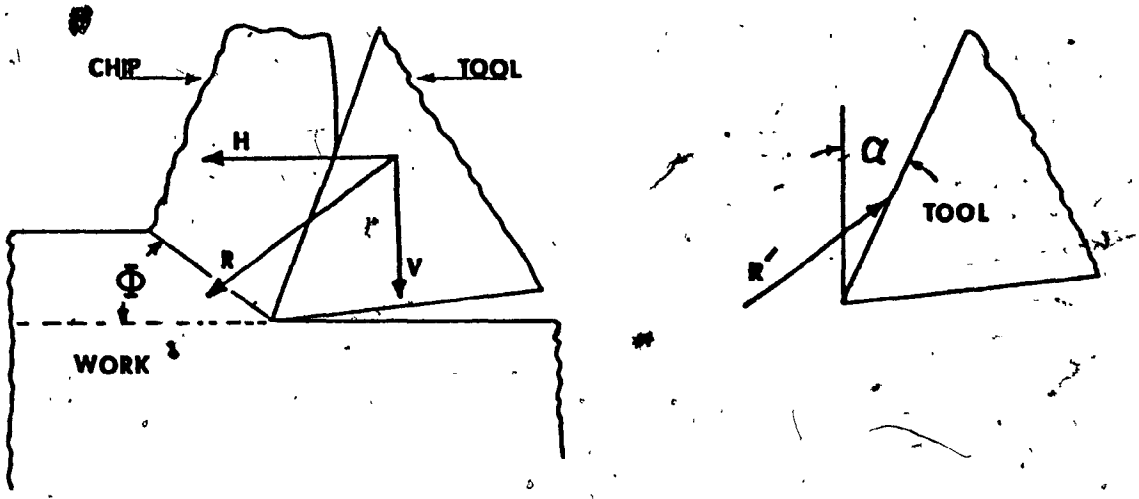

FIG. 3.1 Forces Between Tool and Work Piece

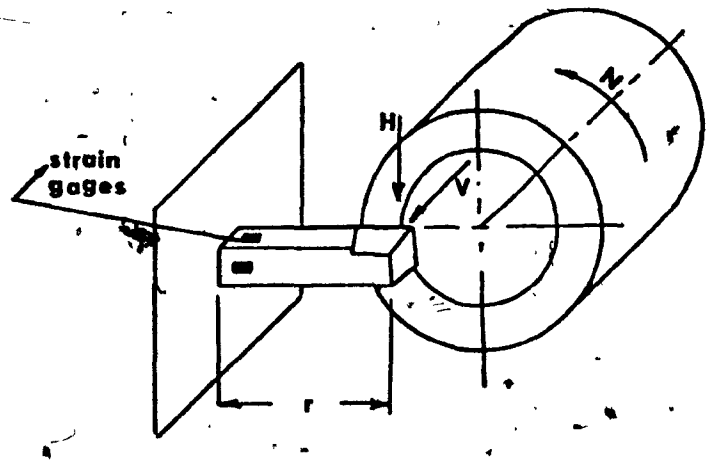

FIG. 3.2a Simple Two-Component Lathe Tool Dynamometer

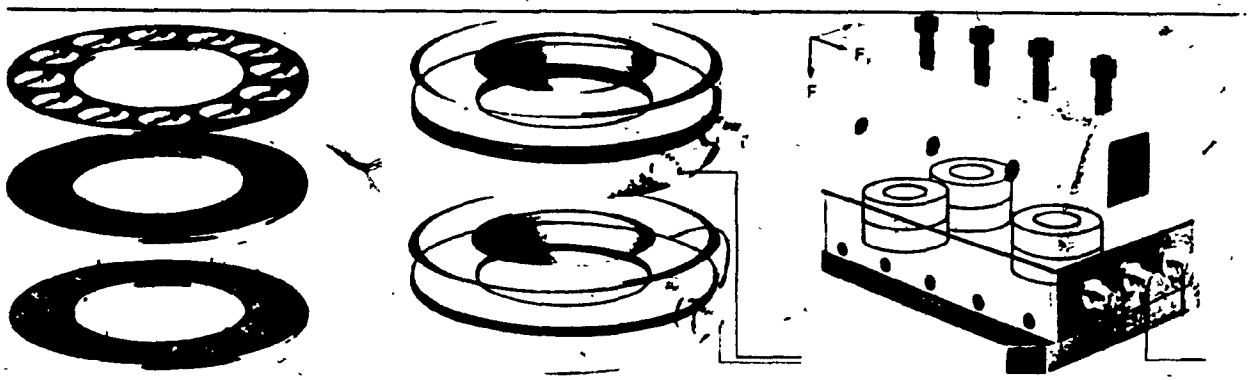

FIG. 3.2b Piezo-Electric Three-Component Dynamometer for Measuring Three Orthogonal Force Components

Maximum Measuring Range $F_x = F_y = 2200$ lbs

$F_z = 4500$ lbs

Resonant Frequency = 2.5 KHZ

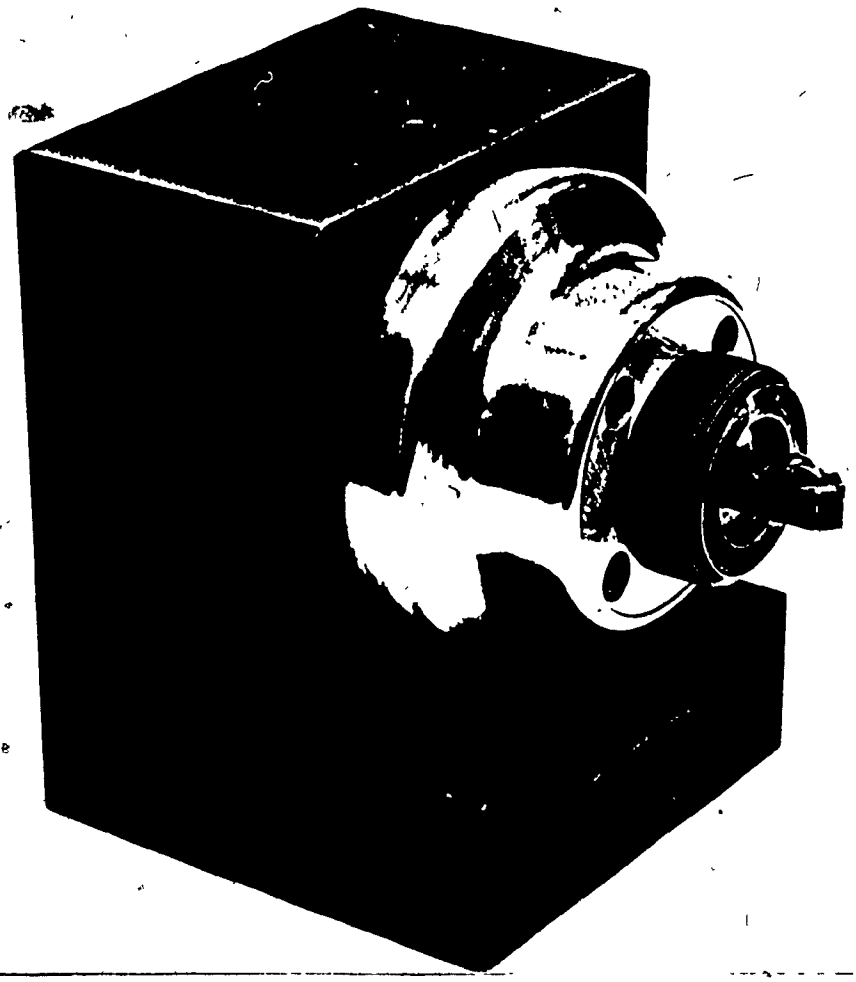

FIG. 3.3 Piezo-Electric Three Component Dynamometer for Measuring the Three-Orthogonal Force Components

Maximum Measuring Range $F_x = F_y = 1100$ lbs

$F_z = 2200$ lbs

Resonant Frequency = 10 KHZ

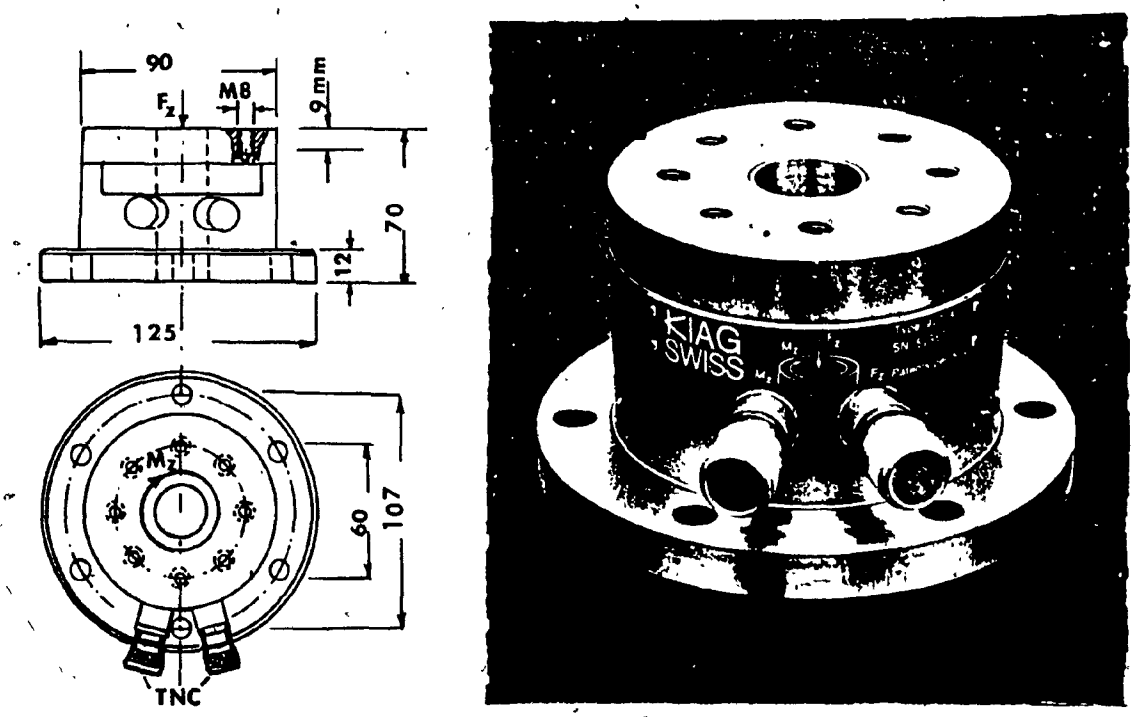

FIG. 3.4 Piezo-Electric Two-Component Measuring Platform

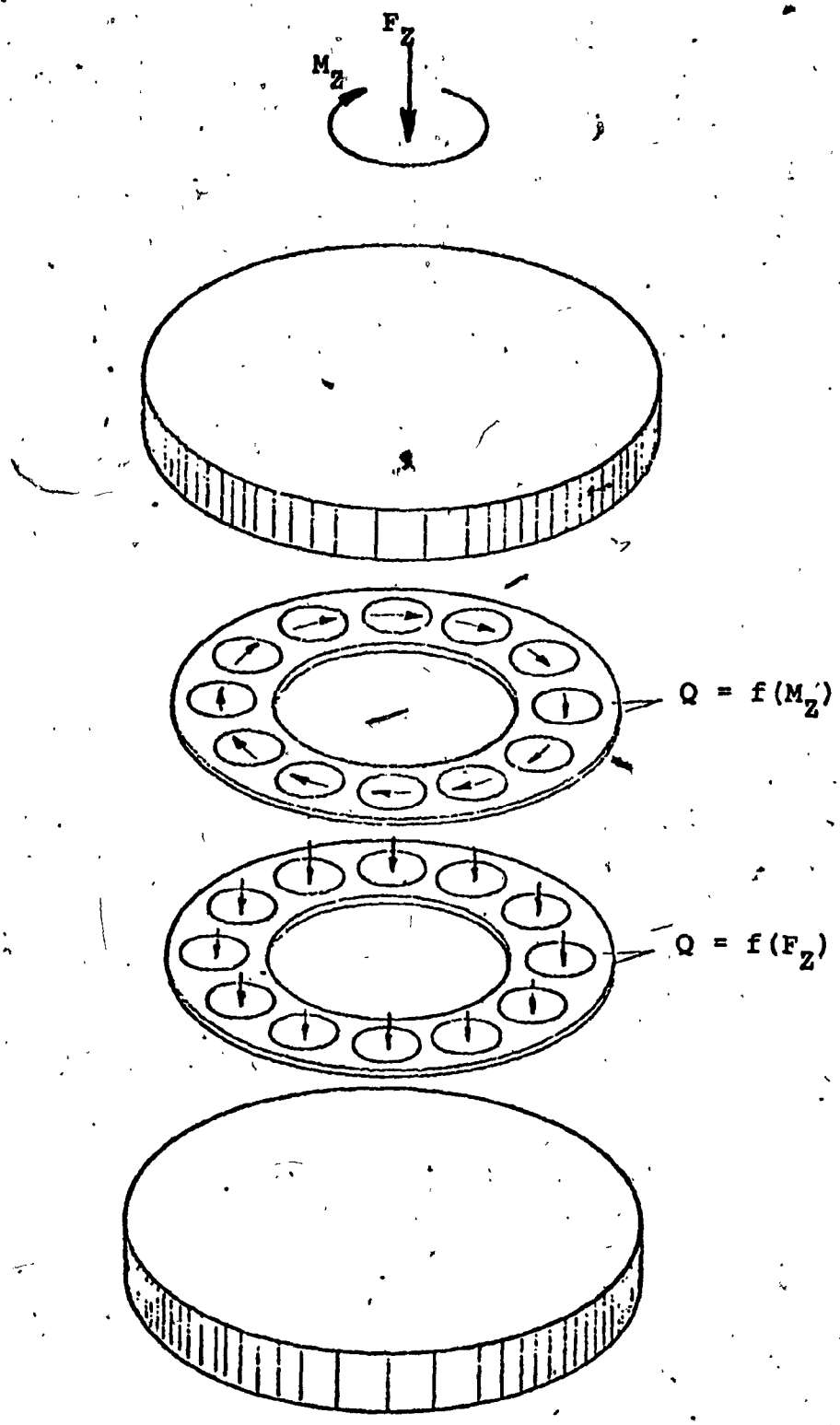

FIG. 3.5 Layout of Platform

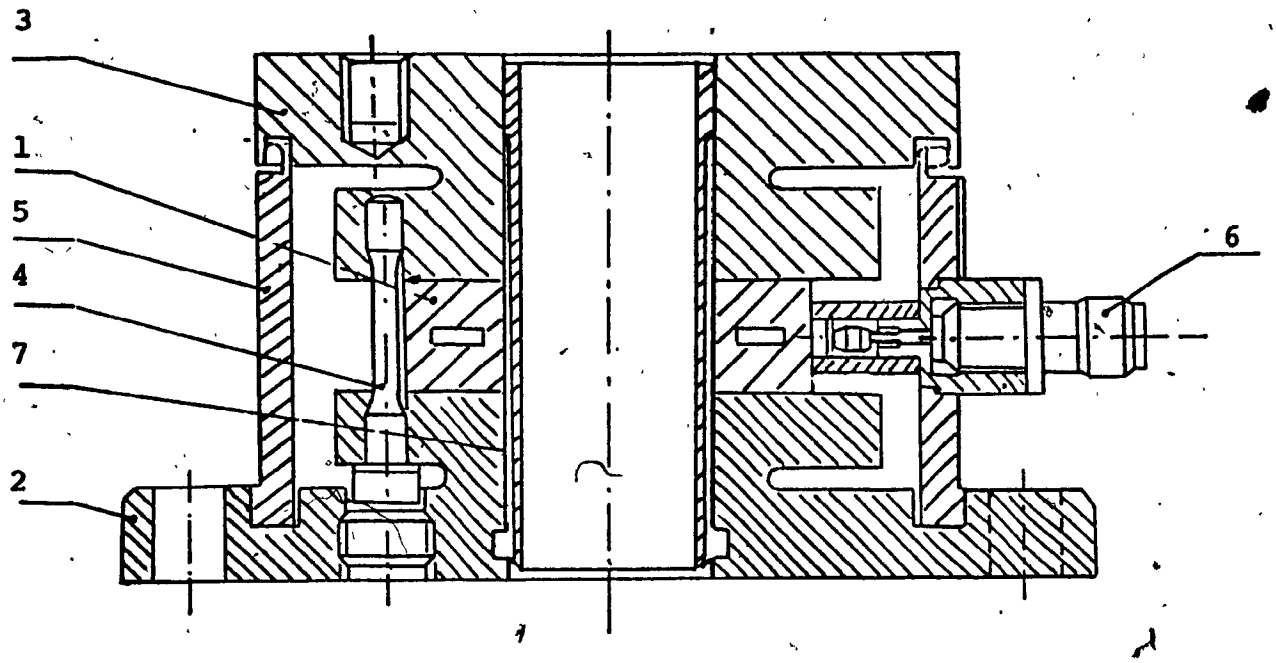

FIG. 3.6 Sectional View of Two-Component Measuring Platform

1 - measuring cell
2 - base plate
3 - top plate
4 - shank bolt
5 - jacket
6 - connecting plugs
7 - steel tube

CHAPTER IV

EXPERIMENTAL SET-UP

CHAPTER IV

EXPERIMENTAL SET-UP

The set-up used for measuring dynamic torque and thrust in drilling consists of

(i) Radial drilling equipment

(ii) Two-component measuring dynamometer

(iii) Two charge amplifiers

(iv) One cathode ray oscilloscope for observing cutting force signals

(v) A magnetic tape recorder for storing signals

The radial drilling machine is a 14HP Meuser & Co. drill unit equipped with a wide range of speeds and feeds. The main function of the charge amplifier is to convert the electrical charge from the piezoelectric crystals of the dynamometers into a proportional voltage. The function of the compensator is to cancel out the undesirable mutual interreference of the 3 independent measuring channels (only two are required for this case). The three operational amplifiers of the compensator are fed with the three force signals from the charge amplifiers. Any desired portion of the output voltage of any one channel may be tapped through a voltage divider and fed as a compensation signal to the input of the other two channels. When this is done for all components, the output from the compensator are the actual cutting forces. Fig. 4.14 shows a functional schematic diagram of the compensator.

The force signal is stored on a magnetic tape and in order to relate the signal to the actual cutting force, the dynamometer must be calibrated statically. The force fluctuations measured by the dynamometer are due to the cutting forces and vibrations of the tool due to resonance in the machine tool - dynamometer system, are excluded. A dynamic test is also required to make sure that the frequency response of the system does not have resonant points close to the frequencies of the forces to be measured.

4.1 STATIC CALIBRATION OF THE DYNAMOMETER IN THE THRUST DIRECTION

Figure 4.1 indicates a block diagram for the static calibration of the dynamometer. The load is increased in steps, and is measured by a force transducer placed between the load and the workpiece. The electric charge produced by the dynamometer is given by:

$$Q = CV$$

Q = charge in pico-coulombs

V = voltage read on oscilloscope-volts

C = gain set on charge amplifier.

For a static calibration of the dynamometer in the F_z direction, the dynamometer was fixed to the machine base. A force transducer was then introduced between the dead load and the dynamometer. The charge from the dynamometer was then converted into a proportional voltage through the Kistler charge

amplifiers, and with application of dead load the proportional voltage was displayed on the oscilloscope. In order to ensure that any form of hysteresis is totally avoided, the loading was increased in steps up to a maximum and then decreased down to zero. The loading and unloading curves were drawn as a function of the charge. A plot of the load versus the charge is shown in Figure 4.7. It may be seen that the curve is linear and hysteresis is not present for the range covered by this investigation.

4.2 STATIC CALIBRATION OF THE DYNAMOMETER IN THE TORQUE DIRECTION

The two-component measuring cells have two sets each comprising of 12 quartz discs arranged circumferentially. Twelve of them respond to the load in the axial direction. They are paralleled electrically and add up the charge proportional to the load. The other set of 12 discs is also arranged circumferentially, but the discs are sensitive to shear. Since they are paralleled in a shear direction, they add up the charge proportional to the torque, Figure 3.5. There may be a cross-sensitivity, but that is eliminated by the use of the compensator.

In order to apply a pure torque, a mechanical lever was welded to a steelplate and the plate was screwed rigidly to the dynamometer. In applying the load to the lever, a special fixture comprising a power nut and screw was made. A Kistler

force transducer which had been calibrated statically, was used as an input force monitoring device. A schematic diagram of the set-up is shown in Figure 4.2 . The output from the dynamometer was displayed on an oscilloscope. The load on the lever was increased step by step, within the range of the dynamometer and then decreased to zero to determine the effect of hysteresis. The force should be perpendicular to the lever arm for the resultant pure torque. As the screw is advanced and the point of load application changes, the line of action of the load may not be perpendicular to the lever. To observe this effect, a dial gauge indicator was attached to the other end of the lever. It was then observed that for the maximum load applied, the maximum deflection was only 0.075" and this deviation does not influence significantly the accuracy of the calibration. A plot of the torque and charge is shown in Figure 4.8. It may be noted that there was no hysteresis present. A photograph of the set-up is shown in Figure 4.15.

4.3 DYNAMIC CALIBRATION

The main purpose here is to establish:

(i) The natural frequencies of the tool dynomometer system along the main cutting direction; and

(ii) whether there is any cross interference between the natural frequencies of the test

set-up and the dominant frequencies of cutting forces to be measured.

For the purpose of finding the natural frequency of the dynamometer, the impulse load method was employed. A steel ball is dropped on the dynamometer and the number of oscillations per second is read on an oscilloscope. The natural frequencies along the axial thrust axis and torque axis are then determined.

The natural frequencies in both directions are found to be greater than 3 kHz. To find the frequency response of the dynamometer and workpiece as well as the machine tool system, a dynamic load was applied at the drill point and kept constant by a feedback loop controlling the Bruel and Kjaer exciter. A diagram of set-up is shown in Fig. 4.3 and a pictorial view in Fig. 4.16. The frequency of the input load was varied from 20 Hz to 4 kHz and the output was observed on an oscilloscope and also recorded on a Bruel and Kjaer Level Recorder 2305. The plot of the output-to-input at different exciting frequencies is shown in Figures 4.9 and 4.10. The dynamometer system, together with machine tool and work piece, shows a resonance at about 1500 Hz. The dynamometer and work piece system shows a resonance at about 2500 Hz. The reduction in resonant frequency clearly indicates the effect of the added masses on the frequency response of the system. Similarly, frequency responses of the system are determined

for the torque direction. The plot of such a response is shown in Figure 4.11.

4.4 ACCURACY OF THE DRILLING TORQUE AND THRUST MEASUREMENTS

In order to obtain an accurate reading of the dynamic variation of the torque and thrust, a steady state component was measured separately from the superimposed fluctuating component. The steady state component was measured by setting the time constant on the charge amplifiers to "long" which in turn, changes the time constant of the measuring system to a high value. After the steady state component has been measured, the charge amplifiers are switched to the "reset" position. After changing to a more sensitive range and the time constant "short", the amplifiers are switched to its operate mode again. This has the effect of shifting the output steady signal to zero and enabling the recording a small variations to be accomplished into greater degree of accuracy. A line diagram, showing the effect of resetting the charge amplifier to a more sensitive range, is presented in Figure 4.12.

4.5 TORQUE AND THRUST MEASUREMENTS

The equipment used for conducting the test is essentially divided into two groups. One group consists of the dynamometer, the drill, the test piece and the radial drilling machine. The second group consists of the electronic instrumentation necessary to measure and record the dynamic signals.

A photograph of the set-up is shown in Figure 4.17. The following cutting conditions were chosen:

Machine:	14 HP Radial drilling machine - MEUSER & CO model
Testpiece:	AISI 1020 steel HB 106
Drill:	as shown in Figure 4.13
Cutting Speed and Feed:	Table 4.1

A series of drilling tests were performed for each feed selected. For three different feeds, photographs of signals were taken by mounting a camera on the oscilloscope. The signals were also recorded on a magnetic tape recorder (Bruel & Kjaer model) and were analyzed as explained in the following Chapter. A constant recording speed of 15 in/sec. was used in all data acquisition runs. Photographs of the signals show that these vary rapidly with time and appear to be random in nature.

4.6 ANALYSIS OF STEADY STATIC TORQUE AND THRUST FORCE

Shaw and Oxford [5] applied dimensional analysis to drilling operation and conducted a number of experiments, using different drill diameters and feeds on steels below 250 H_B hardness number. They showed that torque and thrust depends upon the hardness number and ratio of chisel-edge length to drill diameter. The steady state thrust and torque

required by the drill, may be computed from the semi-analytical equations given below [5].

$$\frac{F_z}{d^2 H_B} = 0.15 \frac{f^{0.8}}{d^{1.2}} \left[\frac{1-c/d}{(1+c/d)^{0.2}} + 2.2\left(\frac{c}{d}\right)^{0.8}\right] + 0.068(c/d)^2$$

$$\frac{M_z}{d^3 H_B} = 0.082 \frac{f^{0.8}}{d^{1.2}} \left[\frac{1 - \left(\frac{c}{d}\right)^2}{\left(1 + \frac{c}{d}\right)^{0.2}} + 3.2\left(\frac{c}{d}\right)^{1.8}\right]$$

where

$$\frac{c}{d} = \frac{\text{Length of chisel-edge}}{\text{Diameter of drill}}$$

H_B = Brinell hardness, psi

f = feed in inch/rev.

d = diameter of drill, inches

In this investigation, AISI 1020 steel was used. The hardness was found on Rockwell Hardness Tester using a scale with 60 kg load and it was found to be 42.

Equivalent $H_B = 106$

$$\frac{c}{d} = 0.105$$

With these substitutions in the above equations

$$F_z = H_B \left[0.186\ f^{0.8}\ d^{0.8} + 0.00075\ d^2\right] \text{ lbs}$$

$$M_z = H_B\ 0.084\ f^{0.8}\ d^{1.8} \text{ lb-inch.}$$

From these equations, thrust and torque were calculated for the three different feeds and the results are tabulated in Table 4.2.

The steady state measurement of torque and thrust were made on an oscilloscope. Because the duration of the signal was not quite long, there could be a slight error in the observation of the signals. In the third cut, measured values are quite lower than the calculated ones. This is partially due to the regrinding of the drill before the third cut was started.

From Table 4.2, it is clear that there is a good correlation between the steady state values given by the equations and those measured in the experimental set-up.

T: force transducer
DYN: dynamometer
CA: charge amplifier
COMP: compensator
CRO: cathode ray oscilloscope
DW: dead weight

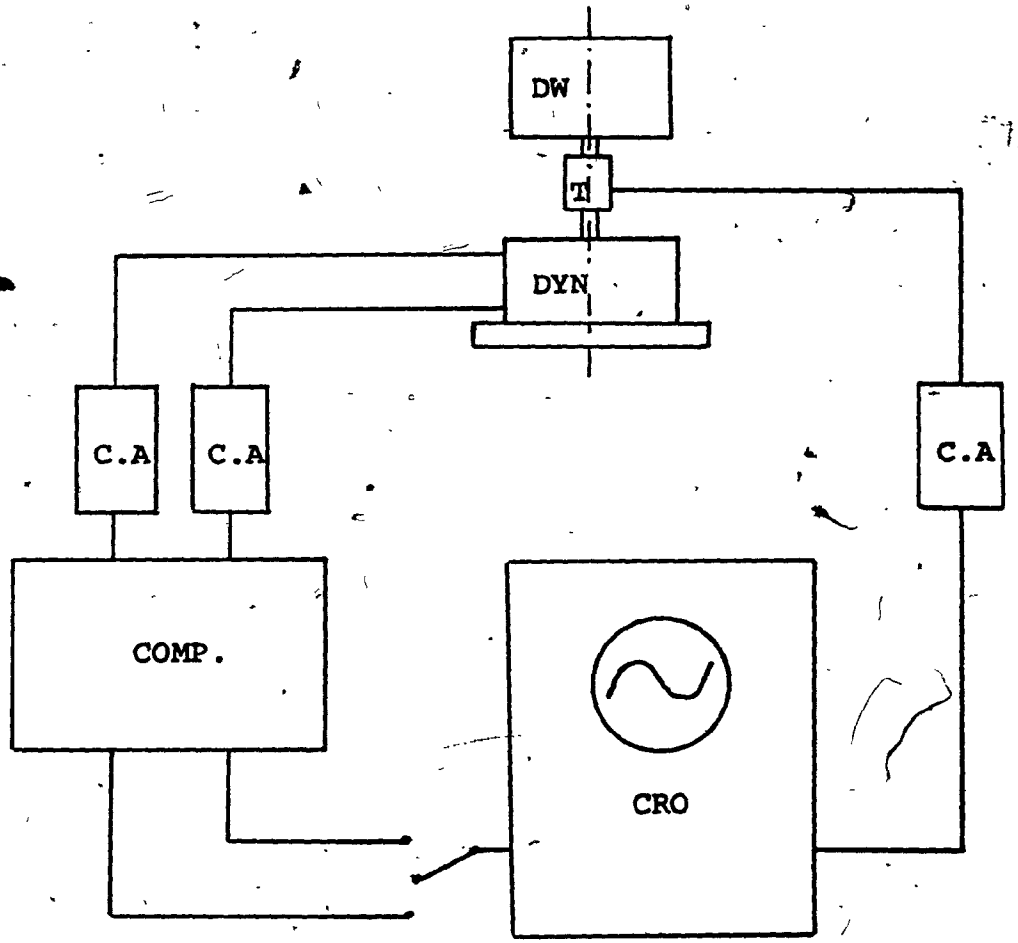

FIG. 4.1 Schematic Diagram of the Set-up for Static Calibration of Dynamometer

G: dial indicator
DYN: dynamometer
T: force transducer
CA: charge amplifier
COMP: compensator
CRO: Cathode ray oscilloscope
F: nut and screw fixture

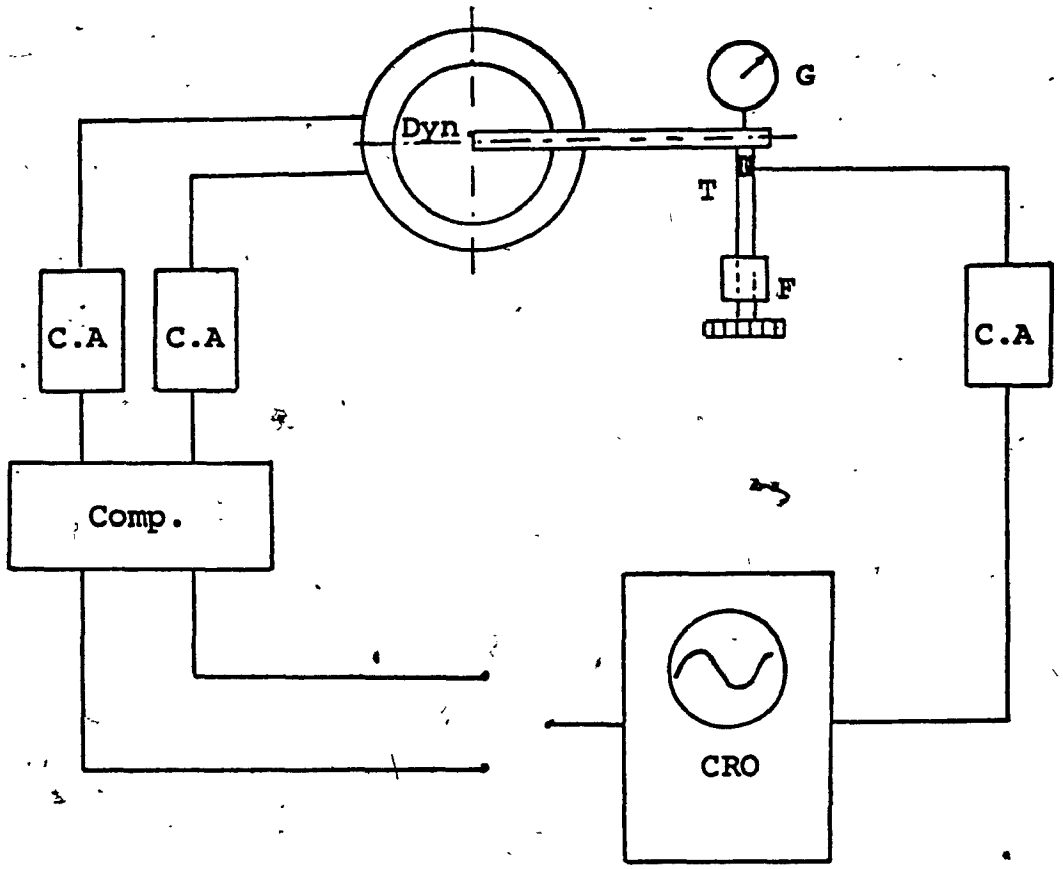

FIG. 4.2 Block Diagram for Static Calibration of Dynamometer for Torque

PA: Power amplifier
T: force transducer
WP: work piece
DYN: dynamometer
CA: charge amplifier
COMP: compensator
CRO: cathode ray oscilloscope
FA: frequency analyzer
LR: level recorder

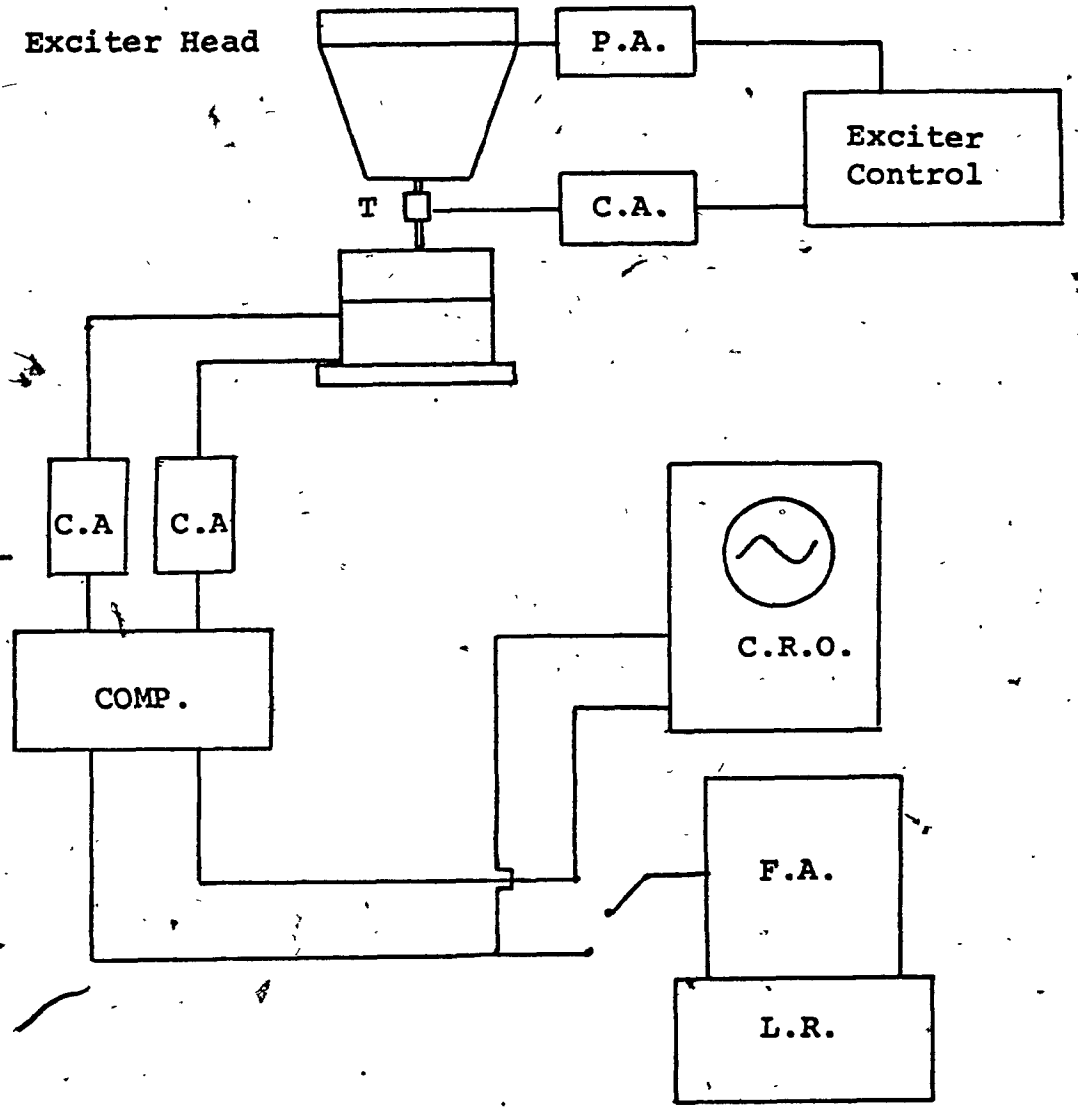

FIG. 4.3 Schematic Set-Up for Dynamic Calibration

WP: work piece
CA: charge amplifier
COMP: compensator
MTR: magnetic tape recorder
CRO: cathode ray oscilloscope

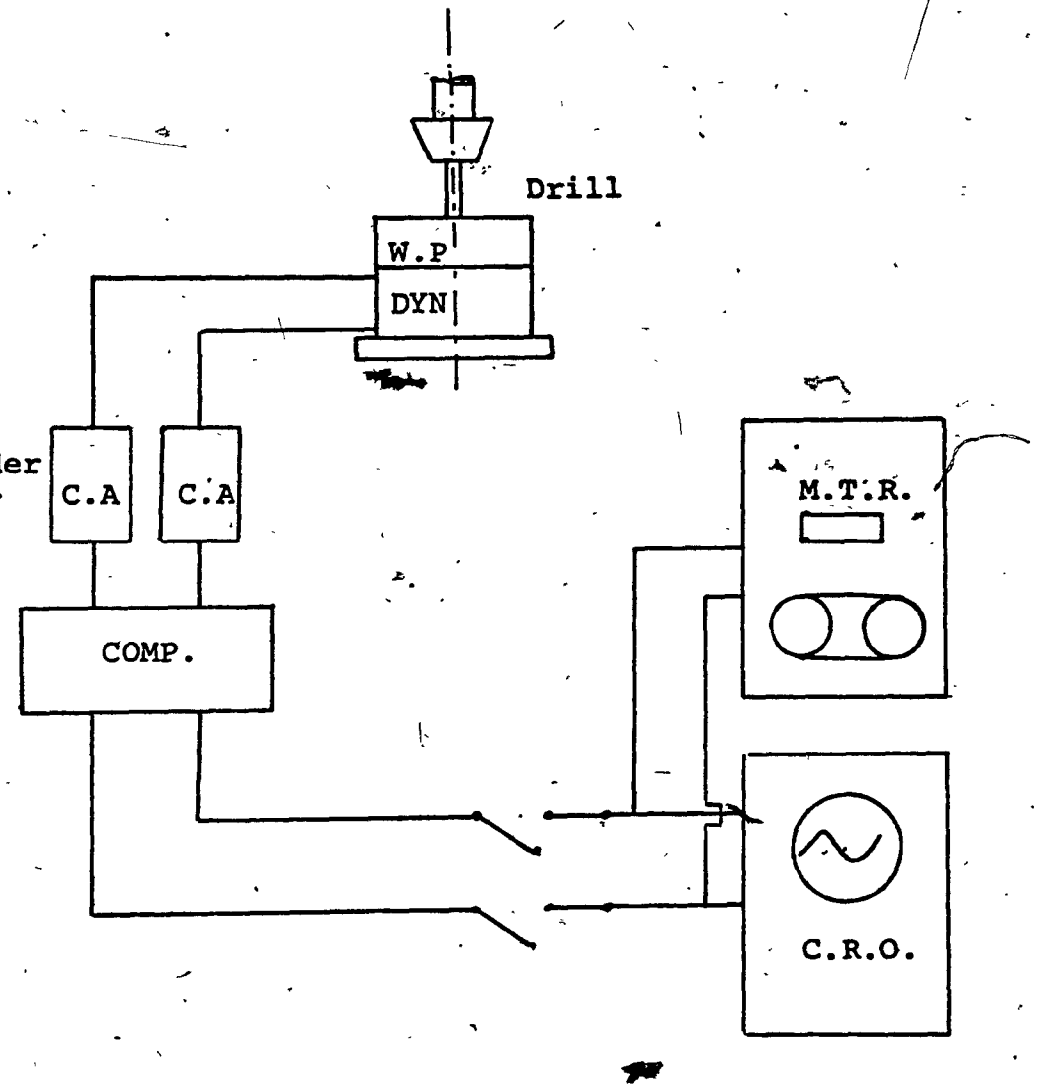

FIG. 4.4 Block Diagram for Dynamic Measurement of Thrust and Torque

TORQUE COMPONENT M_z

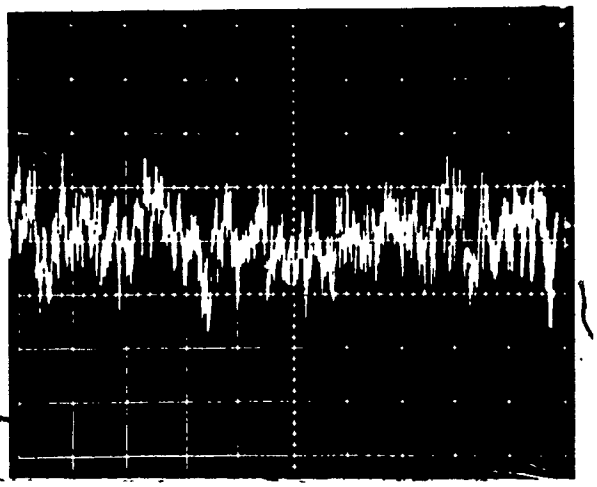

feed 0.0028"/Rev
Static Torque 15 lb-inch
2 lb-inch
0.1 sec

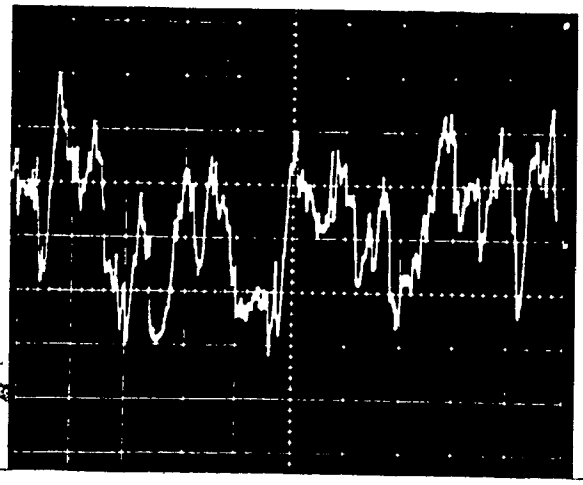

feed 0.007"
Static Torque 34 lb-inch
4 lb-inch
50 m sec

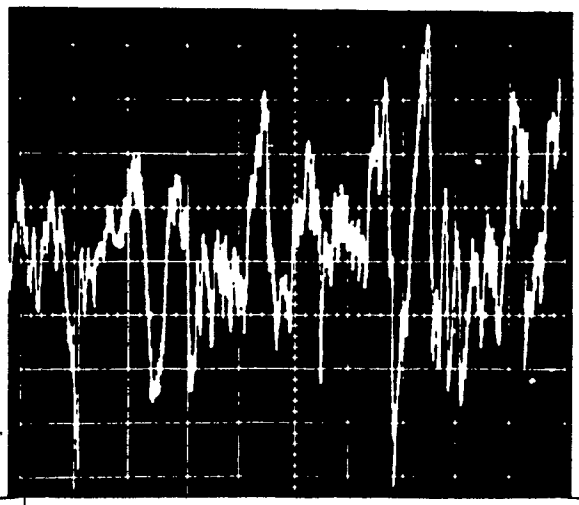

feed 0.0112"
Static Torque 45 lb-inch
5 lb-inch
50 m sec

FIG. 4.5 Fluctuations of Torque Component While Drilling

THRUST COMPONENT F_z

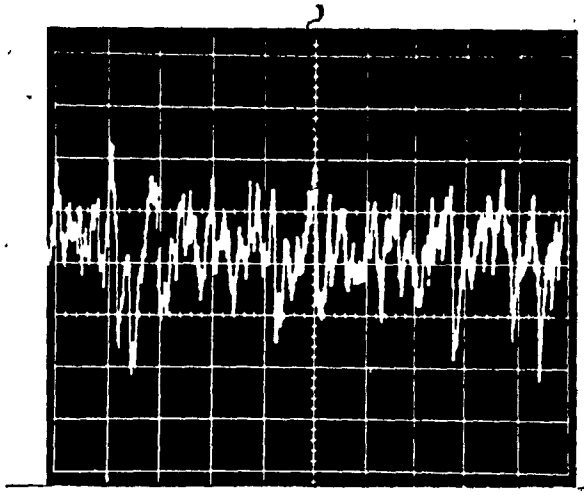

feed 0.0028"/Rev
Static Thrust 100 lbs
10 lbs
50 m sec

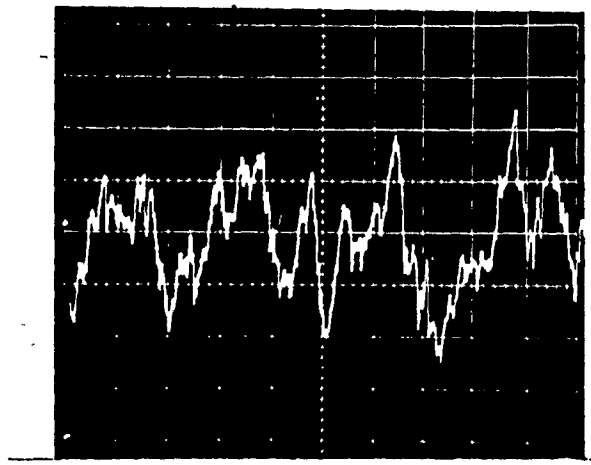

feed 0.007"
Static Thrust 250 lbs
20 lbs
20 m sec

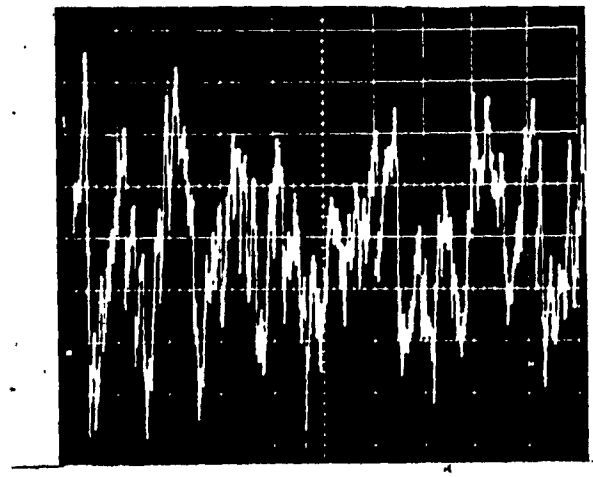

feed 0.0112"
Static Thrust 320 lbs
25 lbs
50 m sec

FIG. 4.6 Fluctuations of Thrust Component While Drilling

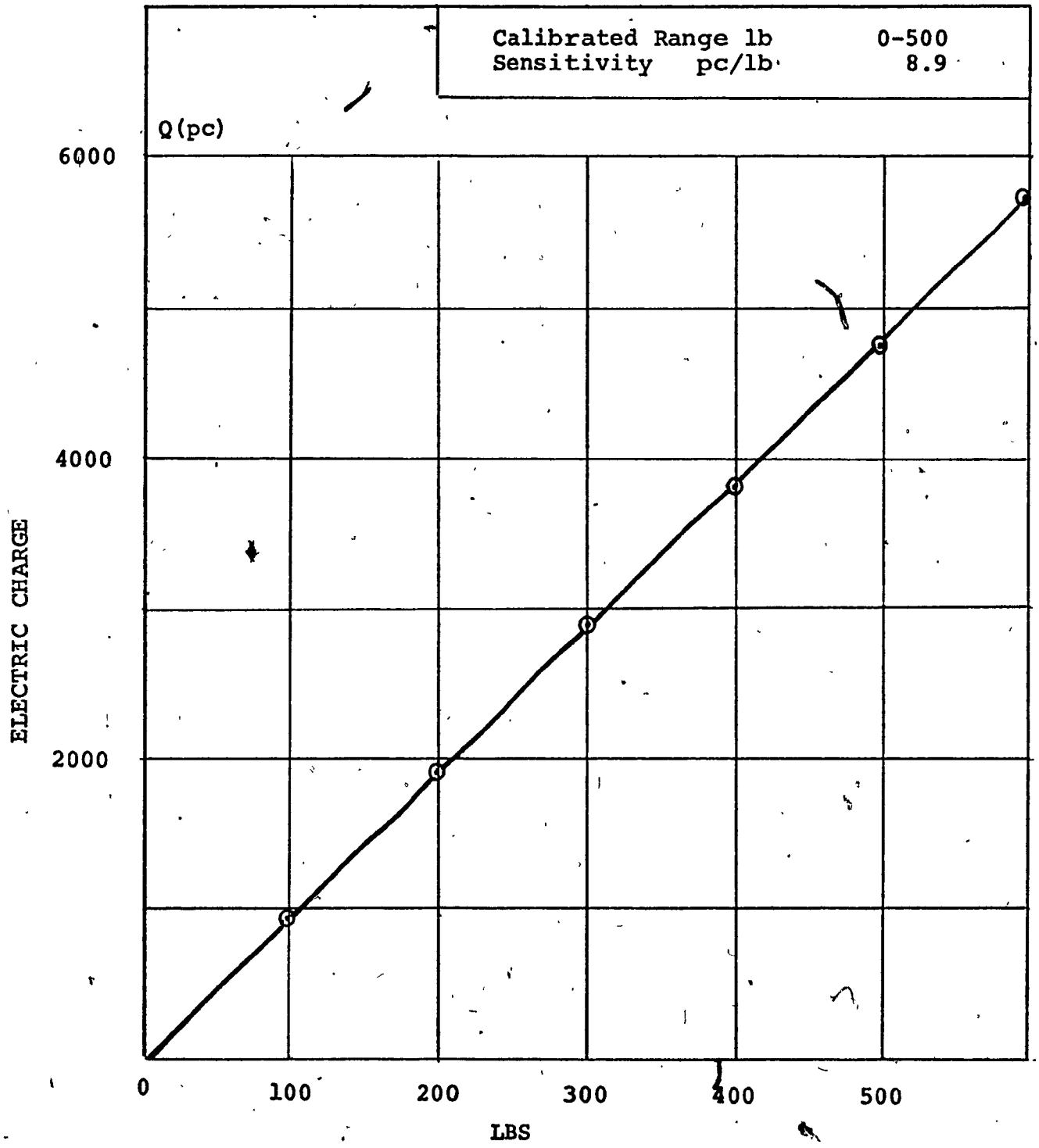

FIG. 4.7 Static Calibration for Two Component Piezoelectric Dynamometer for Thrust

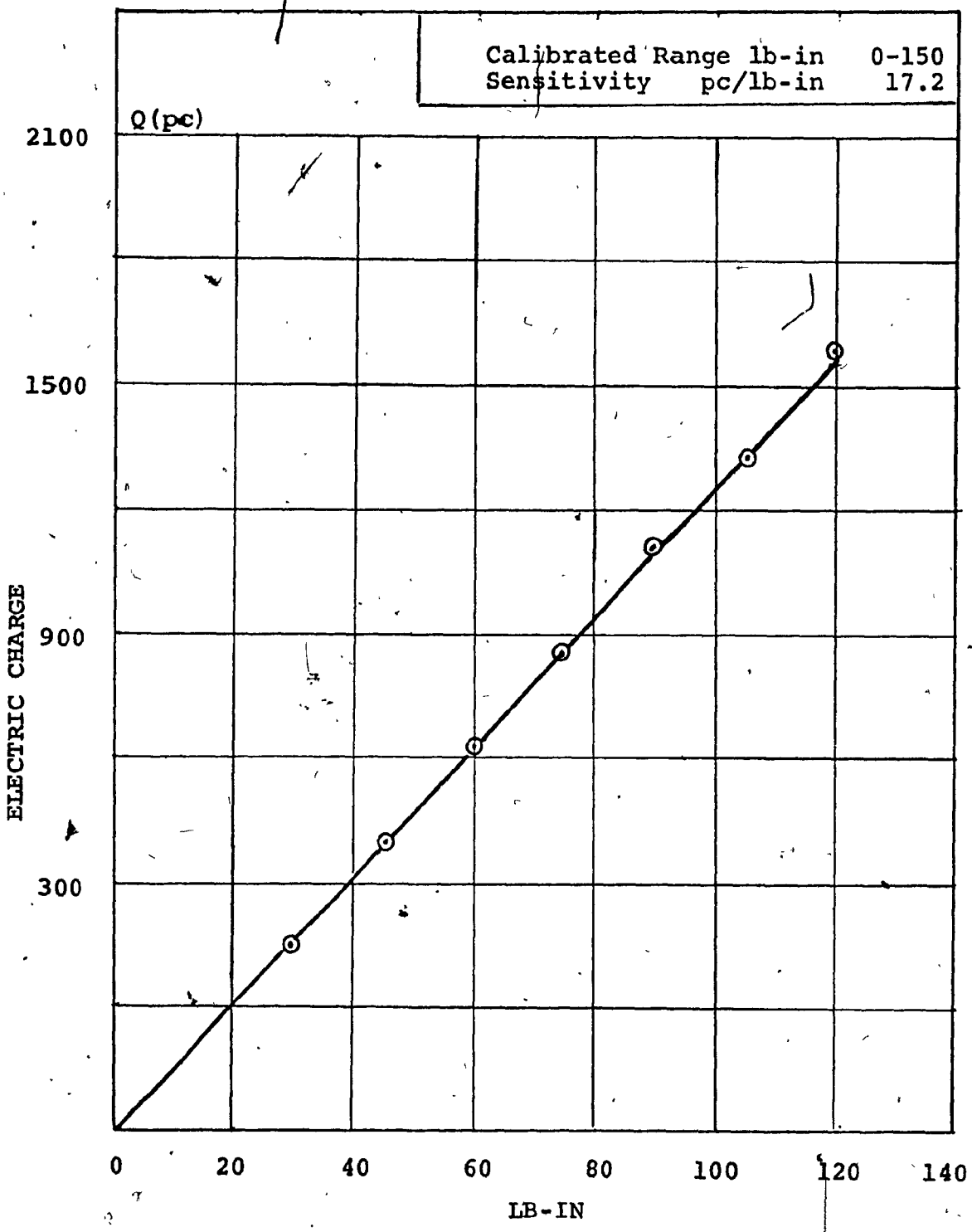

FIG. 4.8 Static Calibration for Two Component Piezoelectric Dynamometer for Torque

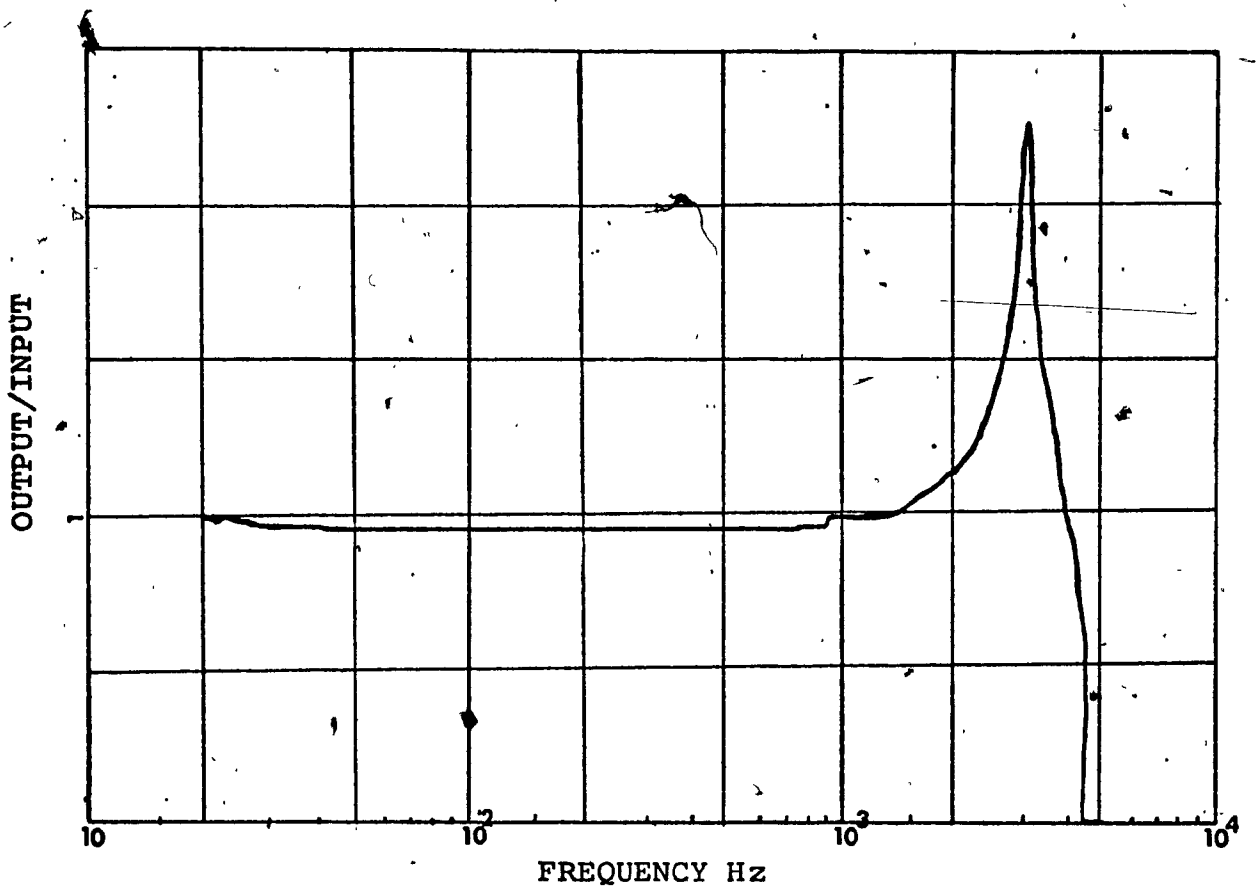

FIG. 4.9 Frequency Response of Dynamometer-Workpiece System in F_z Direction

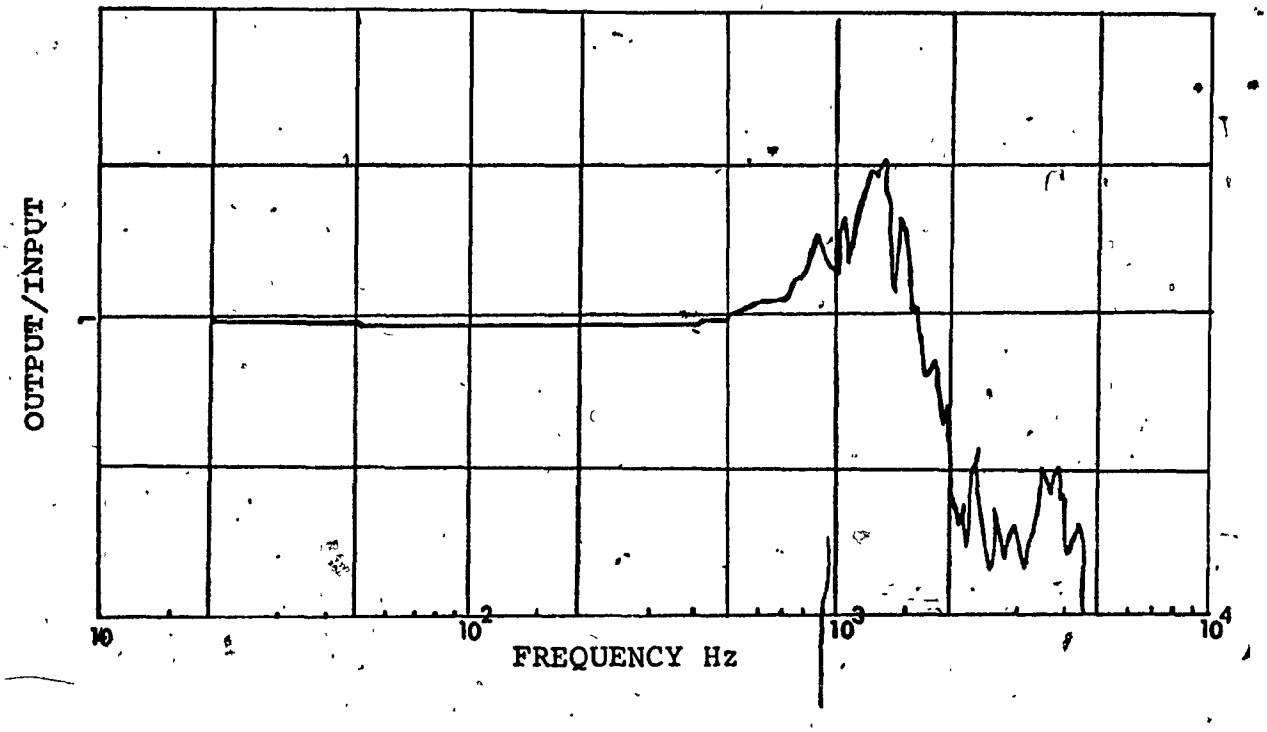

FIG. 4.10 Frequency Response of Drilling Machine-Workpiece-Dynamometer System in F_z Direction

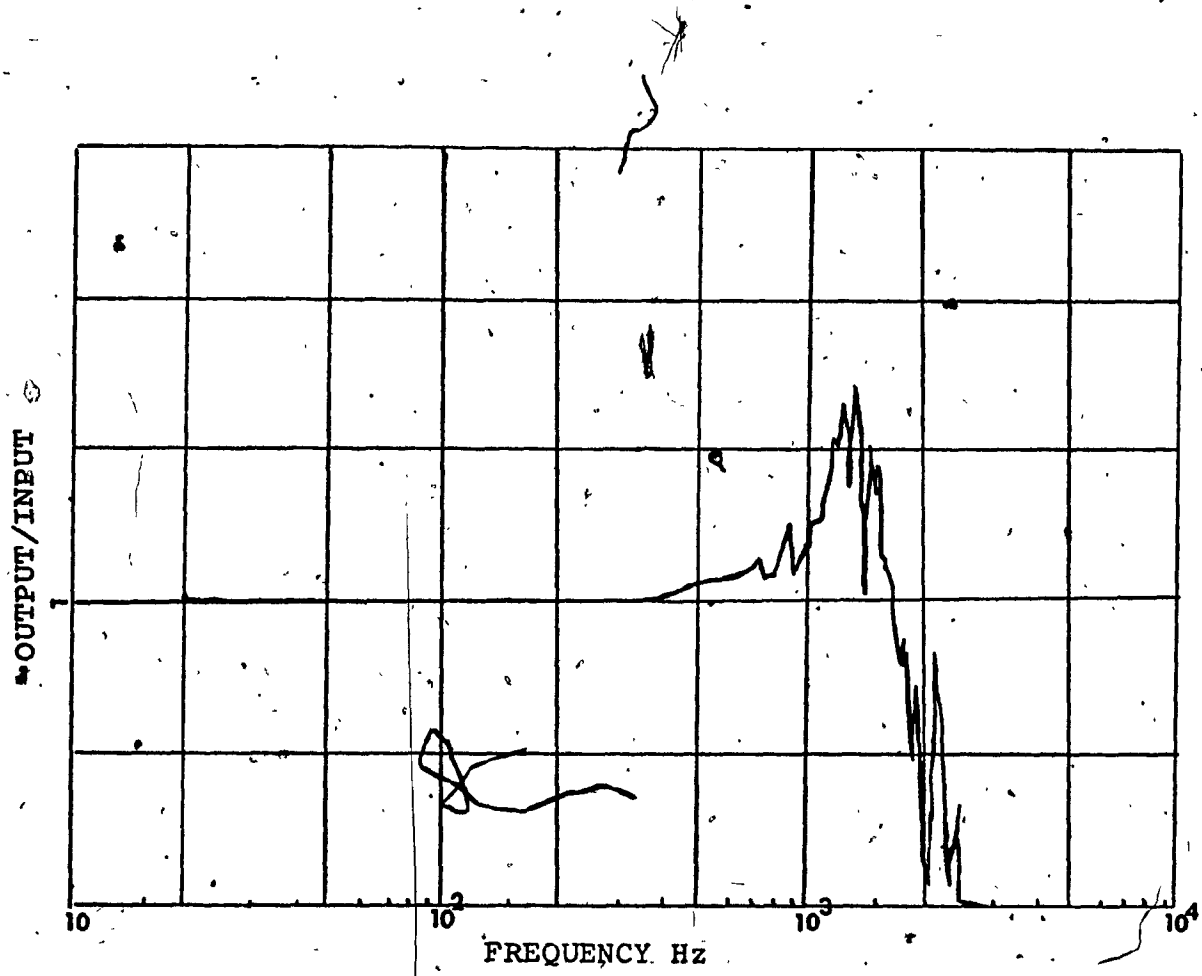

FIG. 4.11 Frequency Response of Drilling Machine-Workpiece-Dynamometer System in M_z Direction

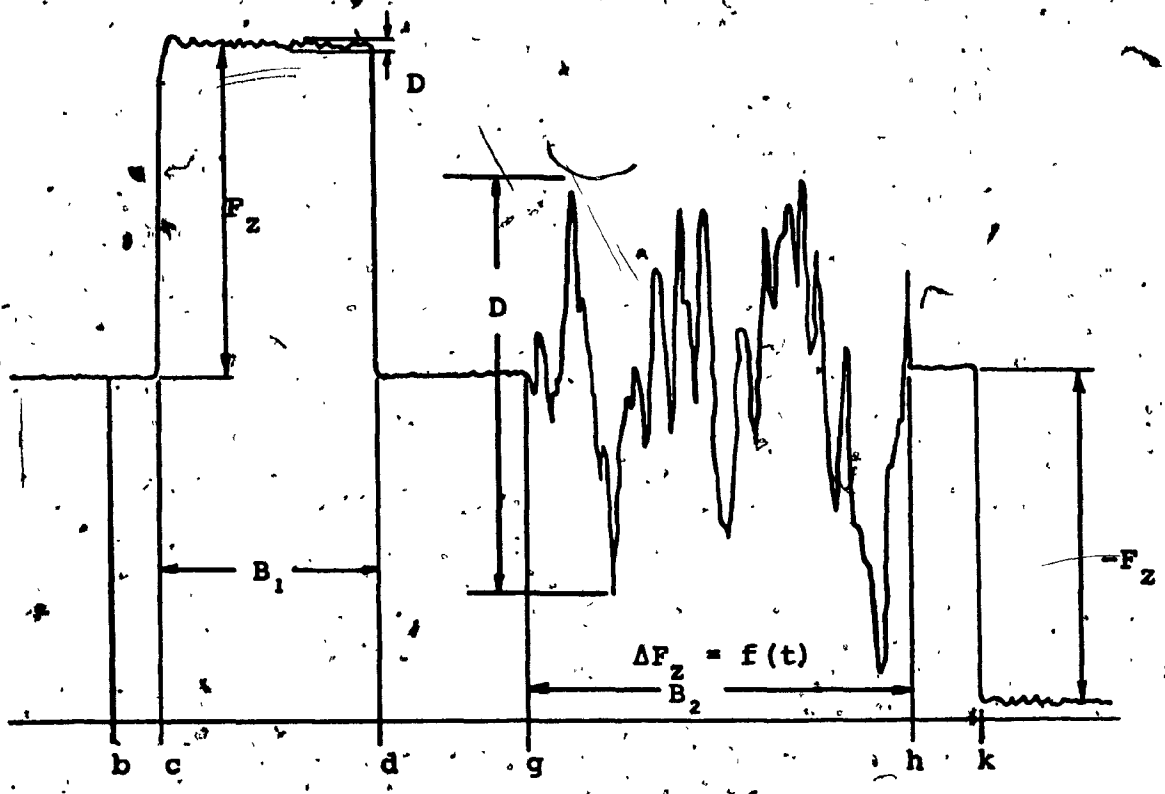

c = F_z is applied

B_1 = Range 1 (1000 lb/v)

B_2 = Range 2 (100 lb/v)

F_z = static force

D = dynamic fluctuations

d = amplifier reset

g = amplifier to operate

FIG. 4.12 Diagram Showing the Effect of Resetting Charge Amplifier to Higher Sensitivity

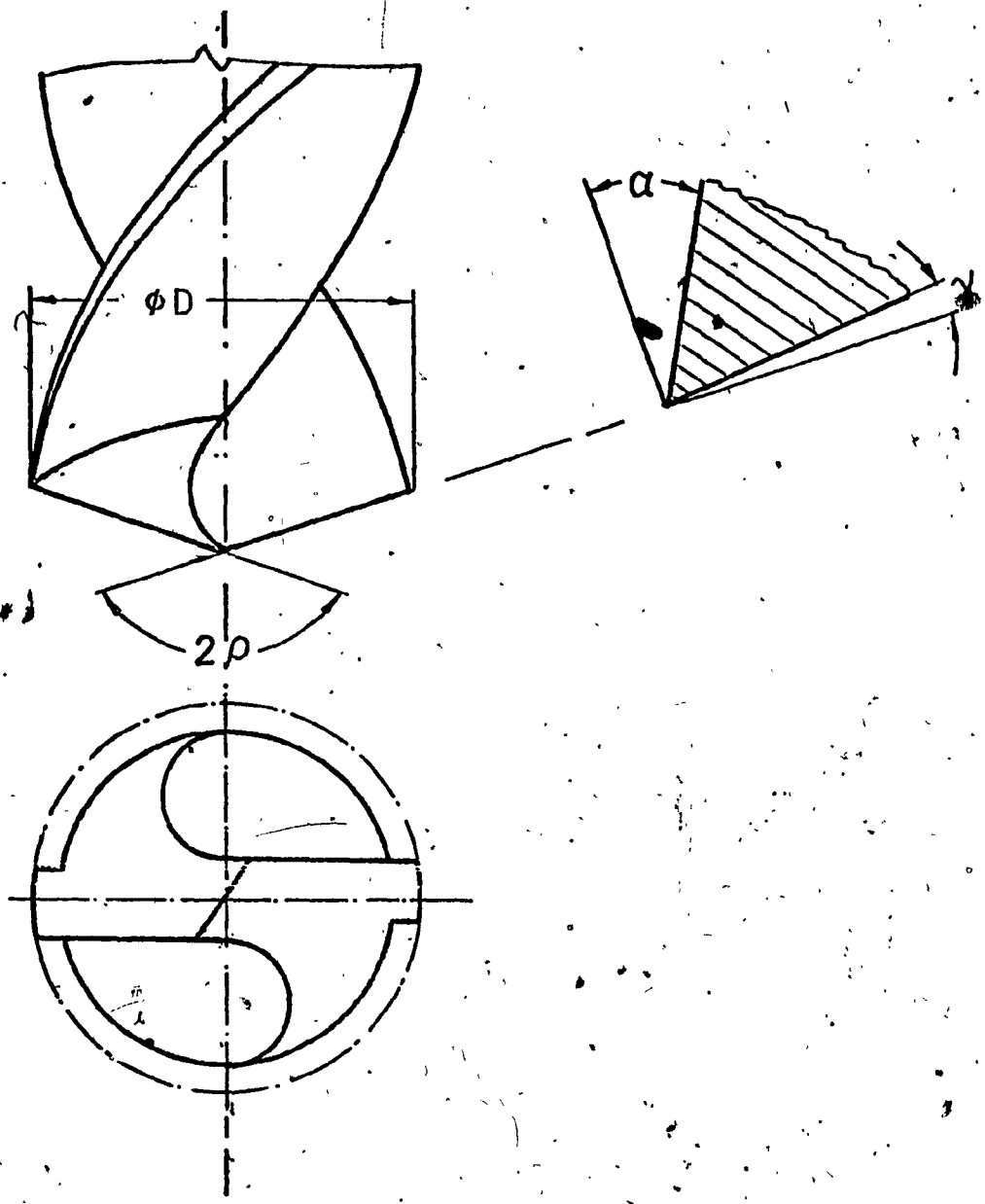

α (Helix Angle) = 30°

2ρ (Point Angle) =116°

φ (Rake Angle) = 30°

ν (Relief Angle) = 7°

D (Diameter of Drill) = 3/8"

FIG. 4.13 Tool Material and Tool Geometry Used in Drilling. Material = High Speed Steel

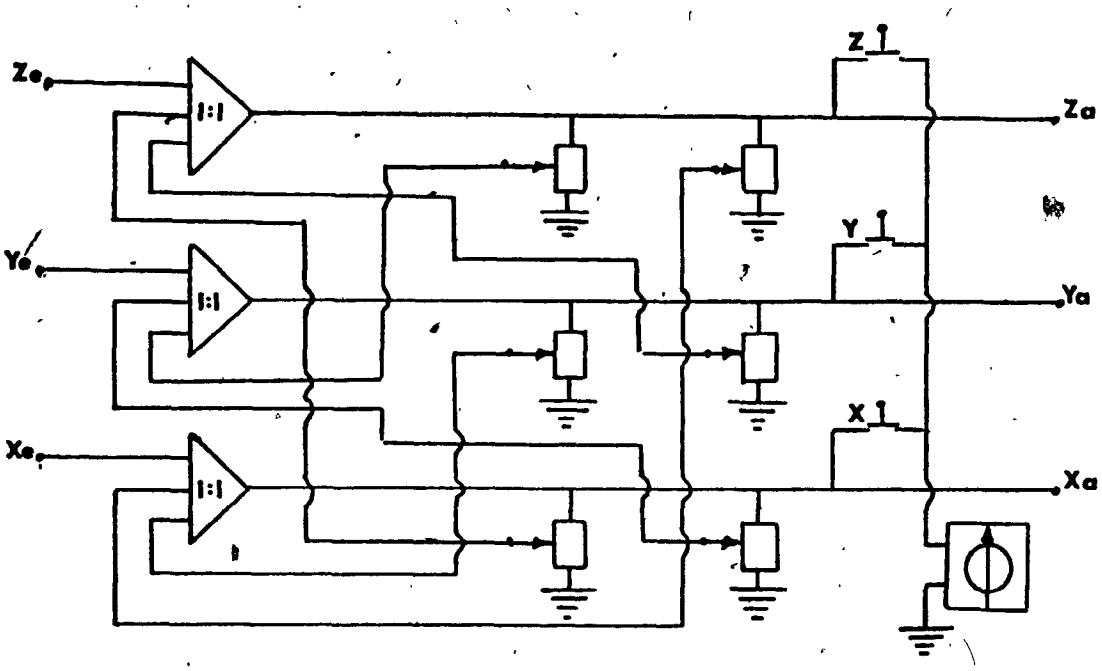

FIG. 4.14 Functional Schematic of x-y-z Compensator

TABLE 4.1 Drilling Conditions Used in Experiments

Feed	Low	Medium	High
Cutting Speed ft/mt	23.55	23.55	23.55
Feed/Rev.	0.0028"	0.0070"	0.0112"

TABLE 4.2 Correlation Between Measured Values and Those Calculated From Steady State Equations

FEED in/Rev	F_{zc} lb	F_z lb	% ERROR	M_{zc} lb inch	M_z lb inch	% ERROR
.0028	131	100	24.2	19.60	15	23.5
.0070	257	250	2.6	40.84	34	14.2
.0112	366	320	12.5	59.5	45	24.3

F_{zc} = calculated thrust lbs

F_z = measured thrust lbs

M_{zc} = calculated torque lb-inch

M_z = measured torque lb-inch

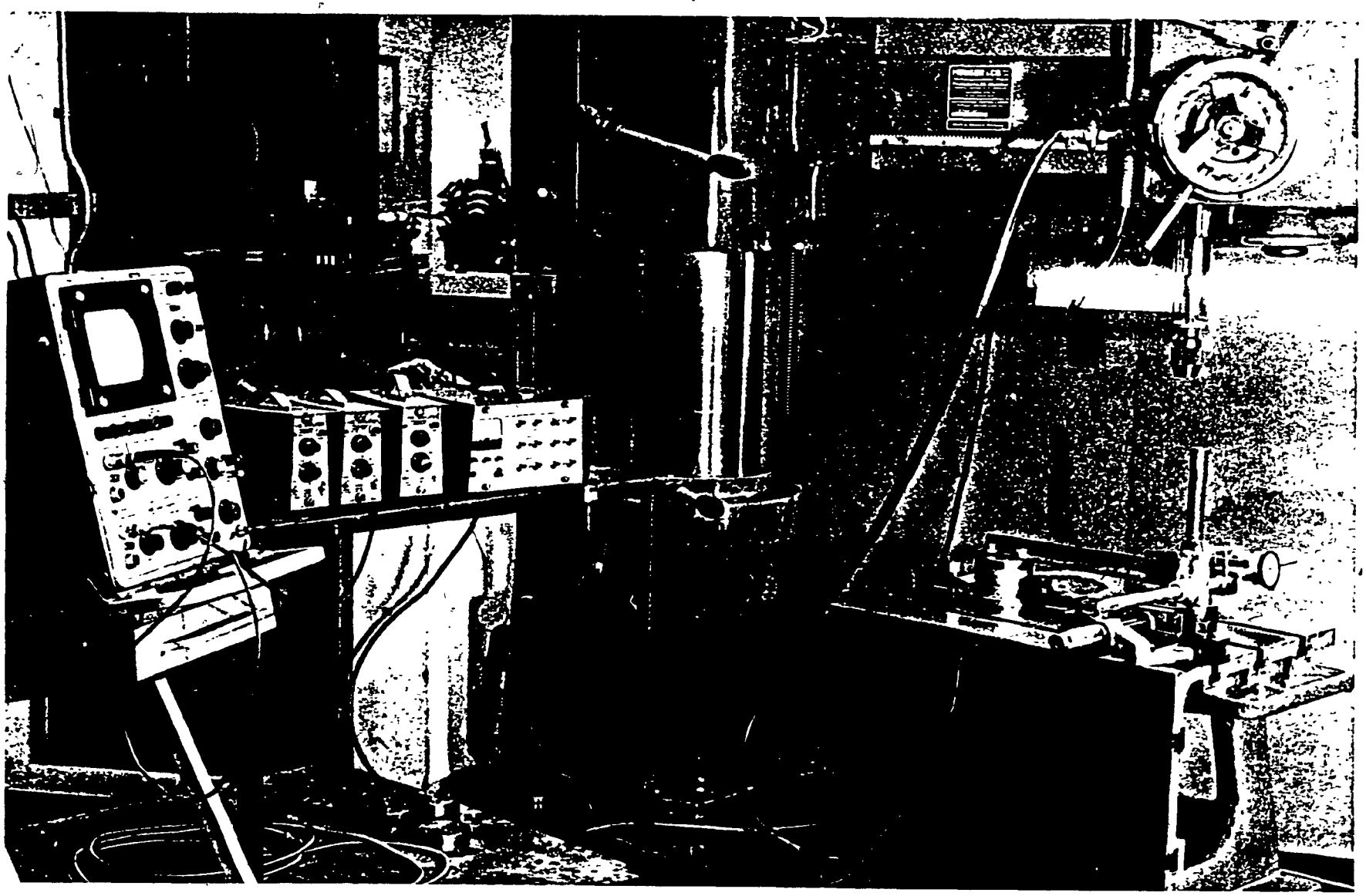

FIG. 4.15 Pictorial View of Equipment Used for Static Calibration in Torque Direction

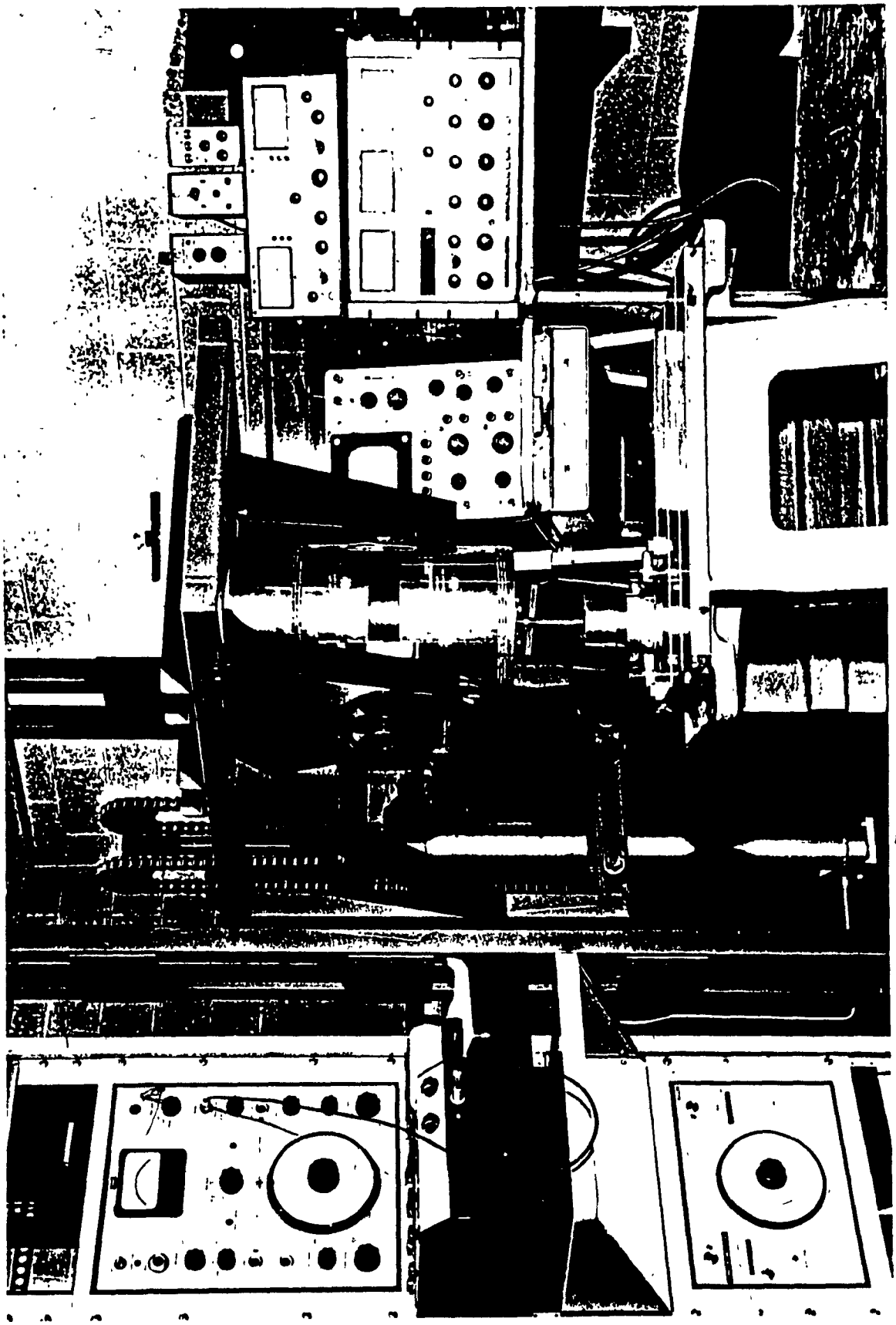

FIG. 4.16. Pictorial View of Equipment Used for Frequency Response of Machine Tool-Dynamometer Worke Piece System

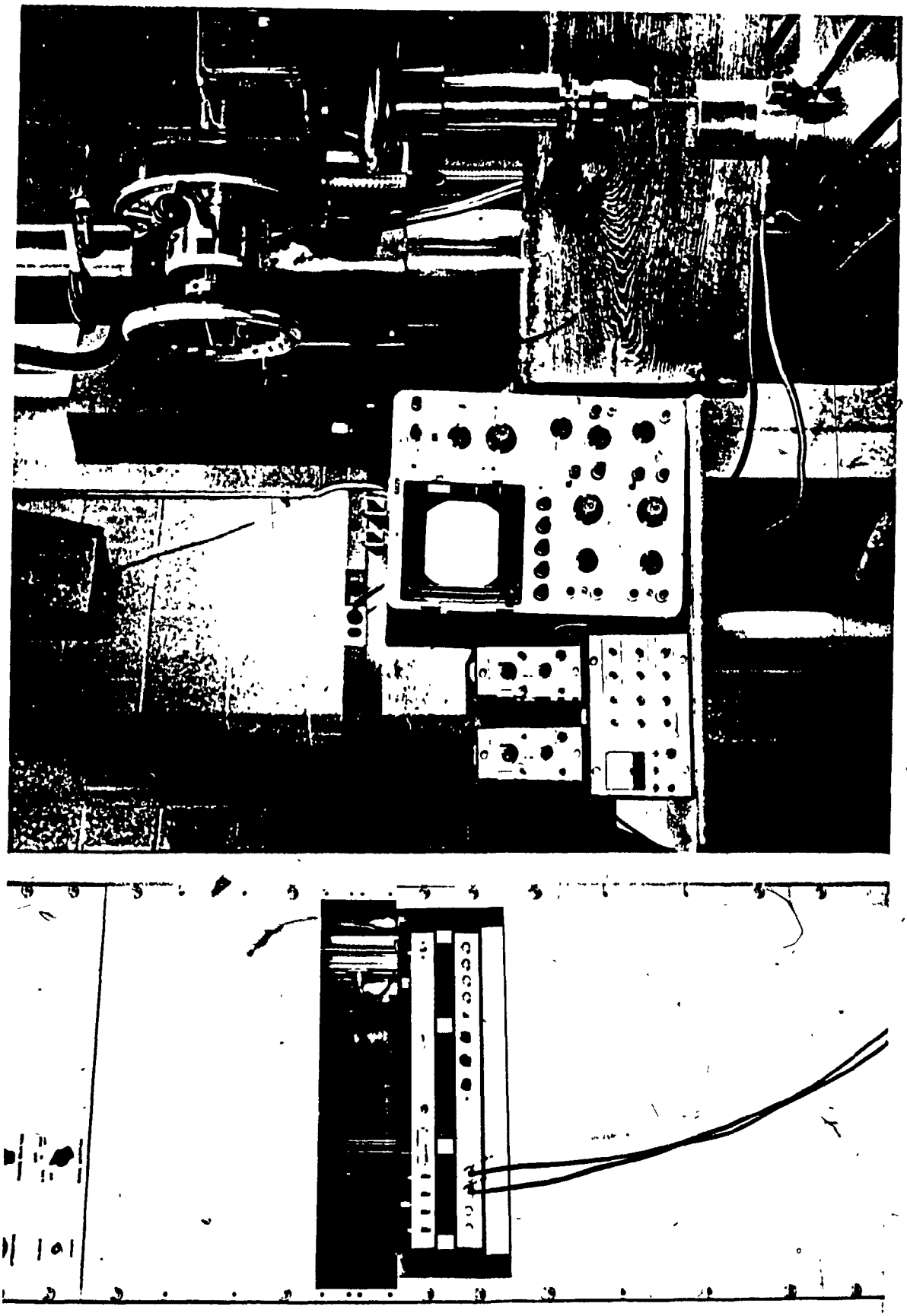

FIG. 4.17 Pictorial View of Equipment Used for Measurement of Thrust and Torque in Drilling

CHAPTER V

DATA PROCESSING AND ANALYSIS OF SIGNALS

CHAPTER V

DATA PROCESSING AND ANALYSIS OF SIGNALS

In this chapter the procedure for data processing, data analysis and mathematical formulation of drilling torque and thrust force are explained. This basically consists of the following three steps.

(1) Analog to digital conversion - carried out using special acquisition system (E.A. 690 HYBRID COMPUTER).

(2) Statistical analysis - using special programs on CDC 6400 and also by Analog Methods.

(3) Proposal of stochastic model - based on the study of statistical properties of the signals obtained above.

5.1 DATA PROCESSING OF CUTTING TORQUE AND THRUST SIGNAL

In order to carry out a detailed statistical analysis, the analog signal is digitized, i.e., it is converted into a series of discrete data points. The conversion is performed by an analog-to-digital conversion package, called the ADCAT SYSTEM. This program was used on an Electronics Associate Incorporated 690 Digital (E.A.I. 690) and a CDC 6400 Computer. The signal from the magnetic tape is connected to the A-D channel of the Analog computer. The ADCAT system is composed of four programmes. The ADCAT programme runs on a CDC 6400 and this receives and records the data and processes the command words. The remaining three programmes are then punched on tapes which run on an

E.A.I. 640, and each one of these performs a particular function and they run in sequence.

Before starting the magnetic tape, the E.A.I. 640 is initialled and the first of three programmes is loaded. The magnetic tape signal is then connected to the A-D channel of the data link. When the "*paper tape*" core image loader is active, all the boot-strapping is complete and the transmission parameters (number of data points and sampling frequencies) supplied to the system, the second programme is automatically loaded. The system is then ready to receive the data. At this stage, the operator gives a command to the computer and the digitizing and storing of the data in the memory starts. When the memory is full, the system starts the transmission of the data.

Communication with the CDC 6400 is maintained through the telephone TDX system, using the interactive sub-system. The normal logging-in procedure is used. The transmission time varies with the amount of data sent. For 10,000 data points, it takes about one hour of processing time. During the transmission, any message sent by the CDC 6400 to the E.A.I. 640 is typed and at that point operator intervention is necessary to re-establish the transmission mode.

The data is transmitted into 18 point records, at the rate of 30 characters per second. At the time of transmission, it is coded into a special format and at the other

end, i.e., the reception end, it is decoded and stored on a disc file on the CDC 6400. After the transmission has been completed, a list of recovered and unrecovered errors is provided. The operator at this stage, can ask to transmit new data or re-transmit old data just transmitted, or terminate any further processing. When all the data stored in the memory are transmitted, a third program is loaded. If more data are to be transmitted, the repositioning of the tape is necessary; otherwise, the system can be outmoded by the normal logging-off procedure.

The number of data points required depends upon the reading rate and record length of the sample. The reading rate is further dependent upon the maximum cut-off frequency. The dynamometer used shows a resonance frequency of 2500 Hz and is reliable to a maximum frequency of 700 Hz. The dynamometer-test piece-tool and machine tool system has a resonance of about 1000 Hz. So, this is the maximum frequency up to which the dynamometer yields accurate results.

As, per BENDAT [26], data sampling is to be spaced suitably, so that it is not correlated, but at the same time it should not be spaced too far apart, which may result in a loss of significant information at high frequencies. Therefore, the minimum sampling rate is twice the cut-off frequency, i.e., in this system, there are 1400 samples per second. For 10,000 data points transmitted, a signal duration contains

7.1428 seconds. All further analyses are based on 10,000 data points. With the selection of a sample size of 10,000 data points, the normalized standard error for spectral calculations is only about 0.10, which is acceptable.

5.2 STATISTICAL ANALYSIS

After the cutting torque and thrust force signals have been digitized and stored on a file in the CDC 6400, the statistical techniques to obtain the characteristic properties of the signals can be applied. From a study of those properties, a mathematical model of the process may then be developed. In the beginning, it is desirable to know whether or not the sampled data is Random Stationary. This facilitates a further analysis. The following procedure for studying the characteristics of the signals was carried out.

(1) A test for Stationarity

(2) A test for randomenss in the time domain

(3) A calculation of the spectral density in the frequency domain

(4) The determination of the probability distribution

5.2.1 Test for Stationarity

A process is said to be stationary, if all its statistical properties do not change with time translations. This is not possible in practice, since there is an infinite

number of possible statistics, and the process has to be described by an infinite number of sample records (ensemble). According to BENDAT [26], certain assumptions which are valid for most of the random data, can be made, and, the following practical tests for stationarity can be applied.

(i) If the process is stationary, the statistical properties calculated using small time intervals of the single time history will not vary significantly from one interval to the other. This means that the data samples will be representative of the process over a large interval of time.

(ii) Verification of invariance of the mean value and an auto-correlation with the time translations is acceptable, as a condition of fulfillment of stationarity.

(iii) The sample record of data to be investigated is very long, compared to the random fluctuations of the data time history. This is necessary so that the short-time averages will truly reflect the average properties of the data.

(iv) If the mean square value of data is stationary, the autocorrelation function is also stationary.

By keeping these assumptions in mind, a single time history of the digitized data is then divided into 100 equal time intervals. Suitable spacing is provided so that the data on one interval remains uncorrelated from the next.

The mean value and mean square value for each interval is evaluated as follows:

$$\bar{Y}_1, \bar{Y}_2, \bar{Y}_3 \ \ldots\ldots\ldots \ \bar{Y}_7$$

$$\bar{Y}_1^2, \bar{Y}_2^2, \bar{Y}_3^2 \ \ldots\ldots\ldots \ \bar{Y}_7^2$$

$$i = 1,2,3 \ \ldots\ldots\ldots \ 100$$

where $\bar{Y}_i$ and $\bar{Y}_i^2$ are the mean value and mean square value in the $i^{\underline{th}}$ interval.

The sequence of the mean and mean square values for the presence of underlying trends other than those due to expected sampling variations is tested. Appendix "A" gives a sample of the computer programme used for the evaluation of these runs and trends. According to the BENDAT "*run test*", the mean value and variance sequences for N = 100 should give the number of runs between the range 38-63. For the "*trend test*", this number should be between 2083-2866. Table 5.1 gives the results of these tests. As can be seen, all these values are within the range and hypothesis of stationarity and are acceptable.

5.2.2 Autocorrelation Function Test

The Autocorrelation function test is a powerful method for detecting the sinusoidal components in otherwise random data. For purely random data, the autocorrelation will monotonously reach a value equal to the mean value squared. This indicates the rapidity of the signal and the behaviour of the wave form repetitions. For stationary data with a mean value of zero, the autocorrelation function with the displacement KH is given as

$$R(KH) = \frac{1}{N-K} \sum_{R=1}^{N-K} Y(R)\ Y(R+K)$$

K = 0,1 100

K = lag number

KH = time lag

N = number of data points in a sample

Y(R) = the sample record

From the above equation, the extent of dependence of Y(R) on Y(R+K) can be established. For a large value of time lag, the autocorrelation reaches the static value of the signal if this is present in the original signal.

Figure 5.2, shows the autocorrelation for some known signals. The rate of decay of oscillation in an autocorrelation function is the index of randomness of the signal.

To calculate the autocorrelation in three signals of cutting torque, 10,000 data points were used for each signal.

The computation was carried out on a digital computer and the programme is given in Appendix A. From the curves, Figure 5.3, it may be seen that they follow the pattern of the curve C of Figure 5.2. This indicates that the cutting torque fluctuations are random and the harmonic content is much less.

5.2.3 Power Spectral Density Estimates for Cutting Torque Signal

The spectral density of the random signal gives useful information about the signal in the frequency domain. It indicates the energy content distributed over the frequency spectrum and the integration of which will yield a total energy associated with the signal. For the calculation of spectral density, an indirect method via the Fourier transform of the autocorrelation function was used in this analysis. For the stationary process with the mean value of zero, the following formula from BENDAT is used.

$$G\left(\frac{CF_c}{M}\right) = \frac{1}{F_c}\left[R(0) + 2\sum_{K=1}^{M-1} R(K)\cos\left(\frac{\pi KC}{M}\right) + (-1)^C R(M)\right]$$

where

$C = 0, 1, 2 \ldots\ldots\ldots M$

F_c = cut-off frequency or critical frequency

M = maximum lag number

$R(K)$ = autocorrelation at lag number K

For the calculation, a programme was prepared and is shown in Appendix "A".

The normalized standard error for the estimate

$$\varepsilon = \frac{1}{\sqrt{BT}} = \frac{1}{\sqrt{14 \times 7.14}} \approx 0.10$$

is given, which is quite acceptable.

The spectral density for the torque signal under three different cutting conditions (different feeds) is evaluated. A plot of the spectral density for the three conditions is given in Figure 5.4. All three graphs exhibit similar characteristics. The first peak is below 30 Hz. Since the cutting torque cannot be expected to have low frequencies, this part is to be neglected. Probably, this is because the machine tool system is being put into resonance at low frequencies and results in this peak. The second peak indicates that the dominant frequency of about 370 Hz exists for f = 0028", .007", and 420 Hz for f = 0112".

5.2.4 Statistical Analysis of the Cutting Torque Signal in Amplitude Domain

The probability density function for the signal is found digitally by dividing the amplitude range into appropriate class intervals. In order to apply a goodness-of-fit test of the data to the Gaussian distribution, a number of class intervals is selected according to BENDAT.

$$\text{Class intervals} = 1.87\,(N-1)^{2/5}$$
$$= 1.87\,(10{,}000-1)^{2/5} = 75$$

This is the minimum class interval and 80 is appropriately chosen. The number of data points in each interval is summed up and a probability histogram is obtained by plotting the number of data points in each interval versus the torque density. Figures 5.8, 5.9 and 5.10 are the results of the plots. The graphs for the three different conditions of cutting exhibit a Gaussian distribution. This is corroborated by Normality Curves, Figures 5.5, 5.6, and 5.7. For high feed, i.e., roughing operations, two portions of the graph are straight lines, but with slight differences of the slopes between them. The middle portion indicates a high slope. The data for this cutting condition still follows the Gaussian distribution, with slight deviations.

The graph of the low feed shows a small variance and more data points that are concentrated about its mean value. The graphs for the medium and high feed have comparatively large variances.

5.2.5 Amplitude Density Analysis by Analog Method

The probability density analysis has already been presented in the previous section, and as indicated, the signals

are Gaussian distributed. The same analysis was confirmed using analog methods which enable the use of longer signal length. For this, a Bruel and Kjae- Amplitude Density Analyzer Model 161 was used. A schematic view of the set-up is shown in Figure 5.11 with a pictorial view in Figure 5.12. To determine whether the equipment is functioning properly, a sinusoidal signal was supplied to the analyzer and its probability density obtained. This is shown in Figure 5.13 and indicates that the analyzer calibration is correct.

It was observed that the torque and thrust signals recorded on magnetic tape (spool type) were not of the same duration as the processing time of the analyzer. The processing time of the analyzer demands that signals be of longer duration. This difficulty was overcome by recording the signal on a closed magnetic tape loop. With the closed loop running on the recorder, there was no problem in matching the processing time of the analyzer. With the proper setting of the analyzer and X-Y Recorder, the thrust and torque signals were fed to the analyzer one-by-one, and the probability density plots were thus obtained, as shown in Figures 5.14, 5.15, and 5.16 for the thrust signal, and Figures 5.17, 5.18, and 5.19 for the torque signal.

This indicates that the signals obtained under different drilling conditions are Gaussian distributed and verifies the results obtained by the Digital Method.

5.3 A MATHEMATICAL MODEL FOR DRILLING TORQUE AND THRUST FLUCTUATIONS

From the experiments conducted to measure the above physical quantities, and from the results of the system analysis as presented, the following conclusions regarding the nature of fluctuations can be drawn:

(1) The nature of cutting torque and thrust force in drilling is dynamic and not static;

(2) the fluctuations are random in nature and there is evidence that they have some harmonic content;

(3) the cutting quantities under three different cutting conditions can be assumed stationary;

(4) from the statistical analysis in amplitude domain, the fluctuations for the three cutting conditions are Gaussian distributed. However, there is evidence that under high feed cutting operations there is a slight departure from the Gaussian distribution:

$$P(y_i) = \frac{1}{\sqrt{2\pi}\sigma} \exp\left[-\frac{(y_i - \mu)^2}{2\sigma^2}\right]$$

(5) From the frequency analysis of the cutting torque and the thrust force fluctuations, it is observed that a simple mathematical formulation is not possible. There is a dominant frequency in all

three cases, but it is not so pronounced. So with this approximation, fluctuations can be assumed to approximate a wide-band random noise between 150 Hz to 700 Hz or a second approximation that the whole frequency range can be divided into suitable intervals for which the spectral density is flat and can be used for the purpose of machine tool stability analysis.

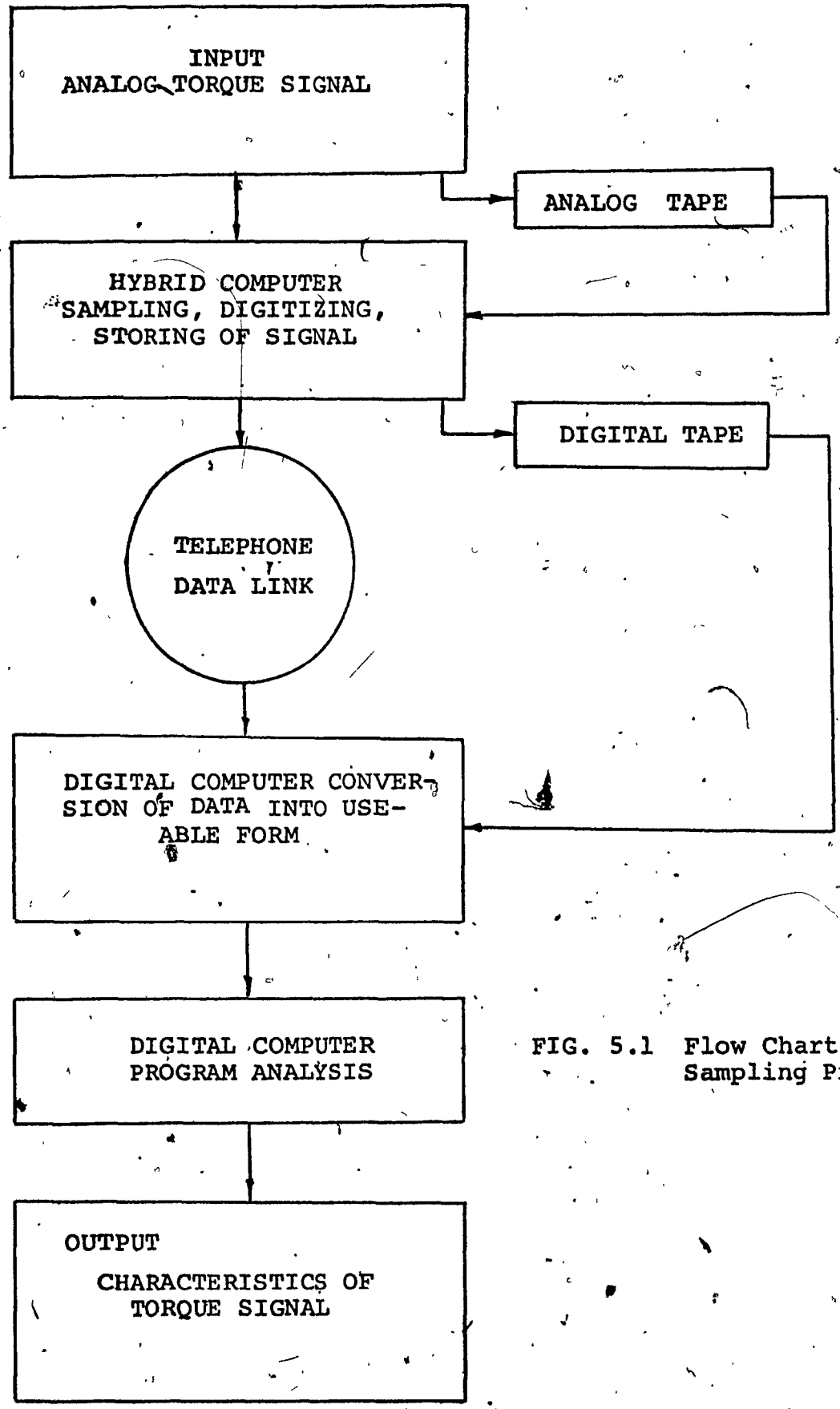

FIG. 5.1 Flow Chart of Data Sampling Procedure

TABLE 5.1 Results of Stationarity Test for the Three Torque Signals

	RUN TEST FOR MEAN VALUE SEQUENCE 38-63	RUN TEST FOR VARIANCE SEQUENCE 38-63	TREND TEST FOR MEAN VALUE SEQUENCE 2083-2866	TREND TEST FOR VARIANCE SEQUENCE 2083-2866
TORQUE COMPONENT feed 0.0028"	58	55	2512	2526
TORQUE COMPONENT feed 0.0070"	57	41	2464	2430
TORQUE COMPONENT feed 0.0112"	54	49	2566	2397

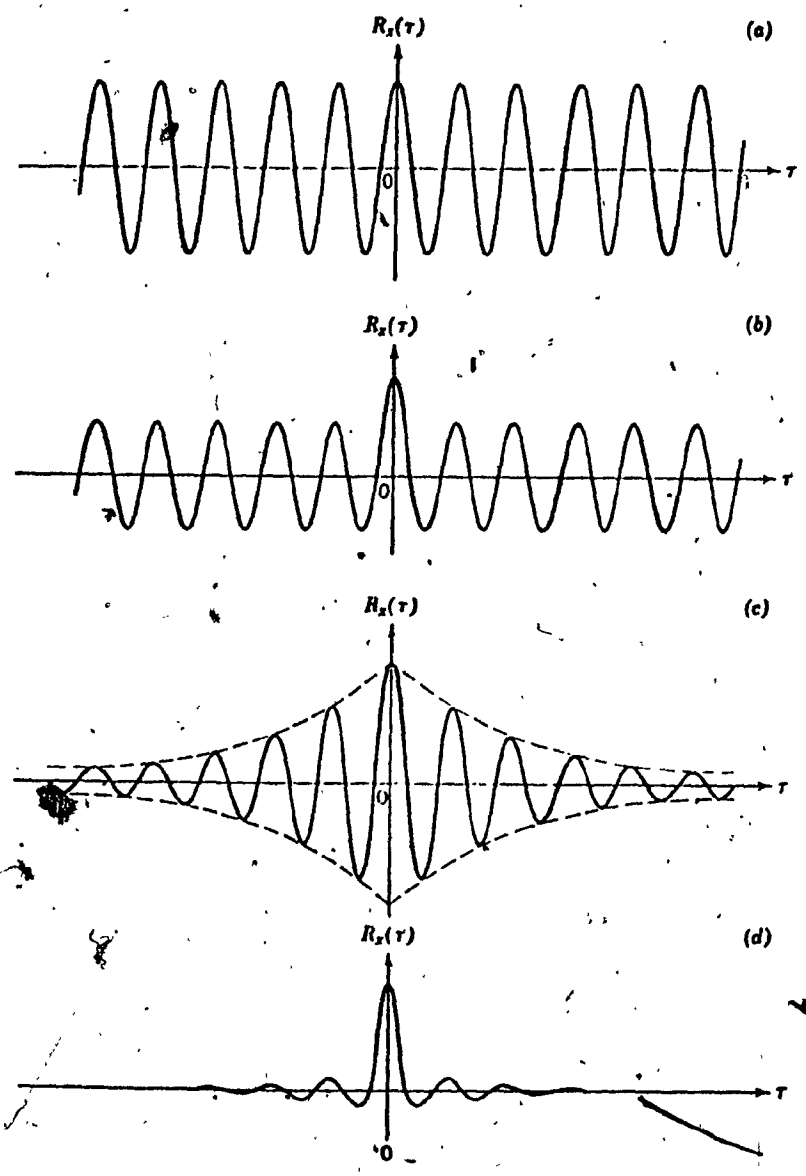

FIG. 5.2 Plots of Auto-Correlation Function[26]

(a) Sine wave
(b) Sine wave plus random noise
(c) Narrow band random noise
(d) Wide band random noise

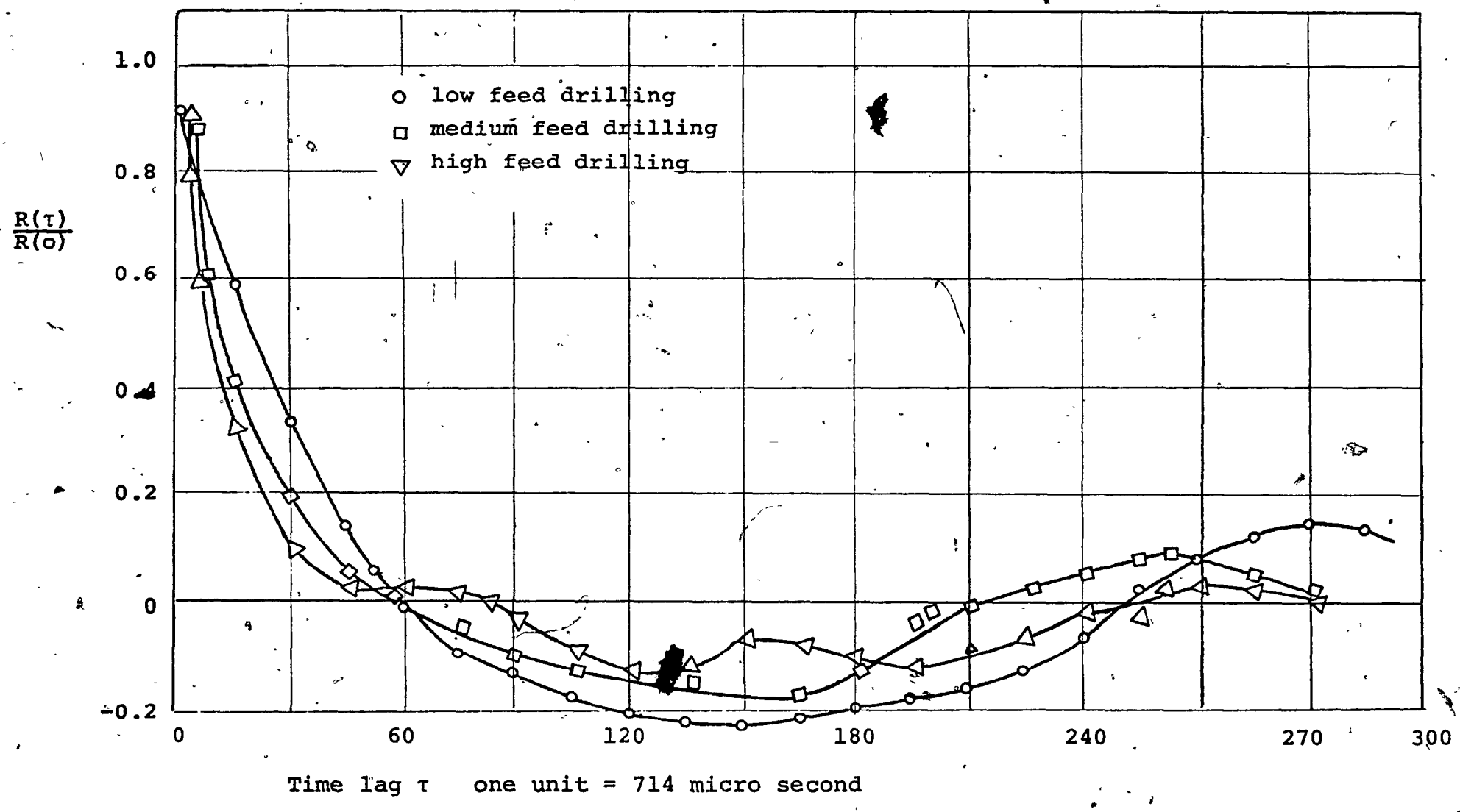

FIG. 5.3 Auto-Correlation Plot for Three Drilling Torque Signals

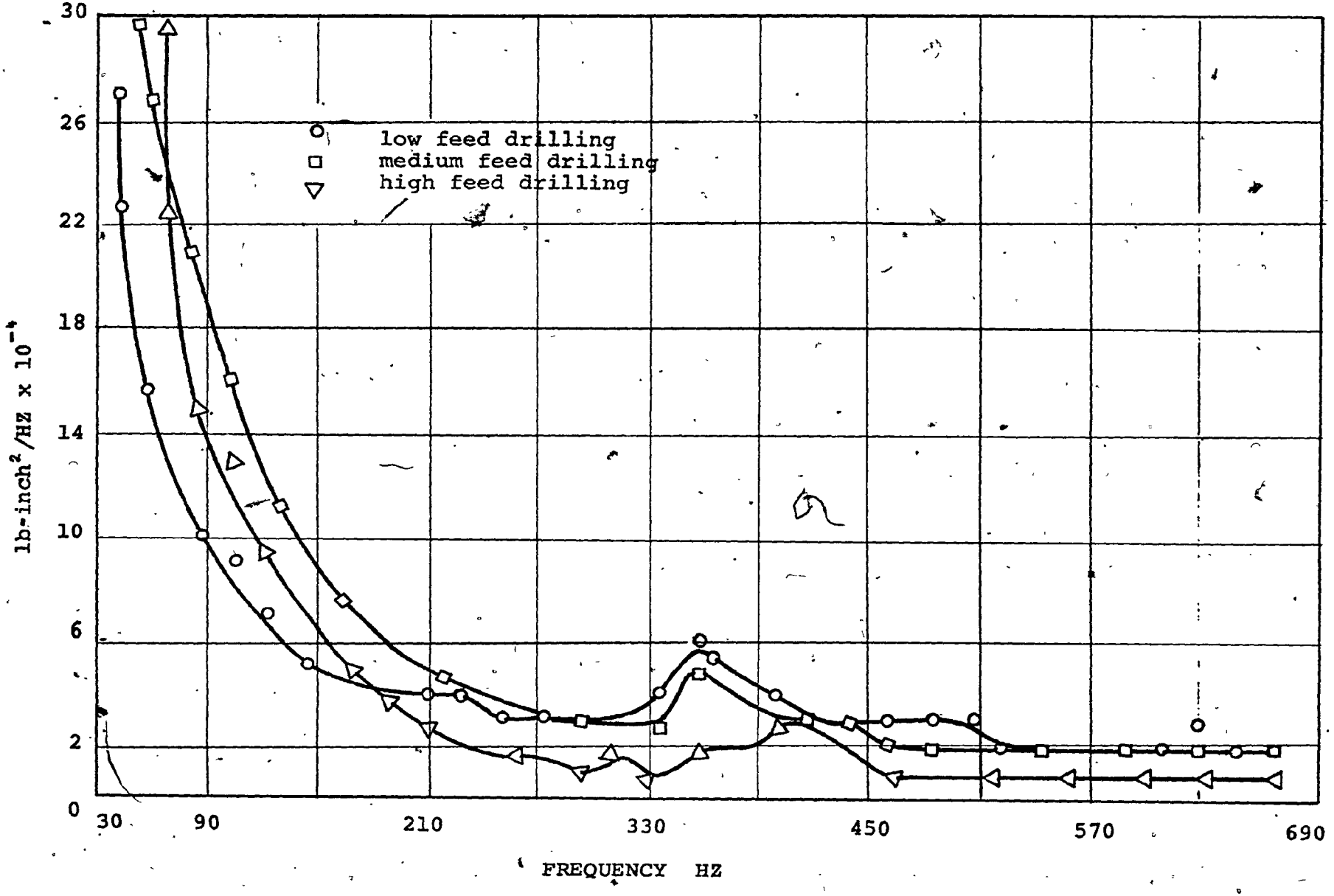

FIG. 5.4 Power Spectral Density Graphs for Three Drilling Signals

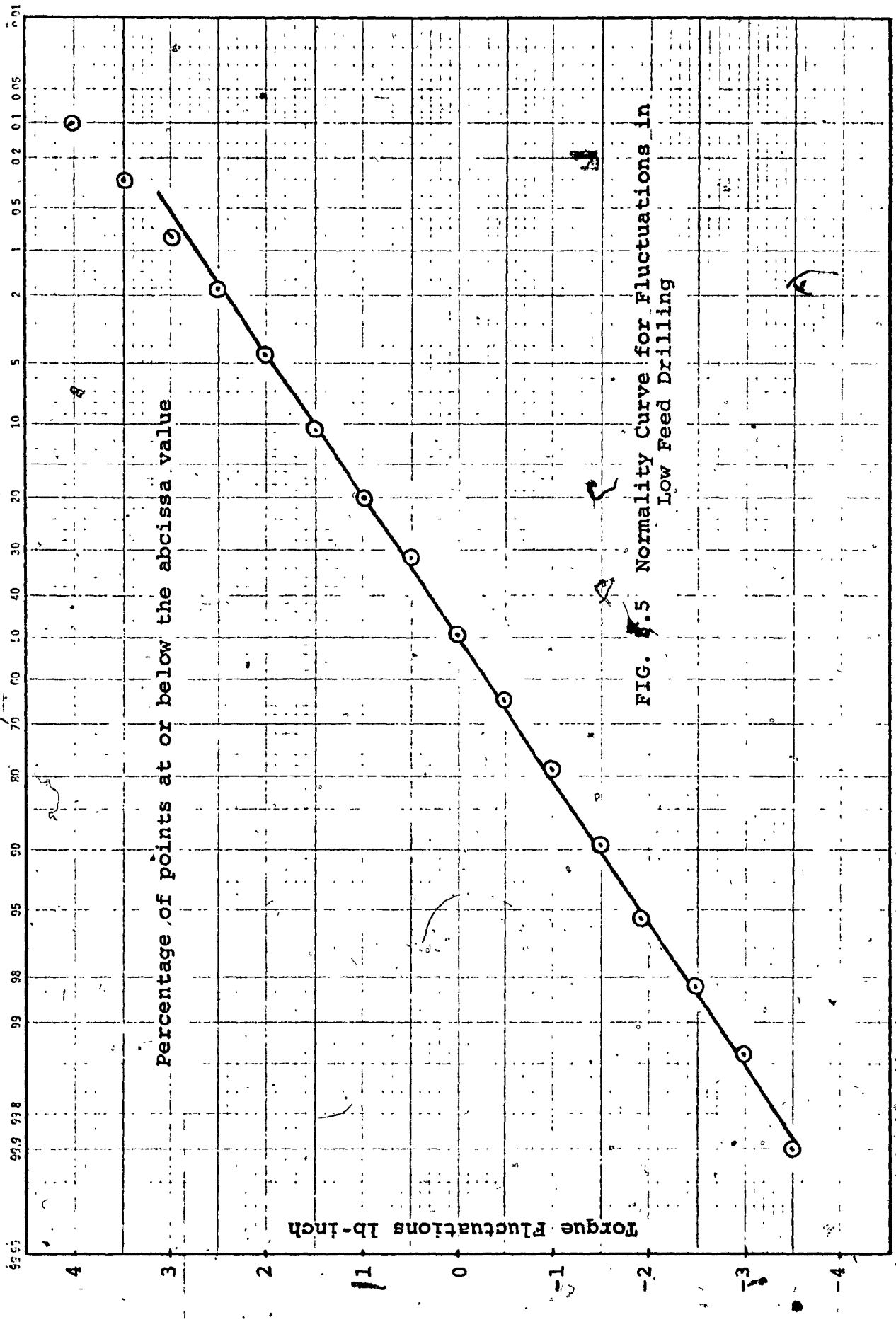

FIG. 4.5 Normality Curve for Fluctuations in Low Feed Drilling

Probability Scale x 90 Divisions

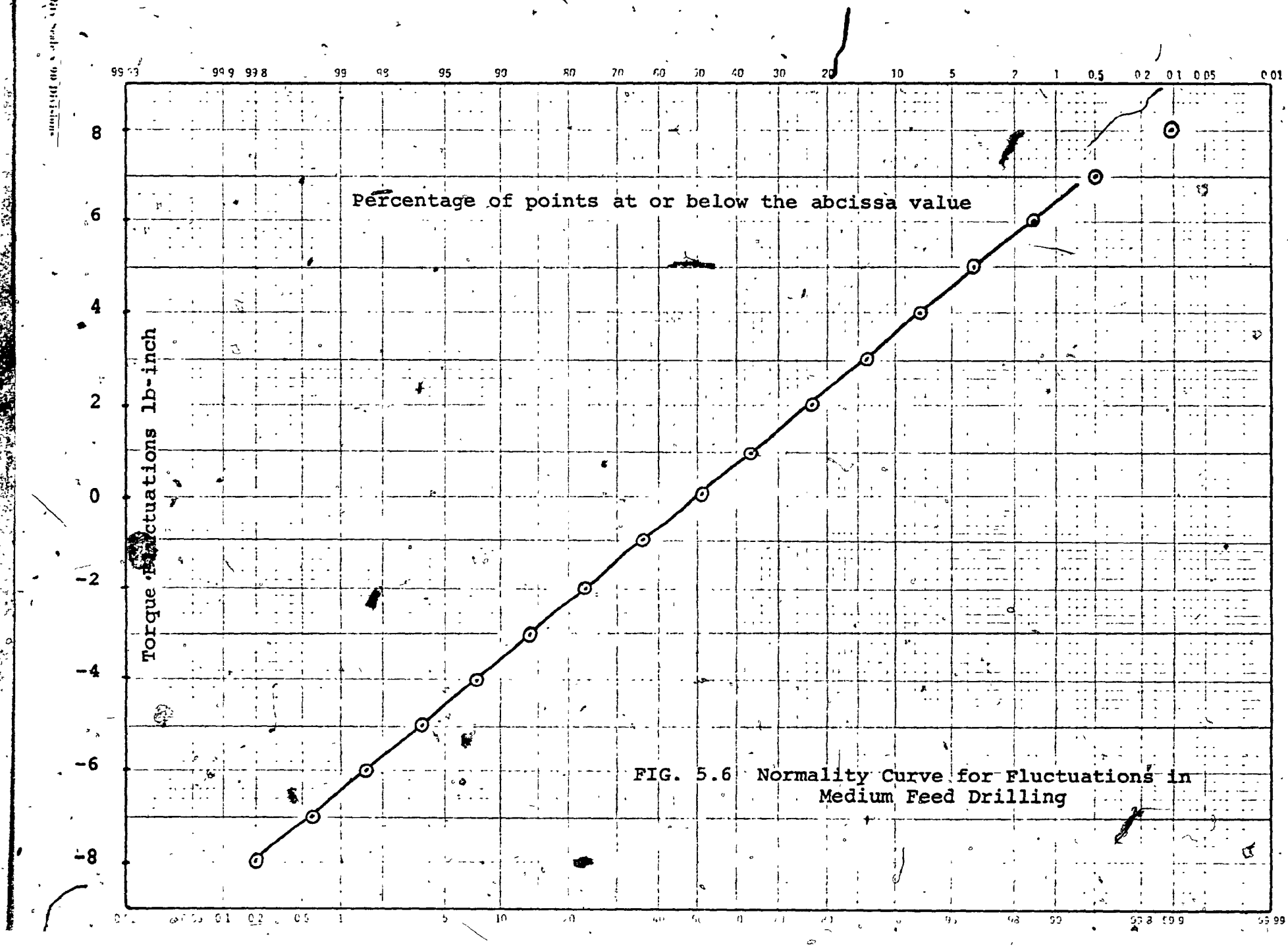

FIG. 5.6 Normality Curve for Fluctuations in Medium Feed Drilling

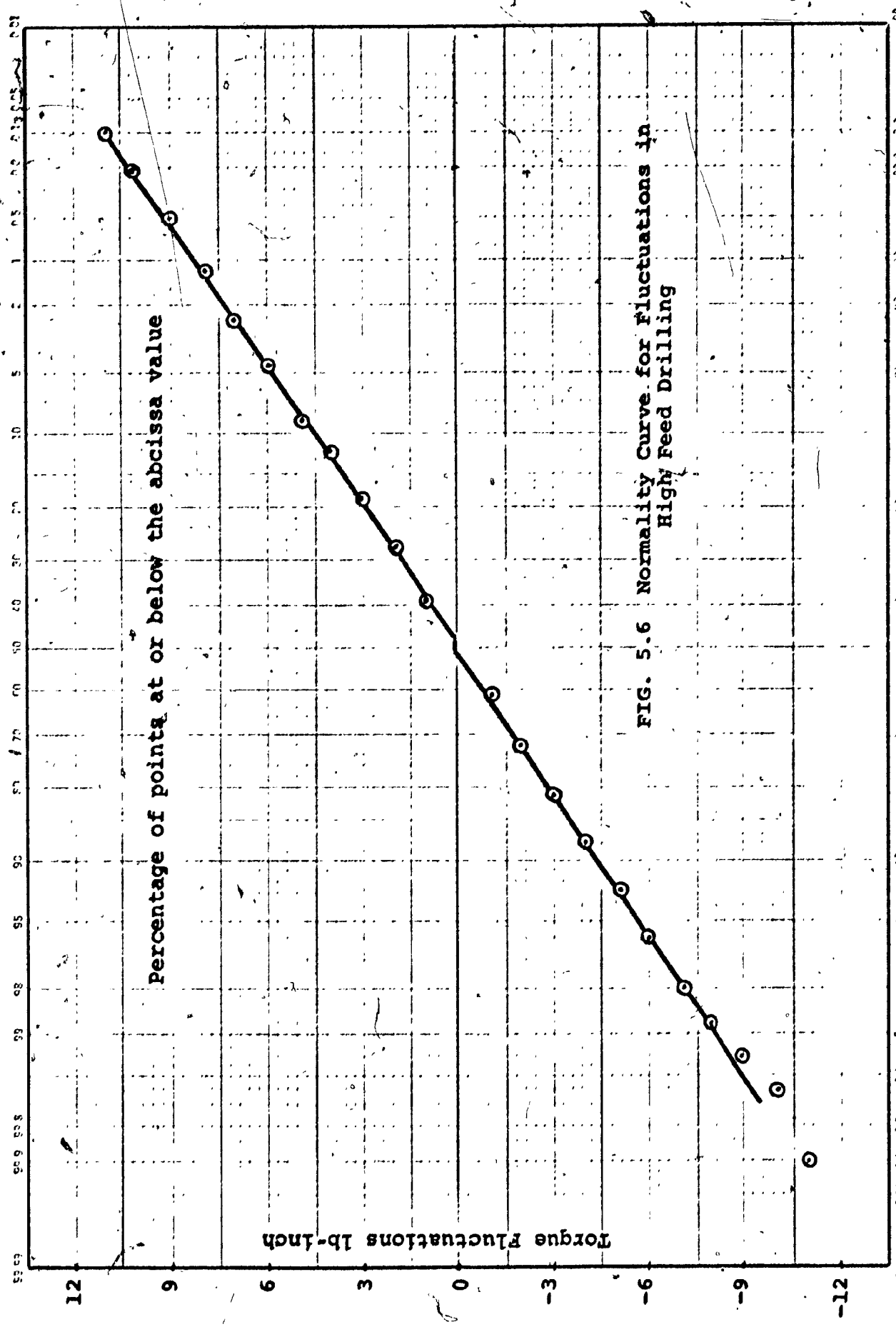

FIG. 5.6 Normality Curve for Fluctuations in High Feed Drilling

Probability Scale x 90 Divisions

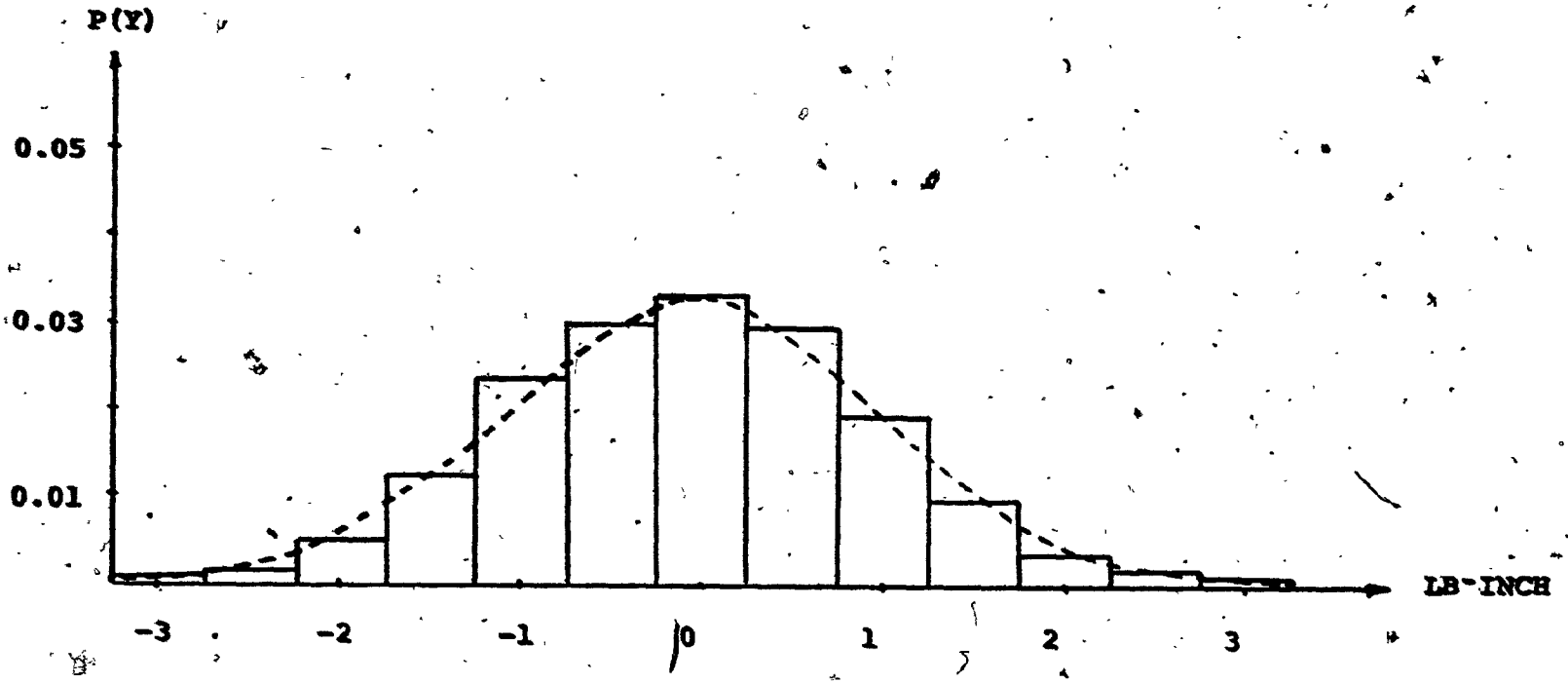

FIG. 5.8 Probability Density Plot for Torque Fluctuations for Low Feed Drilling

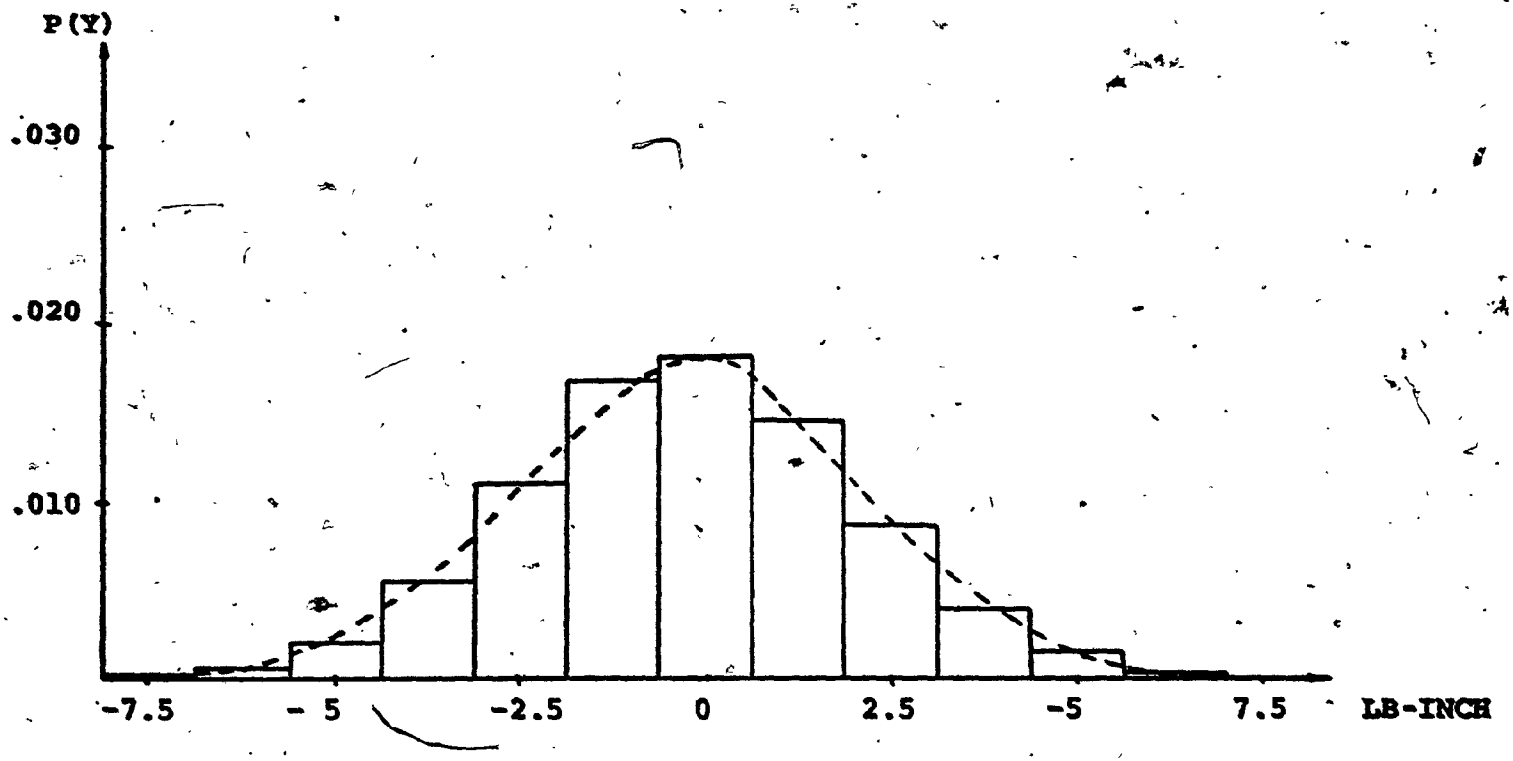

FIG. 5.9 Probability Density Plots for Torque Fluctuations for Medium Feed Drilling

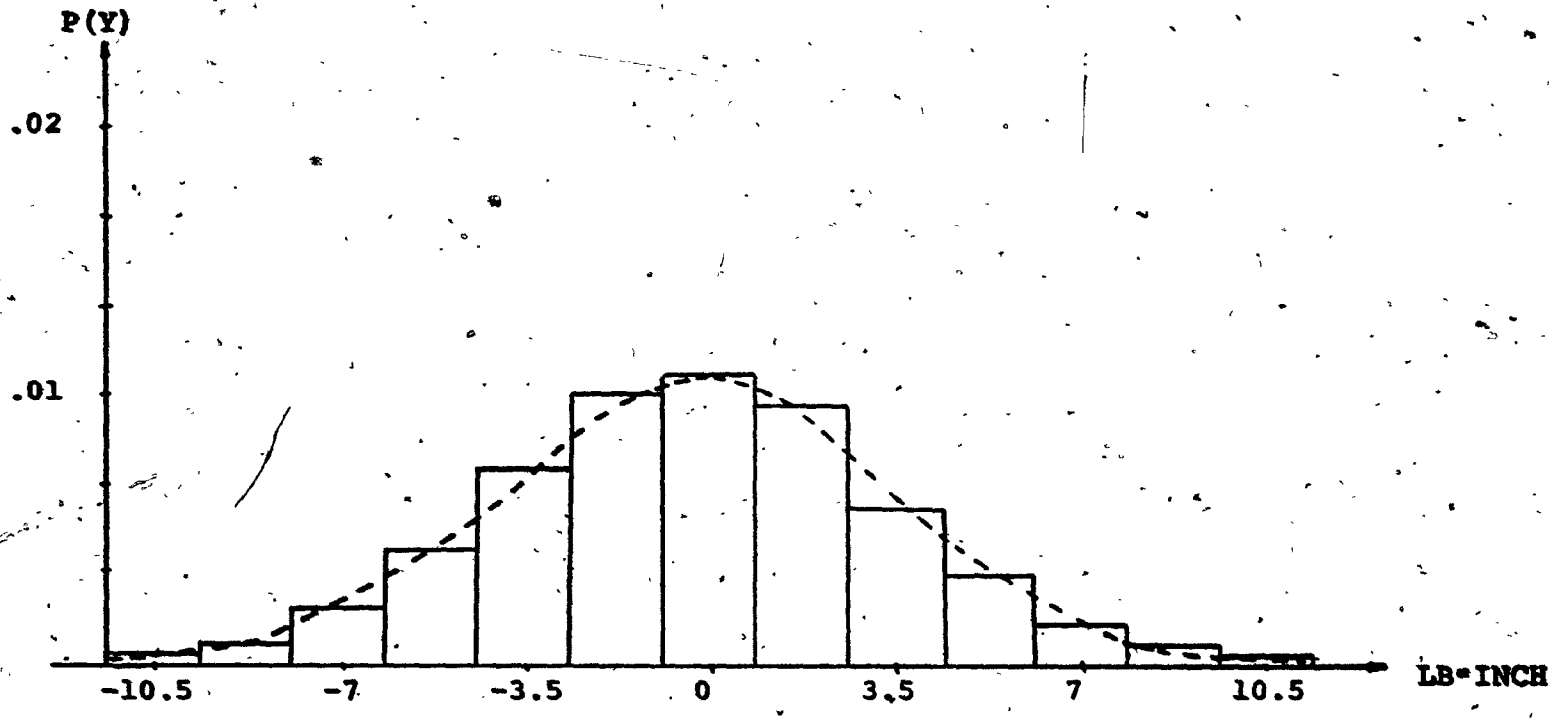

FIG. 5.10 Probability Density Plots for Torque Fluctuations for High Feed Drilling

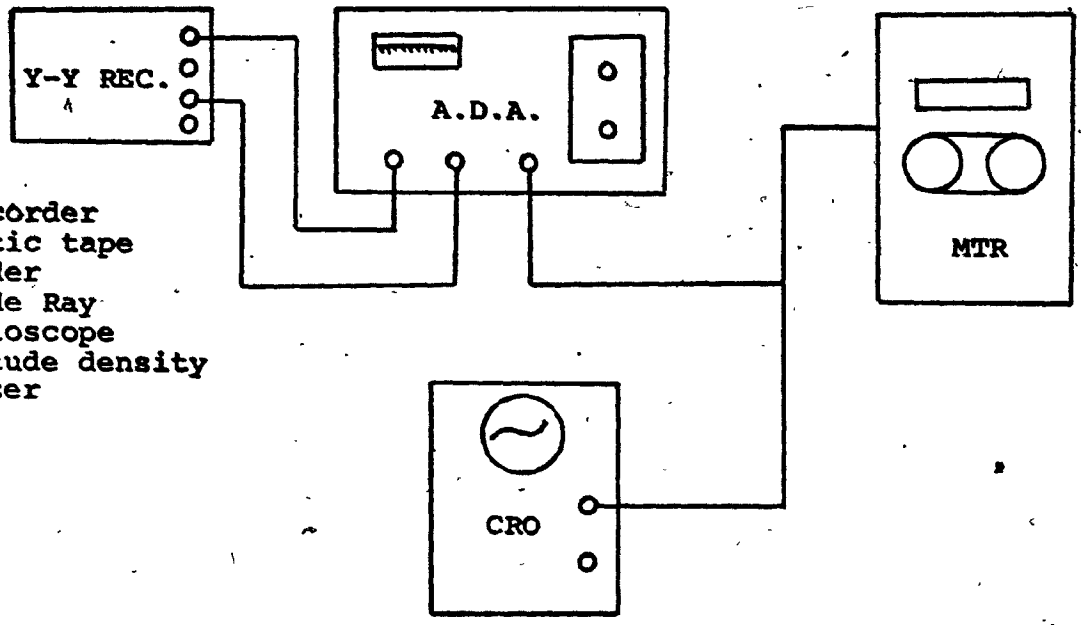

X-Y REC: XY Recorder
MTR: Magnetic tape recorder
CRO: Cathode Ray Oscilloscope
ADA: Amplitude density analyzer

FIG. 5.11 Schematic Set-Up for Amplitude Density Analysis

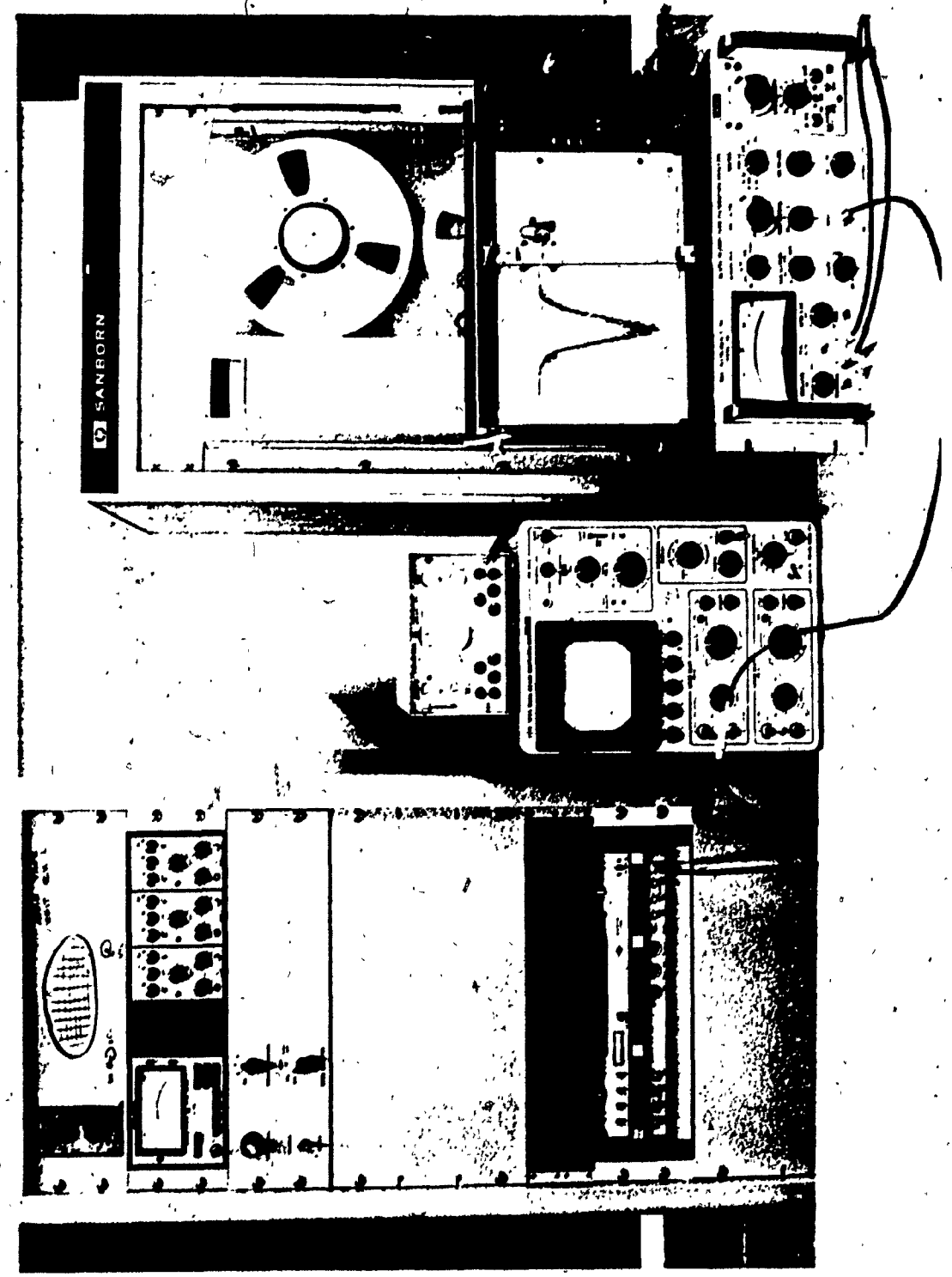

FIG. 5.12 Pictorial View of Equipment Used for Amplitude Density Analysis

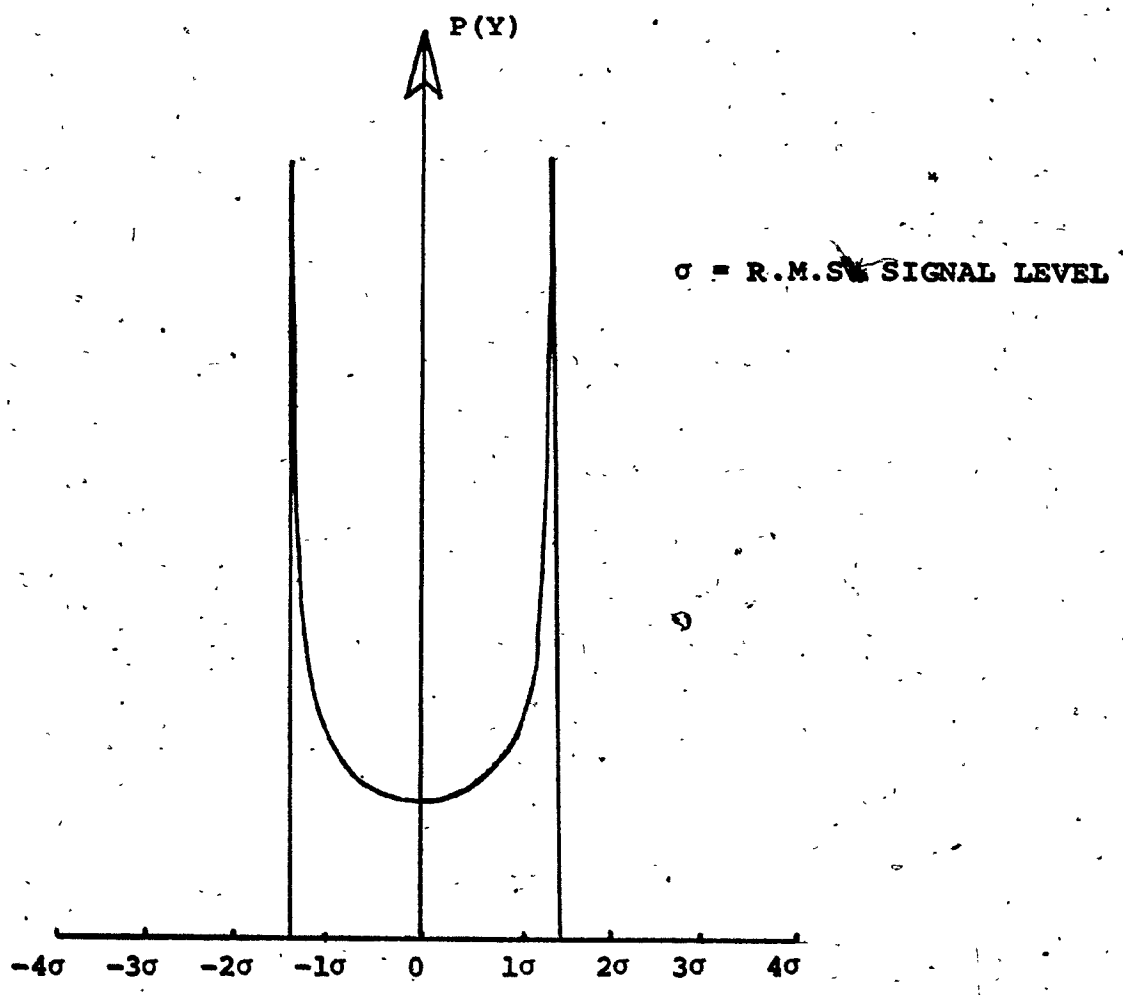

FIG. 5.13 Probability Density of a Known Sine Signal

SWEEP TIME OF ANALYSER = 16 min

σ = R.M.S. SIGNAL LEVEL

FEED = 0.0112 IN

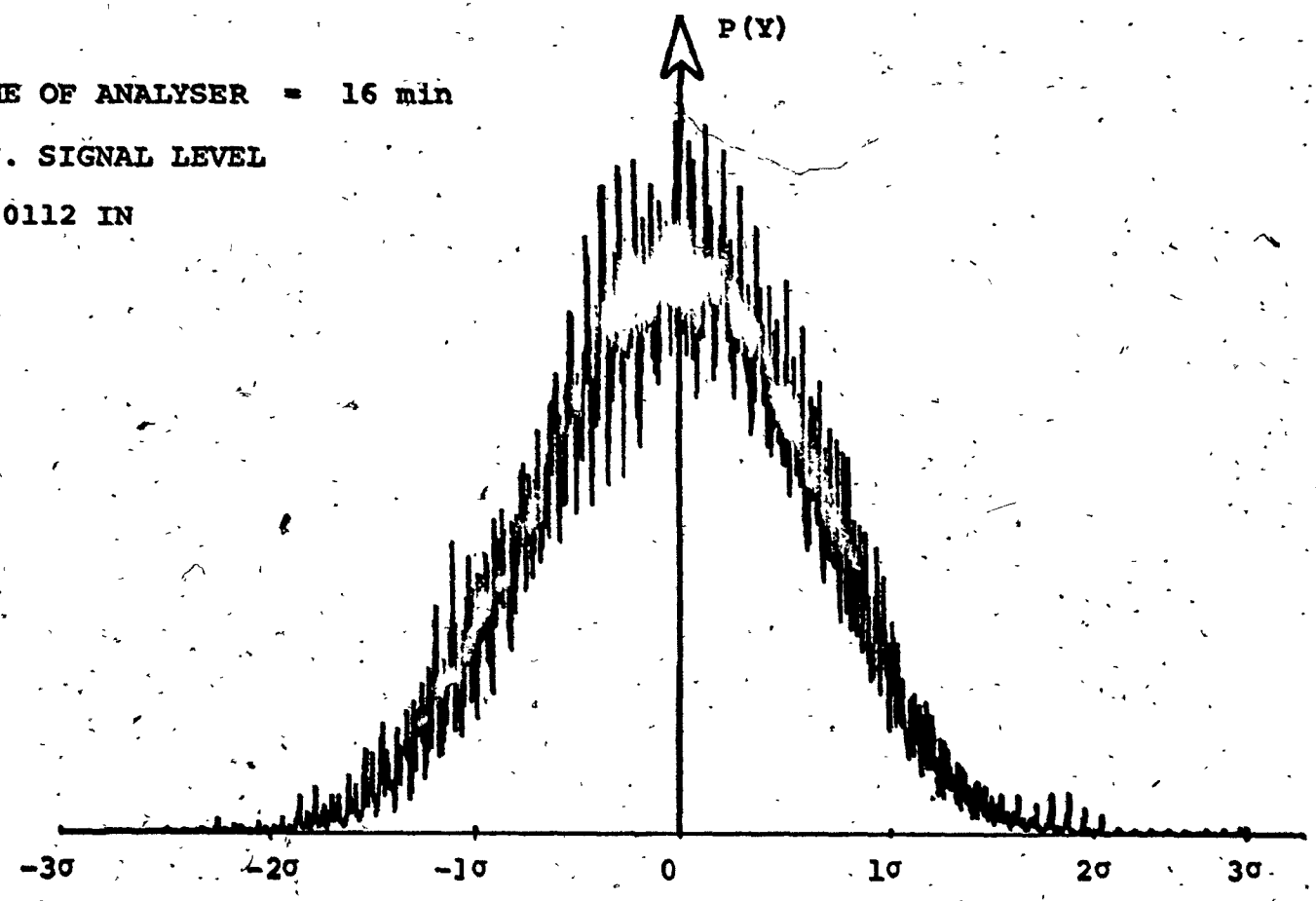

FIG. 5.14 Amplitude Density Plot for Thrust Fluctuations in High Feed Drilling

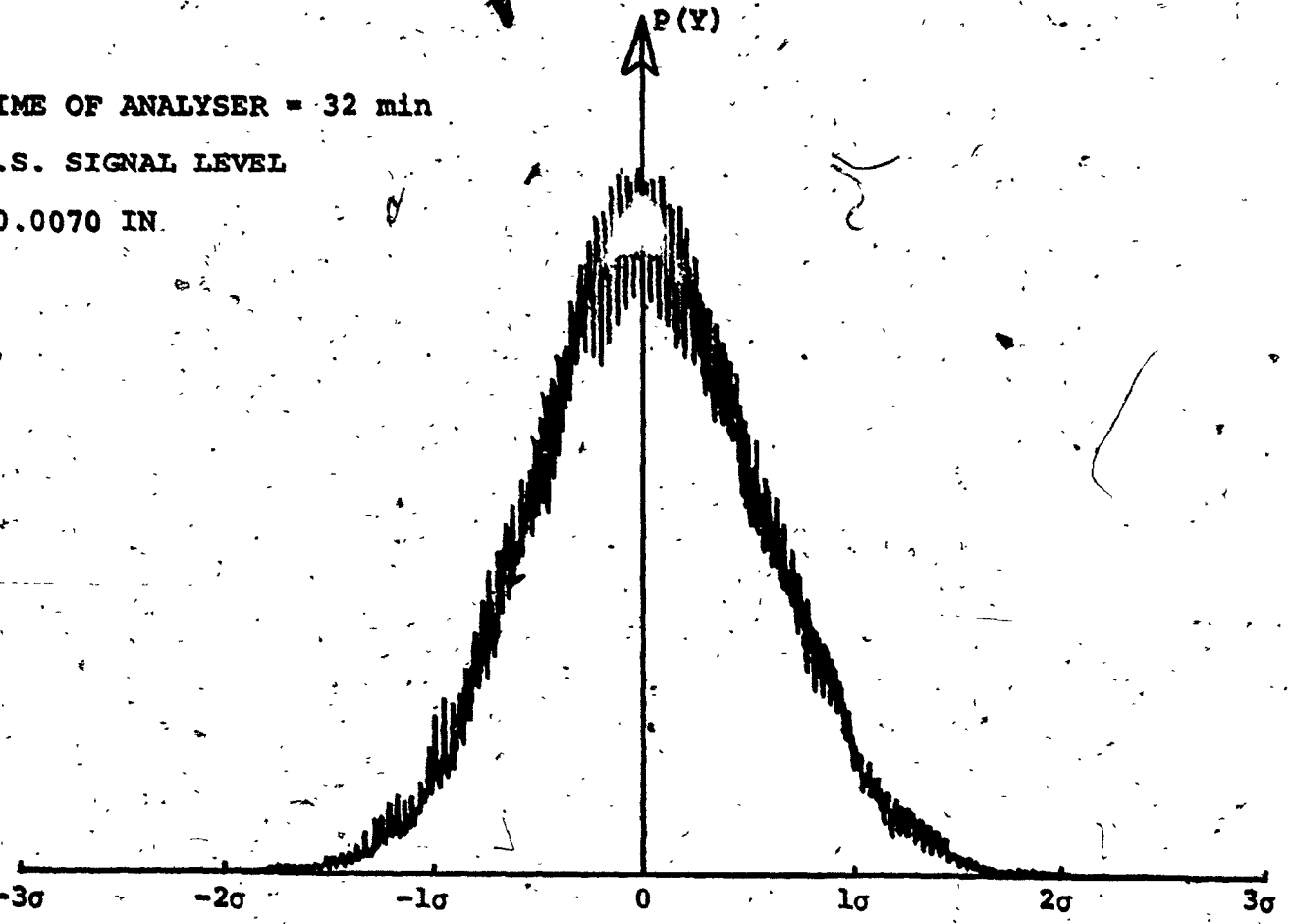

FIG. 5.15 Amplitude Density Plot for Thrust Fluctuations in Medium Feed Drilling

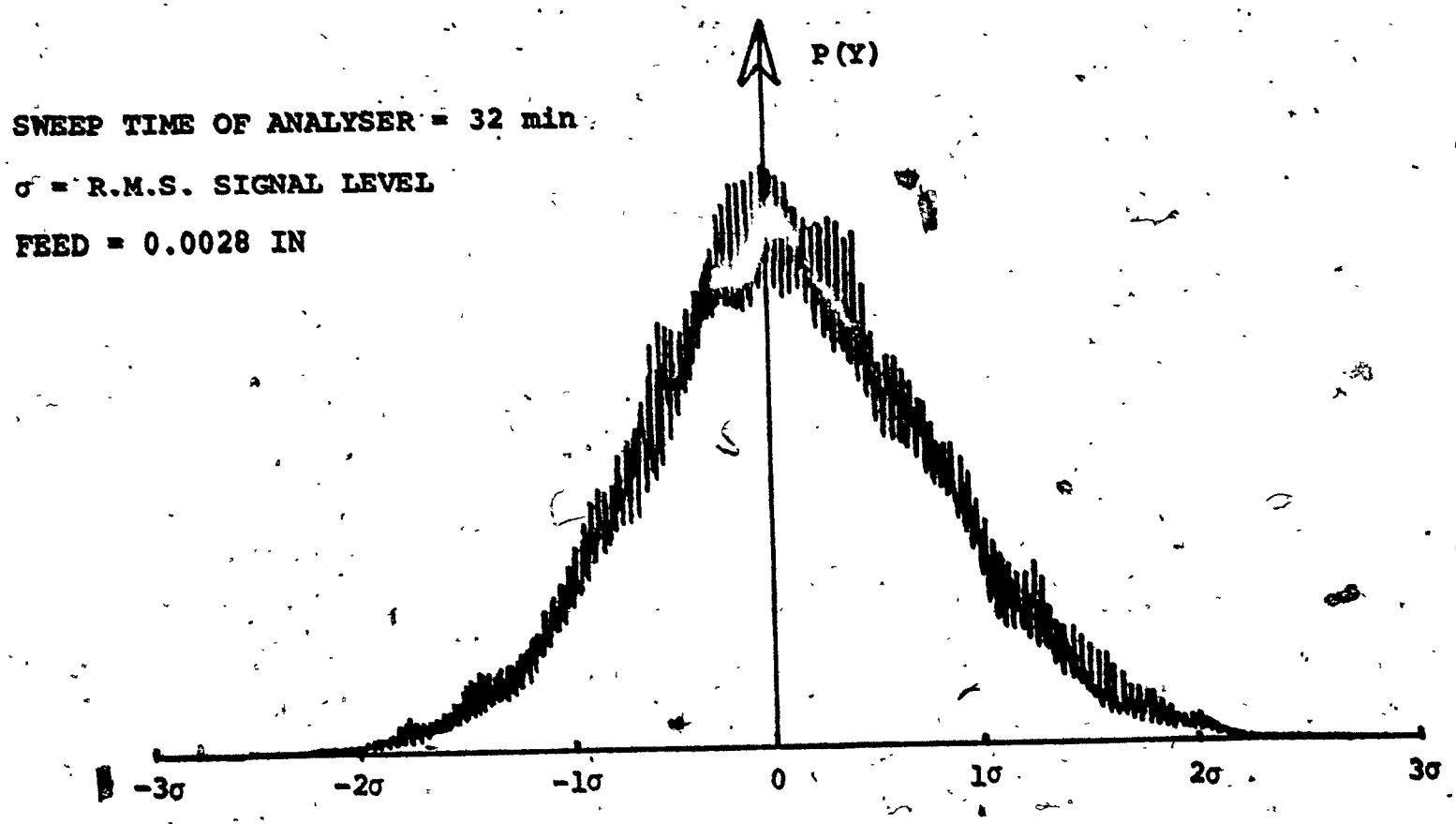

FIG. 5.16 Amplitude Density Plot for Thrust Fluctuations in Low Feed Drilling

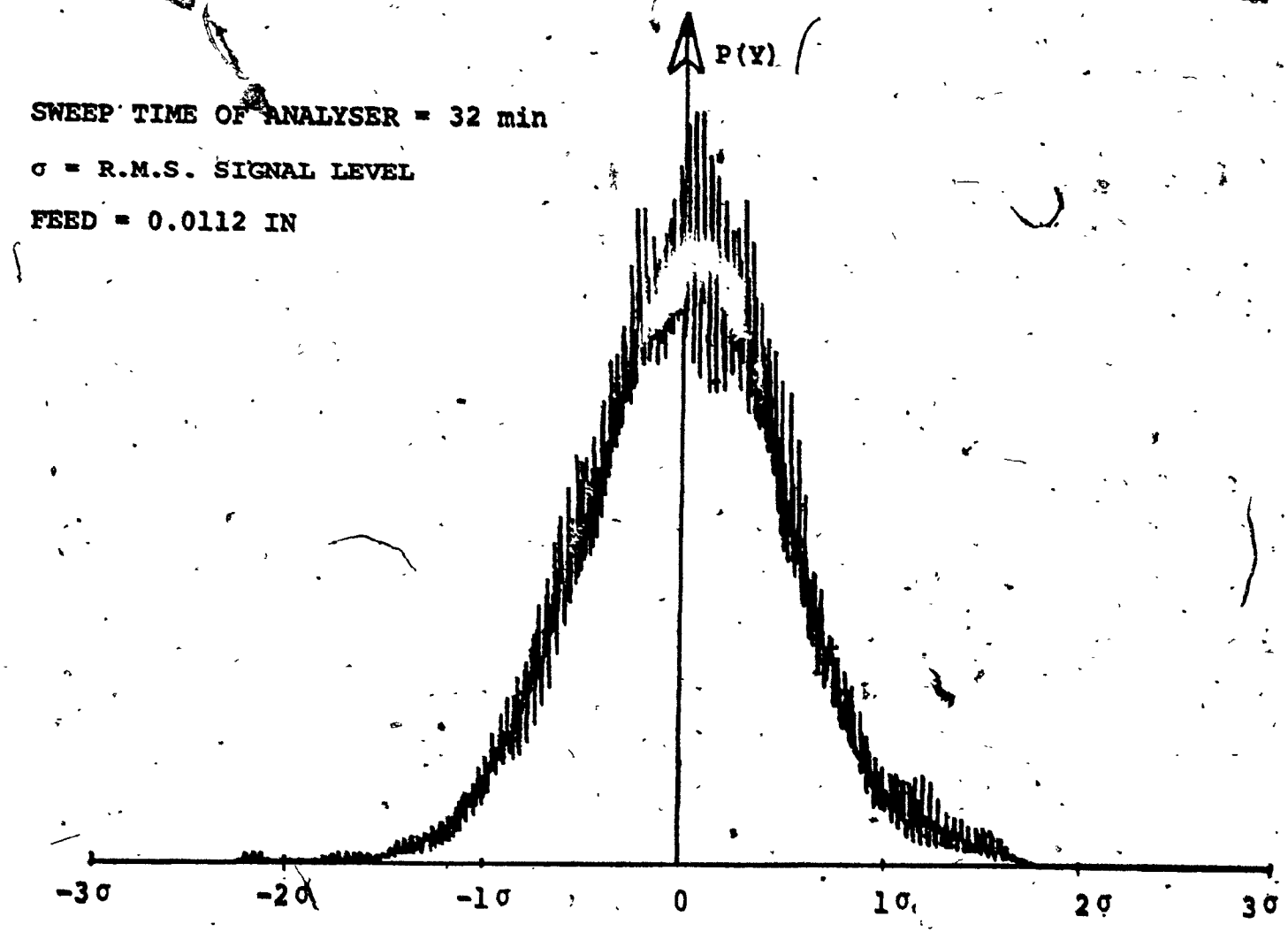

FIG. 5.17 Amplitude Density Plot for Torque Fluctuations in High Feed Drilling

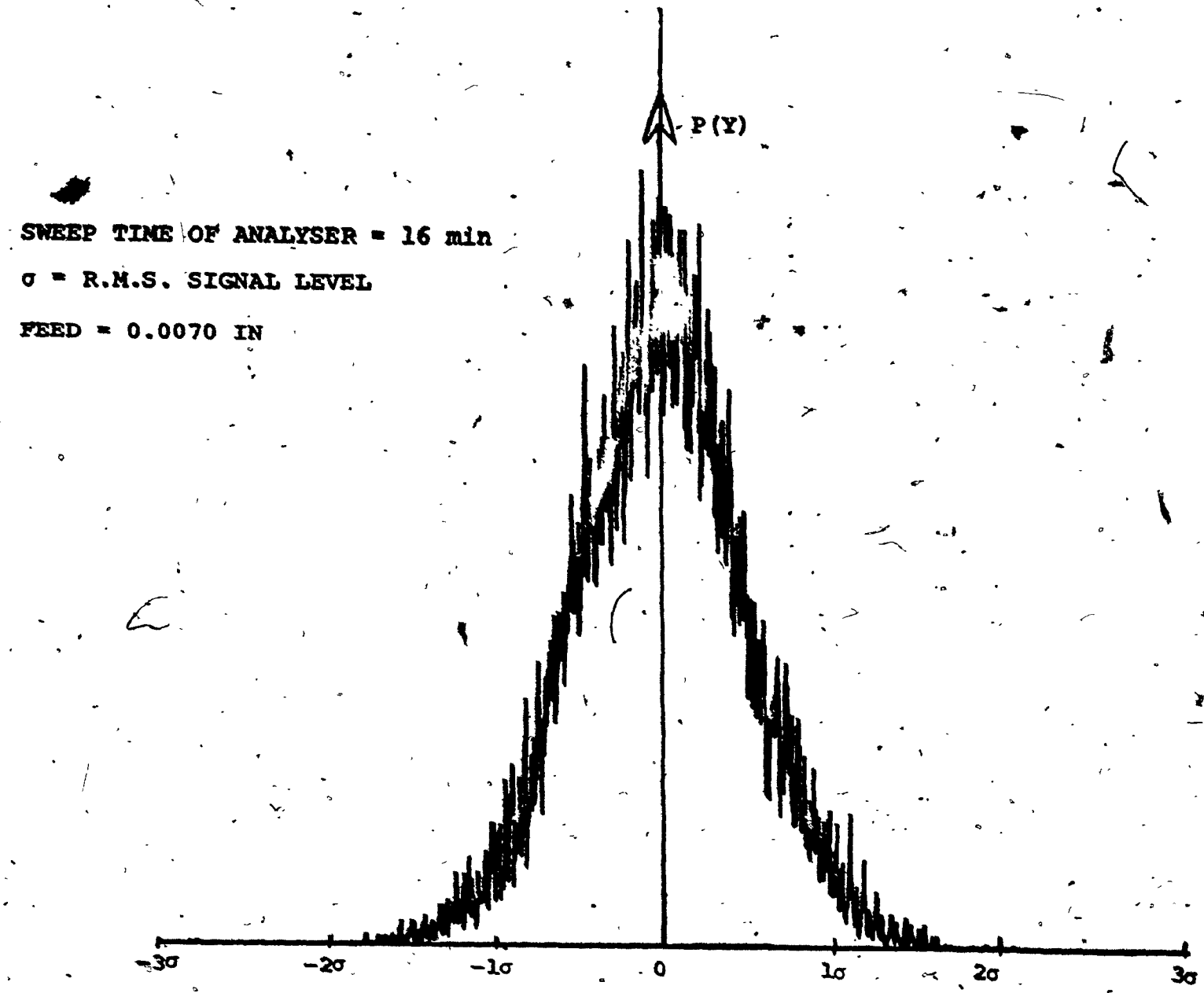

FIG. 5.18 Amplitude Density Plot for Torque Fluctuations in Medium Feed Drilling

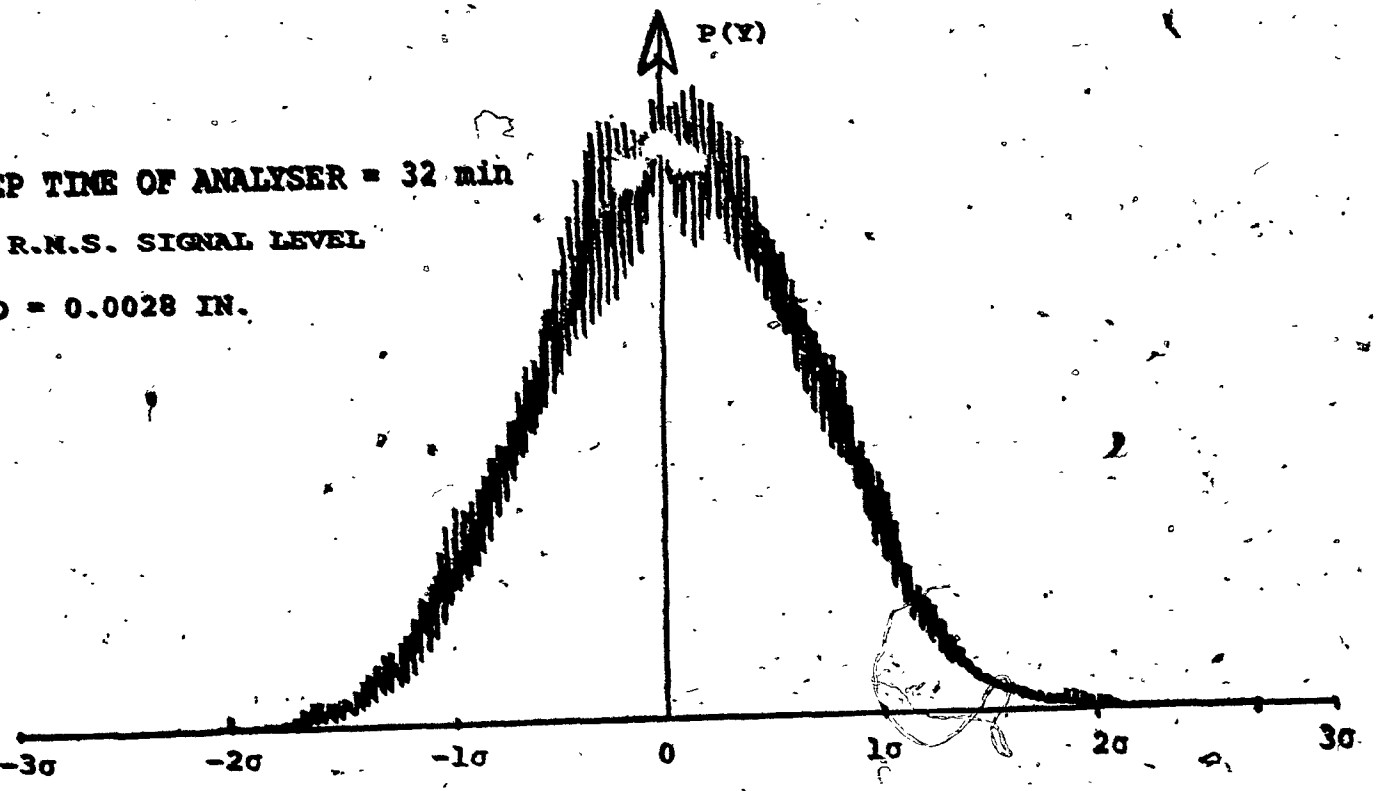

FIG. 5.19 Amplitude Density Plots for Torque Fluctuations for Low Feed Drilling

CHAPTER VI

CONCLUSIONS, LIMITATIONS AND RECOMMENDATIONS OF FUTURE WORK

CHAPTER VI

CONCLUSIONS

The torque and thrust force were measured using a two component piezoelectric dynamometer. Data reduction was carried out to determine their characteristic properties. From the characteristic properties of torque and thrust force, a stochastic model is proposed. Experimental measurements and statistical analysis of the forcing functions yield the following results:

(i) The measured static drilling torque and thrust force under three drilling conditions (low, medium, high feed) are found to be in good agreement with those calculated from semi-analytical steady state equations developed by dimensional analysis [5].

(ii) The nature of torque and thrust force in drilling is dynamic, not static.

(iii) The amplitudes of torque and thrust force fluctuations in drilling are random.

(iv) The study shows that torque and thrust force in drilling operations under three drilling conditions (low, medium, high feed) are stationary. This is in sharp contrast to the study conducted by Maragos [13] and Rakhit [14]. They have shown that cutting forces in turning are

stationary only in finishing operation but non-stationary in medium and rough operations.

(v) Maragos [13], found that amplitudes of cutting forces in single point finishing operations exhibit a single Gaussian distribution whereas those for medium and roughing operations show three superimposed Gaussian distributions. In our statistical analysis in the amplitude domain, the fluctuations of torque and thrust force under low, medium, high feed drilling exhibit Gaussian distribution. However, there is evidence that under high feed drilling, there is a slight departure from a Gaussian distribution.

(vi) The torque and thrust force in drilling exhibit similar spectral density curves, with most of power being concentrated at certain dominant frequencies.

From the signal analysis presented, it is concluded that torque and thrust force in drilling are to be considered stationary random processes with Gaussian distribution. That the processes are truly Gaussian distributed has been confirmed by an amplitude analysis using both the digital and analog methods.

6.1 LIMITATION OF PRESENT WORK AND FUTURE RECOMMENDATIONS

The main purpose of this study has been to investigate the following:

(i) The nature of drilling torque and thrust force under different drilling conditions

(ii) whether the fluctuations are randomly distributed and if they are, then what type of distribution they follow

(iii) power density functions of fluctuations.

(1) In our study, the dynamometer was found to have a natural frequency of 3 kHz. When the frequency response of the combined machine-tool-dynamometer-workpiece system was determined, it was found that the dynamometer could be relied upon for frequency components of only up to 700 Hz. In order that there is no interference between the highest frequency component present in fluctuations and the natural frequency of dynamometer, it is recommended that the dynamometer have a very high natural frequency.

(2) The workpiece was mounted on a two component dynamometer. The effect of added masses has been to reduce the resonant frequency of the system.

However, from statistical analysis considerations, recorded length of signal should be long. Under high cutting speed and feed, for the recorded length of signal to be long, the workpiece dimension has to be greater which adds more mass to the system thereby reducing the resonant frequency. So a compromise has to be found by designing a workpiece of suitable dimensions which does not lower the resonant frequency by the addition of mass and at same time, giving a minimum recorded length of signal necessary for statistical analysis.

It has been found that under high feed, there is a slight departure from Gaussian distribution. More work has to be done to determine the range of drilling speeds and feeds for which the distribution of fluctuations is significantly non-Gaussian.

REFERENCES

REFERENCES

[1] Boston, O.W., and Gilbert, W.W., "The Torque and Thrust in Small Drills Operating in Various Metals", Trans. Amer. Soc. Mech. Engrs. 58, 79(1936).

[2] Merchant, M.E., "Basic Mechanics of the Cutting Process", J. Applied Mech., Vol. 11, (1944), pp.168-75.

[3] Shaw, M.C., Cook, N.H., and Smith, P.A., "The Mechanics of Three-Dimensional Cutting Operations", Trans. Amer. Soc. Mech.Engrs., 74, 1055 (1952).

[4] Oxford, C.J. Jr., "On the Drilling of Metals - Basic Mechanics of Process", Trans. Amer.Soc.Mech.Engrs., 77, 103 (1955).

[5] Shaw, M.C., and Oxford, C.J.Jr., "On the Drilling of Metals - II - The Torque and Thrust in Drilling", Trans. Amer. Soc. Mech.Engrs. 79,139(1957).

[6] De Vries, M.F., "Cutting Forces (Measurement and Applications)", ASTME, Paper No. MR 68-612, (1968).

[7] Crisp, J., Seidel, J.R., and Stockey, W.F., "Measurement of Forces During Cutting With a Single Abrasive Grain", Int.J. of Prod. and Res., Vol.7, No: 2, (1968-69).

[8] Bickel, E., "Die Wechselnden Krafte bei der Spanbildung", C.I.R.P. Annalen, 12(4), (1966), p.206.

[9] Kwiatkowski, A.W., and Al Samarai, H.M., "Progress in the Application of Random Signal Analysis Methods to the Identification of Machine Tool Structures", Advances in Machine Tool Des. Res., (September 1968)

[10] Opitz, H., and Weck, M., "Determination of Transfer Function by Means of Spectral Density Measurements and Its Application to the Dynamic Investigation of Machine Tools Under Machining Conditions", Advances in Machine Tools, Des. Res., (September 1969).

[11] Osman, M.O.M., and Sankar, T.S., "Short-Time Acceptance Test for Machine Tools Based Upon Random Nature of Cutting Forces", Trans. ASME J. of Eng. for Ind., Vol.94, No.4, (November 1972),p.1020.

[12] Sankar, T.S., and Osman, M.O.M., "Flexural Stability of Machine Tool Spindles Under Randomly Fluctuating Cutting Forces", Communication of the Third World Congress for the Theory of Machines and Mechanism, Vol. 9, Paper G-19 (1971),pp.269-280.

[13] Maragos, S.K., "Measurement and Modeling of the Cutting Force Fluctuations During Machining", M.Eng. Thesis, Sir George Williams University, Montreal (1973).

[14] Rakhit,A.K., Sankar, T.S., and Osman, M.O.M., "The Effect of Stochastic Response of Machine-Tool-Workpiece on Formation of Surface Tenture in Turning", ASME Vibration Conference (1973), Cincinnati.

[15] Bhattacharya, A., "Design of Cutting Tools", ASTME Swinahart edition (1969).

[16] Koenigsberger, F., Design Principles of Metal Cutting Machine Tools, The Macmillan Co. (1964).

[17] Armarego, E.J.A., and Brown, R.H., The Machining of Metals, Prentice-Hall, Inc. (1969).

[18] Pal, A.K., Bhattacharya, A., and Sen, G.C.,"Investigation of Torque in Drilling Ductile Materials", Int. J.Mach. Tool Des. Res., Vol. 4, (1965),pp.205-221.

[19] Fujii,S., Devries, M.F., and Wu, S.M., "An Analysis of Drill Geometry for Optimum Drill Design by Computer - 1", ASME, J. of Eng. for Industry, (August 1970).

[20] Williams, R.A., "Dynamic Geometry of a Twist Drill", Int. J. Prod. Res.(1969),Vol.7, No.4.

[21] Hsu, T.C., and Chol,C.Y., "Measurement and Representation of Cutting Force Due to Oblique Machining", Int.J.Mach.Tool Des. Res., Vol.10, (1970), pp.49-64.

[22] Kegg, R.L., "Cutting Dynamics in Machine Tool Chatter", ASME, J., of Eng. for Industry, (Nov.1965).

[23] Gautsch, G.H., "Cutting Forces in Machining and Their Routine Measurement with Multi-Component Piezo-Electric Force Transducers", Advances in Machine Tool Des. Res. (September 1971).

[24] Micheletti, C.F., von Turkovich, B., and Rosseto,S., "Three Force Component Piezo-Electric Dynamometer (ITM MARK 2)",Int.J.Mach.Tool Des.Res., Vol.10, (1970),pp.305-315.

[25] Lathi, B.P., Signals, Systems and Communications, John Wiley and Sons (1965).

[26] Bendat,J.S., and Piersol, A.G., Measurement and Analysis of Random Data, John Wiley & Sons (1966).

[27] Beauchamp, K.G., Signal Processing Using Analog and Digital Techniques, John Wiley & Sons (1973).

APPENDIX A

COMPUTER PROGRAM

```
      PROGRAM TIN (INPUT,OUTPUT,TAPE10)
      DIMENSION Y(10000),X(80),XX(80),HIST(80),PD(80),D(80),SHIST(80)
C     Y=SAMPLE DATA RECORD OF DIMENSION 10000
C     READ RECORD IN
      READ (10,30) (Y(I),I=1,10000)
   30 FORMAT(6(E15.8,1X))
      SUM=0
C     CONVERT VOLT UNITS TO MECHANICAL TORQUE
      FCF=350/120
      DO 40 I=1,10000
      Y(I)=Y(I)*FCF
   40 SUM=Y(I)+SUM
      AVGY=SUM/10000
      PRINT 50,AVGY
   50 FORMAT(1H1,///,15X*AVERAGE OF SAMPLE RECORD=*,E11.4)
C     CONVERT DATA TO ZERO MEAN VALUE
      DO 51 I=1,10000
   51 Y(I)=Y(I)-AVGY
      SUM=0
      DO 3 I=1,10000
    3 SUM=Y(I)*Y(I)+SUM
      RO=SUM/10000
      PRINT 170,RO
  170 FORMAT(/,15X,*VARIANCE OF SAMPLE RECORD=*,E10.4,/)
C
C     TEST FOR STATIONARITY
C     THE RUN TEST
      DO 60 J=1,100
      L=J*100
      K=L-95
      SUM=0
      DO 52 I=K,L
   52 SUM=Y(I)+SUM
   60 X(J)=SUM/96
      SUM=0
      DO 70 I=1,100
   70 SUM=SUM+X(I)
      AVG=SUM/100
      K=1
      I=1
      IF(X(I).GE.AVG) GO TO 12
   13 I=I+1
      IF(X(I).GE.AVG) GO TO 11
      IF(I.EQ.100) GO TO 14
      GO TO 13
   11 K=K+1
   12 IF(I.EQ.100) GO TO 14
      I=I+1
      IF(X(I).GE.AVG) GO TO 12
      K=K+1
      IF(I.EQ.100) GO TO 14
      GO TO 13
   14 PRINT 16,K
   16 FORMAT(15X,*NUMBER OF RUNS FOR SEQUENCE X=*,I3,/)
      DO 75 J=1,100
      L=J*100
      K=L-95
```

```
      SUM=0
      DO 90 I=K,L
   90 SUM=Y(I)**2+SUM
   75 XX(J)=SUM/96
      SUM=0
      DO 91 I=1,100
   91 SUM=SUM+XX(I)
      AVG=SUM/100
      K=1
      I=1
      IF(XX(I).GE.AVG) GO TO 120
  130 I=I+1
      IF(XX(I).GE.AVG) GO TO 110
      IF(I.EQ.100) GO TO 140
      GO TO 130
  110 K=K+1
  120 IF(I.EQ.100) GO TO 140
      I=I+1
      IF(XX(I).GE.AVG) GO TO 120
      K=K+1
      IF(I.EQ.100) GO TO 140
      GO TO 130
  140 PRINT 160,K
  160 FORMAT(15X,*NUMBER OF RUNS FOR SEQUENCE XX=*,I2,/)
C
C     TREND TEST FOR STATIONARITY
      K=0
      DO 21 J=1,99
      JJ=J+1
      DO 21 I=JJ,100
      IF(X(J).GT.X(I)) K=K+1
   21 CONTINUE
      PRINT 22,K
      K=0
      DO 23 J=1,100
      JJ=J+1
      DO 23 I=JJ,100
      IF(XX(J).GT.XX(I)) K=K+1
   23 CONTINUE
      PRINT 24,K
   22 FORMAT(15X,*NUMBER OF REVERSE ARRANGEMENTS FOR THE SEQUENCEX=*,
     CI4,/)
   24 FORMAT(15X,*NUMBER OF REVERSE ARRANGEMENTS FOR SEQUENCEXX=*,I4)
C
C
C     PROBABILITY DENSITY HISTOGRAM
      K=78
      K2=K+2
      DO 88 I=1,K2
   88 HIST(I)=0
      C=K
      A=-4
      B=4
      C=(B-A)/C
      DO 9 I=1,10000
      YI=Y(I)
      IF(A.LT.YI.AND.YI.LE.B) GO TO 18
```

```
      IF(YI.LE.A) GO TO 19
      IF(YI.GT.B) HIST(K2)=HIST(K2)+1
      GO TO 9
   19 HIST(1)=HIST(1)+1
      GO TO 9
   18 E=(YI-A)/C
      II=E
      EE=E-II
      IF(EE.GT.0.001) E=E+1
      IE=E
      HIST(IE)=HIST(IE)+1
    9 CONTINUE
      SHIST(1)=0.5*(HIST(1)+HIST(2))
      DO 215 K=2,79
  215 SHIST(K)=0.25*HIST(K-1)+0.5*HIST(K)+0.25*HIST(K+1)
      SHIST(80)=0.5*HIST(79)+HIST(80)
C
C21   PROBABILITY DENSITY IN TERMS OF PERCENTAGE OFDATA IN
C     EACH CLASS INTERVAL
      N=10000
      DO 27 I=1,K2
      HIST(I)=HIST(I)/N
   27 SHIST(I)=SHIST(I)/N
      PRINT 25
   25 FORMAT(1H1,15X,*PROBABILITY DENSITY HISTOGRAM*/,
     117X,*TORQUE DENSITY*,3X,*TORQUE DENSITY*/,
     217X,*LBINCH    NO     LBINCH    NO*)
      DO 194 J=2,79
  194 D(J)=A+(J-2)*C+0.5*C
      DO 195 J=2,40
      JJ=J+39
  195 PRINT 196,D(J),SHIST(J),D(JJ),SHIST(JJ)
  196 FORMAT(17X,F6.2,F8.4,3X,F6.2,F8.4)
C
C     PROBABILITY DISTRIBUTION
      PD(1)=HIST(1)
      DO 26 I=2,K2
   26 PD(I)=PD(I-1)+HIST(I)
      PRINT 198
  198 FORMAT(1H1,15X,*PROB. DISTRIBUTION*/,
     115X,*TORQUE DIST*,9X,*TORQUE DIST*/,18X,*LBINCH*,9X,*LBINCH*)
      DO 197 J=2,40
      JJ=J+39
  197 PRINT 212,D(J),PD(J),D(JJ),PD(JJ)
  212 FORMAT(17X,2(F5.1,F6.3,3X))
      STOP
      END
```

PROB. DISTRIBUTION

TORQUE DIST LBINCH		TORQUE DIST LBINCH	
-3.9	.000	.1	.563
-3.8	.000	.2	.595
-3.7	.000	.3	.628
-3.6	.001	.4	.658
-3.5	.002	.5	.686
-3.4	.002	.6	.718
-3.3	.003	.7	.748
-3.2	.005	.8	.774
-3.1	.007	.9	.803
-3.0	.007	1.0	.827
-2.9	.010	1.1	.847
-2.8	.013	1.2	.867
-2.7	.016	1.3	.885
-2.6	.020	1.4	.903
-2.5	.023	1.5	.918
-2.4	.030	1.6	.928
-2.3	.036	1.7	.942
-2.2	.043	1.8	.952
-2.1	.050	1.9	.960
-2.0	.061	2.0	.967
-1.9	.072	2.1	.972
-1.8	.086	2.2	.977
-1.7	.100	2.3	.980
-1.6	.119	2.4	.983
-1.5	.137	2.5	.986
-1.4	.157	2.6	.988
-1.3	.181	2.7	.990
-1.2	.205	2.8	.992
-1.1	.229	2.9	.993
-1.0	.256	3.0	.994
-.9	.280	3.1	.995
-.8	.309	3.2	.996
-.7	.338	3.3	.997
-.6	.368	3.4	.997
-.5	.400	3.5	.998
-.4	.432	3.6	.998
-.3	.468	3.7	.998
-.2	.501	3.8	.999
-.1	.532	3.9	.999

PROBABILITY DENSITY HISTOGRAM

TORQUE LBINCH	DENSITY NO	TORQUE LBINCH	DENSITY NO
-3.95	.0001	.05	.0312
-3.85	.0002	.15	.0320
-3.74	.0002	.26	.0321
-3.64	.0004	.36	.0304
-3.54	.0006	.46	.0295
-3.44	.0007	.56	.0303
-3.33	.0012	.67	.0294
-3.23	.0015	.77	.0277
-3.13	.0015	.87	.0271
-3.03	.0016	.97	.0242
-2.92	.0024	1.08	.0211
-2.82	.0028	1.18	.0198
-2.72	.0032	1.28	.0184
-2.62	.0037	1.38	.0169
-2.51	.0043	1.49	.0144
-2.41	.0056	1.59	.0124
-2.31	.0066	1.69	.0120
-2.21	.0067	1.79	.0103
-2.10	.0079	1.90	.0083
-2.00	.0100	2.00	.0068
-1.90	.0120	2.10	.0055
-1.79	.0135	2.21	.0045
-1.69	.0151	2.31	.0036
-1.59	.0173	2.41	.0032
-1.49	.0189	2.51	.0028
-1.38	.0205	2.62	.0022
-1.28	.0228	2.72	.0018
-1.18	.0240	2.82	.0015
-1.08	.0248	2.92	.0012
-.97	.0255	3.03	.0012
-.87	.0260	3.13	.0012
-.77	.0279	3.23	.0011
-.67	.0292	3.33	.0007
-.56	.0301	3.44	.0006
-.46	.0315	3.54	.0006
-.36	.0332	3.64	.0003
-.26	.0344	3.74	.0002
-.15	.0333	3.85	.0002
-.05	.0315	3.95	.0004

ESTIMATES OF THE AUTOCORRELATION AT DIFFERENT LAG NUMBER

.1000E+01

100	-.1582E+00	150	-.2388E+00
101	-.1619E+00	151	-.2407E+00
102	-.1641E+00	152	-.2438E+00
103	-.1671E+00	153	-.2454E+00
104	-.1712E+00	154	-.2472E+00
105	-.1737E+00	155	-.2509E+00
106	-.1756E+00	156	-.2550E+00
107	-.1788E+00	157	-.2558E+00
108	-.1828E+00	158	-.2511E+00
109	-.1865E+00	159	-.2443E+00
110	-.1894E+00	160	-.2382E+00
111	-.1926E+00	161	-.2312E+00
112	-.1949E+00	162	-.2223E+00
113	-.1963E+00	163	-.2157E+00
114	-.1973E+00	164	-.2142E+00
115	-.1977E+00	165	-.2155E+00
116	-.1990E+00	166	-.2164E+00
117	-.2018E+00	167	-.2153E+00
118	-.2048E+00	168	-.2142E+00
119	-.2080E+00	169	-.2144E+00
120	-.2100E+00	170	-.2123E+00
121	-.2113E+00	171	-.2077E+00
122	-.2125E+00	172	-.2052E+00
123	-.2141E+00	173	-.2032E+00
124	-.2151E+00	174	-.1995E+00
125	-.2145E+00	175	-.1976E+00
126	-.2151E+00	176	-.1992E+00
127	-.2162E+00	177	-.2000E+00
128	-.2165E+00	178	-.1977E+00
129	-.2165E+00	179	-.1970E+00
130	-.2171E+00	180	-.1993E+00
131	-.2179E+00	181	-.1986E+00
132	-.2182E+00	182	-.1962E+00
133	-.2184E+00	183	-.1982E+00
134	-.2194E+00	184	-.2019E+00
135	-.2202E+00	185	-.2008E+00
136	-.2204E+00	186	-.1975E+00
137	-.2206E+00	187	-.1979E+00
138	-.2228E+00	188	-.1982E+00
139	-.2249E+00	189	-.1956E+00
140	-.2253E+00	190	-.1935E+00
141	-.2267E+00	191	-.1938E+00
142	-.2281E+00	192	-.1916E+00
143	-.2288E+00	193	-.1872E+00
144	-.2298E+00	194	-.1847E+00
145	-.2328E+00	195	-.1845E+00
146	-.2350E+00	196	-.1828E+00
147	-.2353E+00	197	-.1811E+00
148	-.2363E+00	198	-.1807E+00
149	-.2374E+00	199	-.1799E+00
150	-.2388E+00	200	-.1780E+00

ESTIMATES OF THE AUTOCORRELATION AT DIFFERENT LAG NUMBERS

.1000E+01

1	.9426E+00	51	.8245E-01
2	.8831E+00	52	.7156E-01
3	.8680E+00	53	.6327E-01
4	.8470E+00	54	.5402E-01
5	.7970E+00	55	.4319E-01
6	.7674E+00	56	.3170E-01
7	.7631E+00	57	.2194E-01
8	.7440E+00	58	.1316E-01
9	.7098E+00	59	.3756E-02
10	.6882E+00	60	-.4750E-02
11	.6775E+00	61	-.1155E-01
12	.6565E+00	62	-.1990E-01
13	.6284E+00	63	-.3086E-01
14	.6084E+00	64	-.3962E-01
15	.5956E+00	65	-.4508E-01
16	.5746E+00	66	-.5104E-01
17	.5487E+00	67	-.5748E-01
18	.5305E+00	68	-.6082E-01
19	.5170E+00	69	-.6371E-01
20	.4983E+00	70	-.6847E-01
21	.4771E+00	71	-.7478E-01
22	.4625E+00	72	-.7931E-01
23	.4515E+00	73	-.8314E-01
24	.4357E+00	74	-.8933E-01
25	.4177E+00	75	-.9517E-01
26	.4032E+00	76	-.9654E-01
27	.3914E+00	77	-.9766E-01
28	.3755E+00	78	-.1010E+00
29	.3576E+00	79	-.1033E+00
30	.3437E+00	80	-.1050E+00
31	.3310E+00	81	-.1089E+00
32	.3145E+00	82	-.1141E+00
33	.2977E+00	83	-.1173E+00
34	.2850E+00	84	-.1196E+00
35	.2721E+00	85	-.1233E+00
36	.2559E+00	86	-.1268E+00
37	.2420E+00	87	-.1281E+00
38	.2312E+00	88	-.1284E+00
39	.2180E+00	89	-.1285E+00
40	.2027E+00	90	-.1289E+00
41	.1913E+00	91	-.1298E+00
42	.1820E+00	92	-.1324E+00
43	.1675E+00	93	-.1350E+00
44	.1523E+00	94	-.1383E+00
45	.1424E+00	95	-.1413E+00
46	.1338E+00	96	-.1457E+00
47	.1215E+00	97	-.1500E+00
48	.1099E+00	98	-.1532E+00
49	.1028E+00	99	-.1548E+00
50	.9362E-01	100	-.1582E+00

```
      M=I+50
   29 PRINT 180,I,R(I),M,R(M)
  180 FORMAT(25X,I3,E12.4,10X,I3,E12.4)
      PRINT 11,RO
   11 FORMAT(1H1,20X,*ESTIMATES OF THE AUTOCORRELATION AT DIFFERENT
     CLAG NUMBERS*,//,40X,E10.4)
      DO 27 MM=100,150
      LL=MM+50
   27 PRINT 185,MM,R(MM),LL,R(LL)
  185 FORMAT(25X,I3,E12.4,10X,I3,E12.4)
C
C     POWER SPECTRAL DENSITY ANALYSIS
      FC=700
      DO 5 IK=1,101
      K=IK-1
      F(IK)=FC*K/100
      PI=(3.14159265*K)/100
      SUM=0
      DO 6 IR=1,99
    6 SUM=SUM+R(IR)*COS(PI*IR)
    5 G(IK)=(1/FC)*(RO+2*SUM+(-1**K)*R(100))
      GG(1)=0.5*G(1)+0.5*G(2)
      DO 7 K=2,100
    7 GG(K)=0.25*G(K-1)+0.5*G(K)+0.25*G(K+1)
      GG(101)=0.5*G(100)+0.5*G(101)
      PRINT 171
  171 FORMAT(1H1,15X,*SMOOTH SPECTRAL DENSITY*/,
     113X,*FREQ MAGNITUDE*,4X,*FREQ MAGNITUDE*/,
     214X,*HZ*,4X,*LBINCH/HZ*,3X,*HZ*,4X,*LBINCH/HZ*)
      DO 100 I=1,50
      NI=I+50
  100 PRINT 89,F(I),GG(I),F(NI),GG(NI)
   89 FORMAT(12X,F5.0,F9.4,4X,F5.0,F9.4)
      STOP
      END
```

```
      PROGRAM TIN(INPUT,OUTPUT,TAPE10)
      DIMENSION Y(10000),R(200),GG(101),G(101),F(101)
C     Y=SAMPLE DATA RECORD OF DIMENSION 10000
C     READ RECORD IN
      READ(10,30) (Y(I),I=1,10000)
   30 FORMAT(6(E15.9,1X))
C     CONVERT VOLT UNITS TO MECH UNITS FORCE
      FCF=350/120
      SUM=0
      DO 40 I=1,10000
      Y(I)=Y(I)*FCF
   40 SUM=Y(I)+SUM
      AVGY=SUM/10000
      PRINT 50,AVGY
   50 FORMAT(1H1,///,15X,*AVERAGE OF SAMPLE RECORD=*,E11.4)
C     CONVERT DATA TO ZERO MEAN VALUE
      DO 51 I=1,10000
   51 Y(I)=Y(I)-AVGY
      SUM=0
      DO 3 I=1,10000
    3 SUM=Y(I)*Y(I)+SUM
      RO=SUM/10000
      PRINT 170,RO
  170 FORMAT(/,15X*VARIANCE OF SAMPLE RECORD=*,E10.4,/)
C
C     TEST FOR NORMALITY
      PRINT 15
   15 FORMAT(1H1,10X,*DEVIATION FROM THE   PERCENTAGE OF DEVIATION AT O
     1R*/,13X,*AVERAGE VALUE      BELOW THE GIVEN DEVIATION*/)
      Z=5
      K=0
      DO 20 J=1,19
      Z=Z-0.5
      DO 10 I=1,10000
      IF(Y(I).LE.Z) K=K+1
   10 CONTINUE
      A=K
      DEV=(A/10000.)*100
      PRINT 17,Z,DEV
   17 FORMAT(16X,F6.1,19X,F6.1)
   20 CONTINUE
C
C     TEST FOR THE RANDOMNESS
C     THE AUTOCORRELATION TEST
      N=10000
      DO 1 IR=1,200
      SUM=0
      JJ=N-IR
      DO 2 J=1,JJ
    2 SUM=SUM+Y(J)*Y(J+IR)
      Z=N-IR
    1 R(IR)=SUM/(Z*RO)
      RO=RO/RO
      PRINT 4,RO
    4 FORMAT(1H1,20X,*ESTIMATED OF THE AUTOCORRELATION AT DIFFERENT
     CLAG NUMBERS*,//,40X,E10.4)
      DO 29 I=1,50
```

SMOOTH SPECTRAL DENSITY

FREQ HZ	MAGNITUDE LBINCH/HZ	FREQ HZ	MAGNITUDE LBINCH/HZ
0.	.0574	350.	.0005
7.	.0483	357.	.0006
14.	.0260	364.	.0006
21.	.0095	371.	.0005
28.	.0054	378.	.0005
35.	.0037	385.	.0004
42.	.0027	392.	.0004
49.	.0022	399.	.0004
56.	.0018	406.	.0004
63.	.0013	413.	.0003
70.	.0011	420.	.0003
77.	.0011	427.	.0003
84.	.0010	434.	.0003
91.	.0009	441.	.0003
98.	.0009	448.	.0003
105.	.0009	455.	.0003
112.	.0008	462.	.0003
119.	.0007	469.	.0003
126.	.0007	476.	.0003
133.	.0006	483.	.0003
140.	.0006	490.	.0003
147.	.0005	497.	.0003
154.	.0005	504.	.0003
161.	.0005	511.	.0003
168.	.0005	518.	.0002
175.	.0005	525.	.0002
182.	.0005	532.	.0002
189.	.0004	539.	.0002
196.	.0004	546.	.0002
203.	.0004	553.	.0002
210.	.0004	560.	.0002
217.	.0004	567.	.0002
224.	.0004	574.	.0002
231.	.0004	581.	.0002
238.	.0003	588.	.0002
245.	.0003	595.	.0002
252.	.0003	602.	.0002
259.	.0003	609.	.0002
266.	.0003	616.	.0002
273.	.0003	623.	.0002
280.	.0003	630.	.0003
287.	.0003	637.	.0002
294.	.0003	644.	.0002
301.	.0003	651.	.0002
308.	.0003	658.	.0003
315.	.0003	665.	.0002
322.	.0003	672.	.0002
329.	.0004	679.	.0002
336.	.0004	686.	.0002
343.	.0005	693.	.0002

SMOOTH SPECTRAL DENSITY

FREQ HZ	MAGNITUDE LBINCH/HZ	FREQ HZ	MAGNITUDE LBINCH/HZ
0.	.0574	350.	.0005
7.	.0483	357.	.0006
14.	.0260	364.	.0006
21.	.0095	371.	.0005
28.	.0054	378.	.0005
35.	.0037	385.	.0004
42.	.0027	392.	.0004
49.	.0022	399.	.0004
56.	.0018	406.	.0004
63.	.0013	413.	.0003
70.	.0011	420.	.0003
77.	.0011	427.	.0003
84.	.0010	434.	.0003
91.	.0009	441.	.0003
98.	.0009	448.	.0003
105.	.0009	455.	.0003
112.	.0008	462.	.0003
119.	.0007	469.	.0003
126.	.0007	476.	.0003
133.	.0006	483.	.0003
140.	.0006	490.	.0003
147.	.0005	497.	.0003
154.	.0005	504.	.0003
161.	.0005	511.	.0003
168.	.0005	518.	.0002
175.	.0005	525.	.0002
182.	.0005	532.	.0002
189.	.0004	539.	.0002
196.	.0004	546.	.0002
203.	.0004	553.	.0002
210.	.0004	560.	.0002
217.	.0004	567.	.0002
224.	.0004	574.	.0002
231.	.0004	581.	.0002
238.	.0003	588.	.0002
245.	.0003	595.	.0002
252.	.0003	602.	.0002
259.	.0003	609.	.0002
266.	.0003	616.	.0002
273.	.0003	623.	.0002
280.	.0003	630.	.0003
287.	.0003	637.	.0002
294.	.0003	644.	.0002
301.	.0003	651.	.0002
308.	.0003	658.	.0003
315.	.0003	665.	.0002
322.	.0003	672.	.0002
329.	.0004	679.	.0002
336.	.0004	686.	.0002
343.	.0005	693.	.0002

AVERAGE OF SAMPLE RECORD= -.3193E-01

VARIANCE OF SAMPLE RECORD= .1453E+01

NUMBER OF RUNS FOR SEQUENCE X= 58

NUMBER OF RUNS FOR SEQUENCE XX=55

NUMBER OF REVERSE ARRANGEMENTS FOR THE SEQUENCEX=1894

NUMBER OF REVERSE ARRANGEMENTS FOR SEQUENCEXX=2526

DEVIATION FROM THE AVERAGE VALUE	PERCENTAGE OF DEVIATION AT O R BELOW THE GIVEN DEVIATION
4.5	99.9
4.0	199.8
3.5	299.5
3.0	398.7
2.5	496.9
2.0	592.5
1.5	682.2
1.0	761.9
.5	827.2
0.0	877.3
-.5	911.6
-1.0	932.7
-1.5	943.4
-2.0	948.0
-2.5	949.8
-3.0	950.4
-3.5	950.5
-4.0	950.5
-4.5	950.5